Utilities Policy 55 (2018) 129–141

Contents lists available at ScienceDirect

Utilities Policy

journal homepage: www.elsevier.com/locate/jup

Challenges of India's power transmission system

Naveen Upreti[a], Raju Ganesh Sunder[b], Narendra N. Dalei[c,*], Sandeep Garg[d]

[a] Department of Energy Management, School of Business, University of Petroleum and Energy Studies, Dehradun, 248007, India
[b] CCE Academic Unit, School of Business, University of Petroleum and Energy Studies, Dehradun, 248007, India
[c] Department of Economics and International Business, School of Business, University of Petroleum and Energy Studies, Dehradun, 248007, India
[d] India Electronics Semiconductor Association, Delhi, India

1. Introduction

The critical infrastructure defining a country's economic prosperity and welfare is its power supply infrastructure. Generation, transmission, and distribution sectors collectively represent a complete power value chain (Singh, 2006). Globally, India's power sector is the fifth largest in terms of installed power generating capacity with a complex network reaching 200 million diverse consumers spread across the country (Daruka, 2015). With the deregulation of the power sector along with the goal “power accessible to all”, the onus of Indian power sector lies with Central and State utilities. With initiatives such as “Make in India” and “Digital India”, this emerging country is passing through the most energy-intensive phase of its economic growth.

India is ranked third in power production among other countries in the world (Thakur et al., 2005) and has witnessed commendable growth in generation capacity over past decades totaling more than 320 GW (MOP, 2018). Prospective comparison of the growth in generation capacity with respect to load is depicted in Fig. 1. With enough availability of conventional and non-conventional resources, power generation is not a concern today.

Despite being a power surplus nation with a moderately low power demand of 164 GW (as of March 2018), India still faces a delivery shortfall of 4 GW (2%) (CEA, 2017). There are persistent issues of power outages for several hours due to lack of adequate transmission capacity. There are also a few thousands of towns not associated with the national grid due to the absence of transmission infrastructure (Sinha et al., 2011). Although the power is available, power accessibility issues have unfavorably influenced the nation's economy and accounted for substantial GDP loss, which in turn has impacted various other sectors (Singh, 2013). Policymakers are perplexed with the distressing state of power deficit, regardless of having surplus power.

Problems of power deficiency and accessibility in India lie mainly with the transmission infrastructure and are expected to increase in the next few years without appropriate attention. Pressure on the existing network to transfer more power has led to transmission congestion (CEA, 2016; Xue and Xiao, 2013). It has been estimated that the generated energy wasted due to transmission bottlenecks is approximately 1.93×10^9 kWh of electricity (Kovendan and Sridharan, 2017). To overcome these persisting issues in Indian Power Transmission System (IPTS), it is important to understand its overall structure as provided in Fig. 2.

Unlike many other countries, IPTS follows a federal structure wherein the power and controls are distributed between central as well as state governments of the country. Consequently, the responsibility of the sector lies with both central and state governments. The Inter-State Transmission System (ISTS) is mainly owned by the central government with the goal of developing a national grid. ISTS is the prime responsibility of the Powergrid Corporation of India, a Central Transmission Utility. Similarly, Intra-State Transmission System (InSTS) within the state is owned by State Transmission Utilities (STU) of each state under the powers of state governments (CEA, 2016). ISTS and InSTS are described in the Appendix.

Further, the Indian Transmission structure is divided among the North Route (NR), the South Route (SR), the East Route (ER), and the West Route (WR). Power is routed into the grid from one point to another through Open Access (OA). OA provides a non-discriminatory provision to customers connected with a load of one megawatt (MW) or above to choose and purchase power from the lower cost power companies available from large power companies. OA ensures regular supply of electricity to large consumers at competitive prices. The categorization of OA is provided in the Appendix.

Despite the fact that various key bodies such as the Ministry of Power (MoP) and POWERGRID are involved in national power grid planning, IPTS may not be able to evacuate power (especially from power surplus to power deficit regions) due to unavailability of transmission corridors and transmission congestion at ISTS and InSTS levels, leading to inefficiencies in meeting demand (CEA, 2016). A few examples are provided in the Appendix for reference purposes.

The increasing power demand of the country remains unfulfilled despite the steady increase in transmission capacity. This is due to various strategic as well as operational challenges within the IPTS. These challenges have been indirectly reported in the literature and are

* Corresponding author.
E-mail addresses: upreti.naveen@yahoo.com (N. Upreti), raajuganieshsunder@gmail.com, rgsunder@ddn.upes.ac.in (R.G. Sunder), nndalei@gmail.com, ndalei@ddn.upes.ac.in (N.N. Dalei), sandeepgarg05@gmail.com (S. Garg).

https://doi.org/10.1016/j.jup.2018.10.002
Received 13 November 2017; Received in revised form 7 October 2018; Accepted 7 October 2018
Available online 16 October 2018
0957-1787/ © 2018 Elsevier Ltd. All rights reserved.

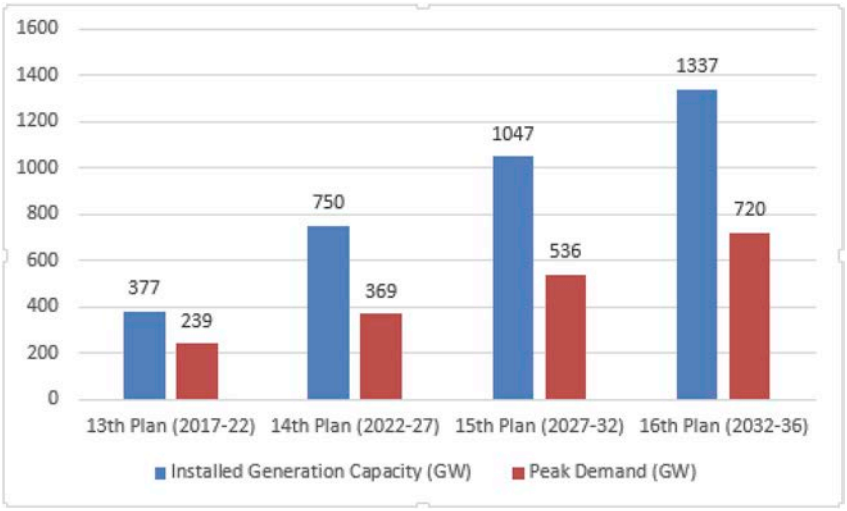

Fig. 1. Installed Capacity vs Demand in GW (Source: Central Electricity Authority, 2016).

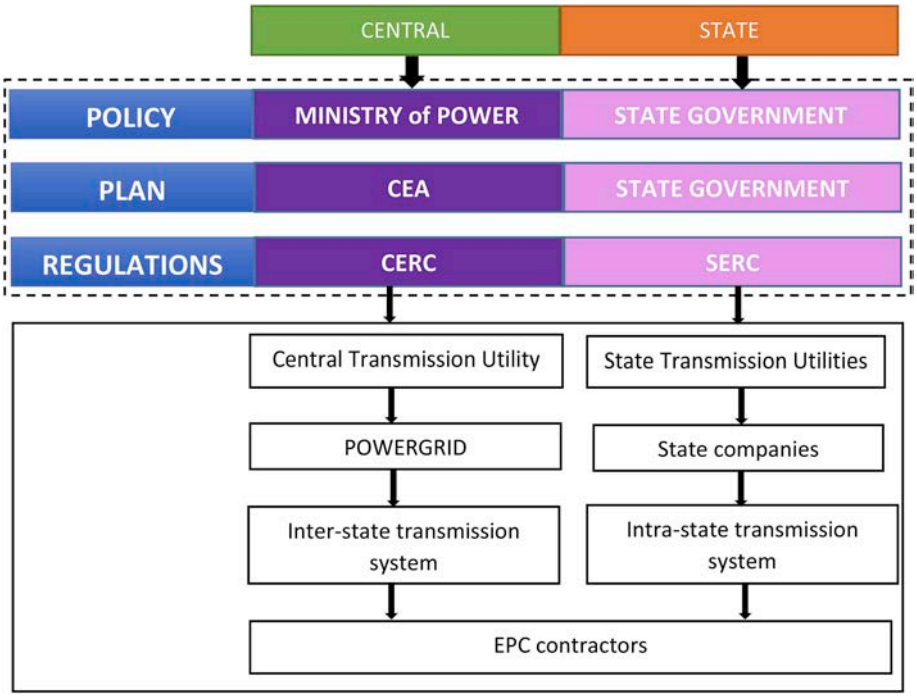

Fig. 2. Structure of Indian power transmission system.

presented in a fragmented manner. This paper focuses on enhancing the IPTS by identifying and assessing various persistent issues that act as key constraints on improving transmission adequacy. To date, no study has attempted to provide a combined list of the various factors that influence the general functioning of the IPTS. To fill this gap, this paper reviews the literature on the Indian power sector, and the transmission system in particular. We discuss the role of each factor to understand its major implications on the overall transmission system. The study further examines relationships among the different factors using Decision Making Trial and Evaluation Laboratory (DEMATEL) approach. The DEMATEL method is considered to be one of the best multi-criteria decision-making (MCDM) techniques to decipher direct and indirect relationships among factors mathematically.

DEMATEL was selected for its capability to develop a visual representation of the causal factors and effect factors affecting the IPTS and relationships among them. This approach can be used to improve understanding of the challenging elements in the policy scheme. It also helps decision-makers prioritize their focus on causal factors and offer policy recommendations to make the transmission network more robust for power evacuation. The paper provides value-added insights that can contribute to making an efficient and cost-effective transmission system in India. Other countries engaged in transmission system policy and planning can also draw lessons from the analysis.

The rest of the paper is organized as follows. Section 2 provides a detailed discussion of key factors inhibiting the development of IPTS. In Section 3, we describe the DEMATEL methodology and the results are analyzed and discussed in Section 4. Lastly, in Section 5, conclusions and policy implications of this work are provided.

2. Key challenges of India's power transmission system

In India, the installation of transmission networks was initiated immediately after independence (1947) to meet increasing demand. At present, these transmission lines are functioning but performing

inefficiently due to age. Replacing old lines is needed to reduce losses and achieve demand targets (Omer et al., 2013). The instability of India's grid infrastructure drew attention when more than a dozen of transmission towers with 765 kV and 400 kV capacities collapsed in the face of pre-monsoon winds between April and June in the year 2015 (Sasi, 2015).

To revive the power sector, a reform was introduced in 1991 in the country and is considered to be sustainable, economically efficient, financially viable, environmentally benign, and feasible in implementation (Bhattacharyya, 2007). The reform was introduced with a focused objective to convert technically inefficient power sector into a commercially viable power-trading sector (Sharma et al., 2005). One of the major changes was to link accountabilities of generation and transmission to both state and central government, but the state government regulates distribution (Shukla and Thampy, 2011). These major changes alleviated some immediate concerns but long-term sustainability requires further deepening of the reform process.

Despite market restructuring and policy reforms, there still exist substantial inefficiencies in the system and stress in the transmission sector (Bhattacharyya, 2007). Also lacking is an integrated managerial approach to improving transmission capabilities. The initial focus of policymakers on the addition of generation capacities to meet surging market demand has turned to inadequacy, limited transfer capability, and inefficiencies within the transmission sector, as this has become a major constraint for the Indian Power System to meet the increasing demand. The key challenges faced by the IPTS, identified in the literature are summarized below:

2.1. Absence of strategic planning by the government

Transmission planning is a continual process of identifying the expansion prerequisites of the transmission sector. Growing demand, additions to generation, and the need to strengthen the existing system will ultimately require more transmission capacity (MOP, 2012).

The Central Electricity Authority (CEA) is the nodal planning agency for preparing five-year plans for the power sector. Installed capacity and peak demand of the country, planned by CEA is presented in Table 1 below.

Presently, transmission capacity is insufficient relative to generation capacities and load requirements (Singh, 2013). Growth in transmission capacity was only 27%, compared to 50% growth in generation capacity during the years 2011–2016 as shown in Fig. 3.

According to National Electricity Policy, the power transmission system is considered to be a vital link that must be in place before the addition of any generation capacity (CAC, 2015). The 20-year (2016-36) perspective Transmission Plan Report was prepared in December 2014 by CEA, the Technical wing of the Ministry of Power to bring focus on the transmission sector. This report was amended in January 2016 with more precise inputs on power transmission planning. Transmission planning is done at the central level for ISTS and at the state level for InSTS.

2.2. Low investments in power transmission

Despite investing USD 75 billion in the power sector within the period of the 12th and 13th Five-Year Plans (2012–2022),[1] the funds allocated to the transmission sector are still insufficient. This has resulted in the unavailability of required transmission networks in a number of states (Bhattacharyya, 1994). It has been estimated that at least half of the total investments of the power sector must be made in transmission. The ratio stands at only 30% in India (Singh, 2013). For

[1] A Five-Year Plan in India is premised on the concept of centralized economic planning for effective and balanced utilization of resources. The plans are formulated for every sector in the country.

Table 1
Total installed Generation Capacity and Demand.

Year	Installed Generation Capacity (GW)	Peak Demand (GW)
9th Plan **(1997–2002)**	105	75
10th Plan **(2002–2007)**	132	101
11th Plan **(2007–2012)**	199	130
12th Plan **(2012–2017)**	326	159
13th Plan **(2017–22)**	377	239
14th Plan **(2022–27)**	750	369
15th Plan **(2027–32)**	1047	536
16th Plan **(2032–36)**	1337	720

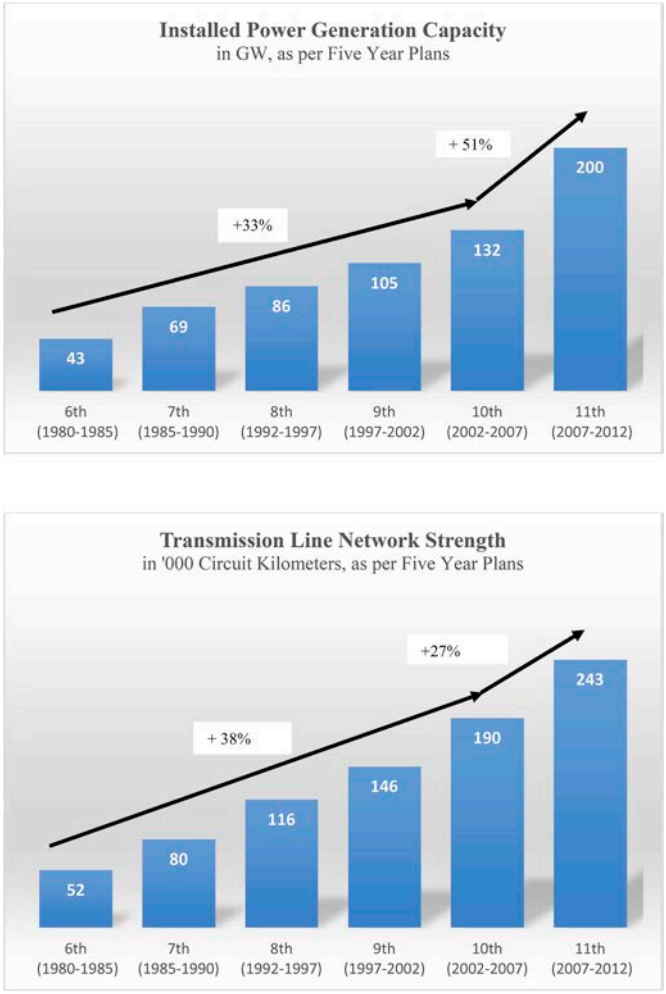

Fig. 3. Comparative Analysis of Generation and Transmission capacities (Source: Planning Commission, 2014).

immediate addition of transmission capacity, financial limitations have been seen as one of the major bottlenecks (Sanghvi, 1991). Resource-rich areas like Chhattisgarh are witnessing substantial industrial development and a surplus of power. However, the transmission infrastructure in the state is still inadequate (Kovendan and Sridharan, 2017).

To add 90,000 circuit-kilometer (ckm) of 220–765 kV lines, substation with a capacity of 154,000 MVA and national grid with a capacity of 27,350 MW are required during the years 2017–2022, and this requirement will increase with increasing demand. Thus, there is an urgent need to invest in the transmission sector so as to add more power evacuation capacity.

2.3. Fewer private players in transmission

In 1991, the government encouraged more participation of private enterprises in the Indian power sector (Singh, 2013). Since then, the generation sector has been de-licensed resulting in continuous generation capacity additions. Policymakers encourage captive production (localized source of power) to increase total generation. Private captive producers were advantaged by the Electricity Act 2003, which opened the generation sector. Therefore, captive producers are able to serve numerous consumers in the bulk market by acting as private generators. Similarly, distribution companies can purchase power from private producers competing with the state utilities (Joseph, 2010). Thus, the private sector has contributed to adding generation (to 35% of the total) as compared to transmission, where policymakers have not focused on private participation (MOP, 2005).

Adding transmission capacity poses a major challenge for IPTS in a de-licensed regime (Bhattacharyya, 2007). As per the 12th Five-Year Plan (2012–2017), the investment required in the transmission sector was estimated at about USD 35 billion. The public utility had planned to provide about USD 19 billion and the remaining USD 16 billion were planned to come from private players (Singh, 2013). However, private participation in the transmission sector constitutes only 3% of the total transmission capacity (CAC, 2015). As a result, to add transmission capacity, funds are mainly gathered from budgetary allocations, internal accruals from public-sector undertakings, and borrowing (Planning Commission, 2014). Competitiveness based on costs and quality of the project decreases due to the lesser participation of private players.

The Indian Power sector faces a shortage of financial resources in the center and state utilities (Gupta and Sarvat, 1998). To attract private sector participation, an initiative was taken in the transmission sector in the year 2000, when the Central Government issued guidelines under joint venture and independent routes. However, the sector has not yet seen much private participation (Planning Commission, 2014).

Fig. 4 depicts the unsteady investments attracted by the Power sector in last 20 years. Investments were mostly attracted during the period when policymakers were viewing the revival of the sector through generation. The entire focus of Public Private Partnership (PPPs) was on power generation, with the transmission and distribution sectors left out.

Policy reforms are necessary to make PPPs successful and ensure that they contribute to the aims of developing the grid, meeting demand, and effectively utilizing generation capacity (Singh, 2013).

2.4. Transmission congestion

According to the Indian Electricity Grid Code 2010, transmission congestion is a situation where the load on transmission network exceeds its available transfer capability (Swami, 2013). In the wake of the de-licensing of generation and the recent surge in power generation, IPTS faces a serious transmission congestion arising from increasing demand, waning networks, and integration of renewable energy into the existing grids (Kumar et al., 2004). Ideal Energy Projects Limited (IEPL) commissioned a 270 MW thermal power plant and Maharashtra state commissioned a 1980 MW Tiroda Generation Plant in May 2013 and June 2013 respectively, without commissioning of the required number of transmission lines (CAC, 2015), resulting in congestion in the existing networks.

In 2014-15, Indian Energy Exchange (IEX) experienced the impact of congestion, which was estimated at 3.1×10^9 kWh loss of electricity (Bahuguna, 2015) as shown in Fig. 5, enough to serve the monthly demand of Delhi or Maharashtra for more than a week.

Congestion and choking lead to power interruptions, outages, and deficits and add to large power losses (Xue and Xiao, 2013). As a result, power demand is not fulfilled even if surplus power is available elsewhere (Bahuguna, 2015). Congestion also limits the capacity of the network and meddles with the efficient power exchange from an arrangement of power transactions (Nappu et al., 2014; Brunekreeft et al., 2005). The current transfer capability of the transmission network ranges between 20 and 30 percent of its total transmission capacity (CAC, 2015).

Most of the states do not purchase power as per the plans of power sourcing due to transmission congestion. This results in deficiency on one system and surplus on another and Also inflates the cost of power, which reached to USD 0.17–0.31 per kWh during summer season (Jai, 2016). There is thus an urgent need to make transmission system robust to mitigate congestion in the transmission network (CAC, 2015; Verma, 2016).

2.5. Transmission losses

The difference between total power generated and total units of power distributed is known as transmission and distribution (T&D) losses and comprised of technical and commercial losses. Technical losses occur due to energy dissipation in the electrical equipment such as conductors, transformers used in transmission lines, sub-transmission lines and distribution lines. Commercial losses occur at the distribution side due to bypassing meters, use of error-prone meters, and errors in meter reading (Bhattacharyya, 1994).

Fig. 6 reveals that power losses in India are higher than those of

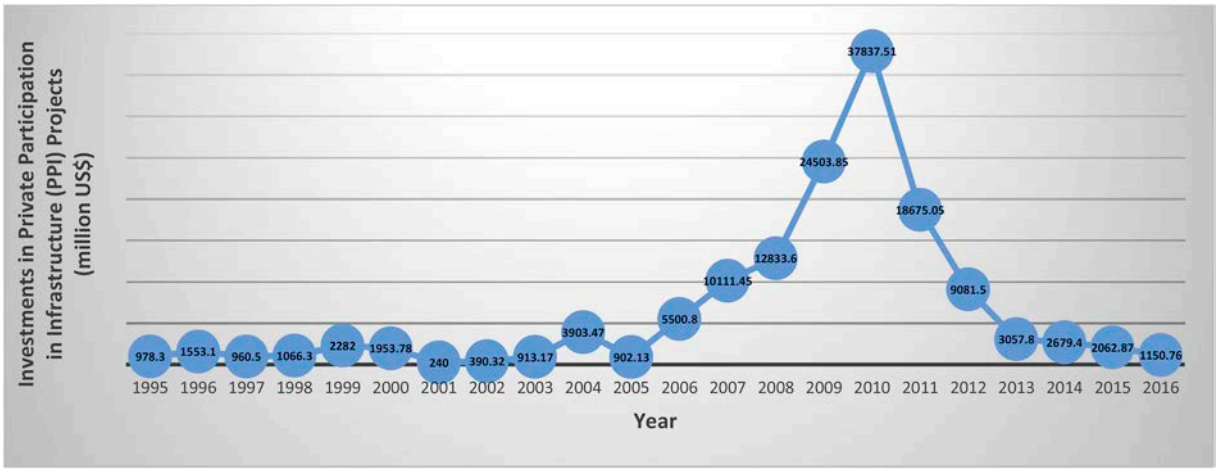

Fig. 4. Public private partnership in power sector in India (source: World Bank, 2016a,b).

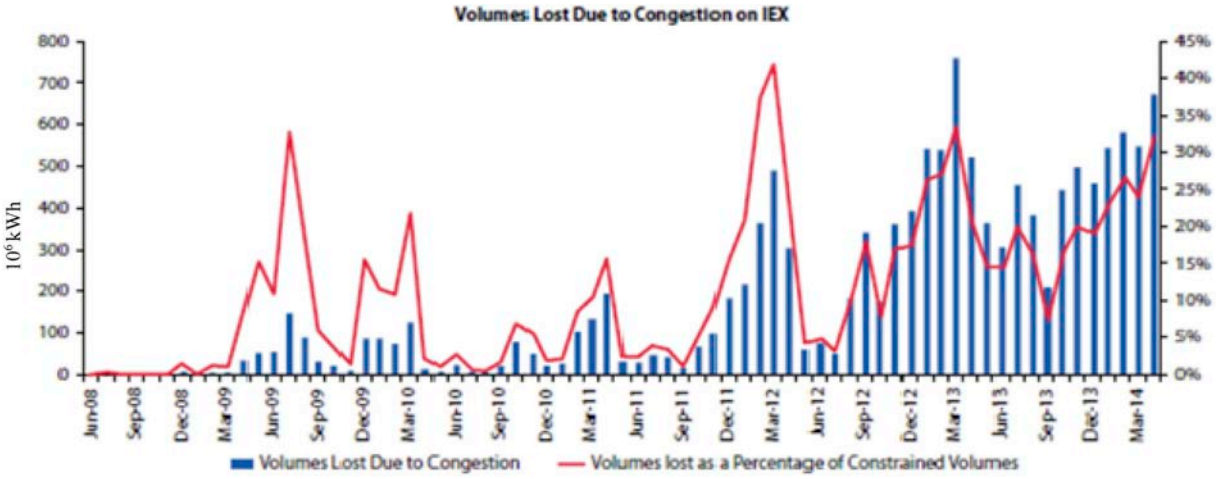

Fig. 5. Total Volume Lost due to congestion on IEX from 2008 to 2014 (Source: IEX, 2014).

other countries, and are estimated to be approximately 21.5% of total power available. Such losses are very high compared to developed countries like the United States, where T&D losses are approximately 6% (Omer et al., 2013). The cost of T&D losses has been estimated to account for 1.5% of the country's annual GDP. Out of these cumulative 21.5% T&D losses, transmission losses are approximately 6% due to highly leaking and aging transmission lines (Sachchidanand, 1999; CEA, 2014).

Aggregate technical and commercial losses in India are estimated at 27% (Planning Commission, 2014). These losses further strain the finances its public electricity providers (Min and Golden, 2014; Omer et al., 2013). For instance, in the country's largest state Uttar Pradesh, it was found that 29% of the power distributed from 1970 to 2010 remained unbilled due to technical losses, irregularities in billing, and theft. Such losses cumulatively estimated to be about 300 million megawatt-hours (MWh). Transmission losses in Uttar Pradesh are continuously increasing since the 1970s despite several policy initiatives and measures to minimize power theft (Min and Golden, 2014).

2.6. Delay in project execution

The Indian transmission system faces serious issues of related to rights of way (ROW), land acquisition, forest clearance, and statutory approvals. ROW is a key reason for the delay in new capacity addition (Rahman and Khan, 2007). The licensees are empowered with ROW according to the Electricity Act 2003. However, it is uncommon to execute transmission projects without any delays due to ROW or land acquisition issues (Omer et al., 2013; Schmidt and Lilliestam, 2015). Due to delays, the gap between the number of planned transmission lines and the number of lines actually achieved is widening (Omer et al., 2013; Singh, 2013). There also are various inherent risks associated with overhead line projects, such as disproportionate allocation of budget to the projects, lack of coordination among key stakeholders, lack of skilled personnel, and inefficiencies in the execution of projects that lead to further delays (Moazzam Jazi et al., 2015).

In 2011, more than 120 transmission projects were delayed as developers failed to get timely approvals. In the same year, the Power Grid Corporation of India (PGCIL) was unable to spend its planned USD 901.88 million for building the transmission lines between states primarily due to land acquisition and ROW problems (Singh, 2013). The list of delayed line and substation projects totals 378 (MOP, 2017a,b) as shown in Table 2.

The Ministry of Power (MoP) has acknowledged ROW as a major issue and emphasized its implications for improving the national grid. In addition, CEA guidelines also emphasize ROW as a key challenge to setting up new transmission lines (Singh, 2013). Fig. 7(a) and 7(b) demonstrates the percentage delay in Transmission Line and Substation projects repectively.

Facing ROW issues, transmission infrastructure developers are

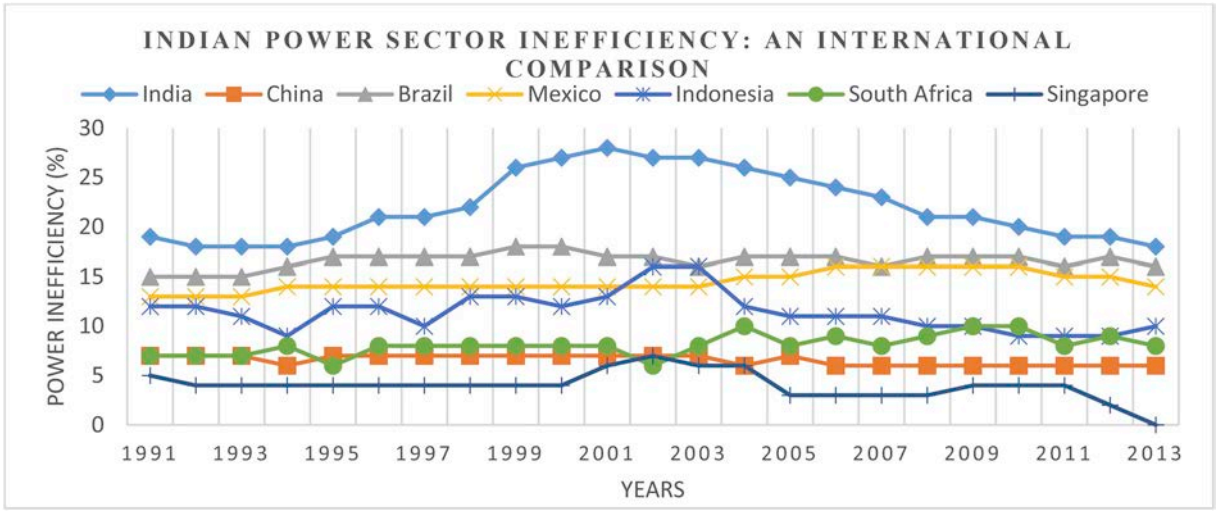

Fig. 6. Power sector inefficiency in terms of Transmission and Distribution (T&D) losses (World Bank, 2016a,b).

Table 2
Delayed transmission line and substation projects.
Source: Ministry of Power, 2017.

Line/ Substation	Total Projects (A)	Commissioned (B)	Reason for delay/stall known (C = D)	At least one of the reasons for delay (D = E+F+G+H+I)				
				RoW (E)	Forest Clearance (F)	Force Majeure (G)	Legal (H)	Other (I)
Delayed								
Transmission Line	552	199	93	52	23	7	11	–
Substation	16	1	2	–	–	2	–	–
Stalled								
Transmission Line	7	N.A.	7	–	–	–	7	–
Substation	2	N.A.	2	–	–	–	2	–

compelled to use alternate routes, leading to an entire revision of the project plan and further escalating the costs and timelines.

For instance, in order to draw power from the Koodankulam Nuclear Power Project (KKNPP), Kerala government has planned to re-route the 310-km-long transmission corridor on the Edamon to Pallikkara stretch; 170 km of this corridor was stalled in view of the absence of ROW clearances (Singh, 2013).

2.7. Failure to upgrade technology

India has an immediate need to upgrade the degree of innovation and technology in the power sector as a whole (Singh, 2013). There is less technological awareness among transmission utilities and low investment in research and development. Technology utilization must be encouraged due to meet demand, electricity rural areas, manage load optimally, and reduce financial and technical inefficiencies (Samantaray, 2014).

Currently, there are no guidelines for the utilization of these technologies. The sector focuses instead on lowering costs through competitive bidding. The standard bidding documents, varying from state to state, allows changes in the route and tower design as per the geography of the region. However, no provisions or policies are available in these bidding documents that allow or incentivize the use of any new technology or construction methods. Table 3 shows the difference in conventional conductor and high performance conductor in constructing a new transmission line.

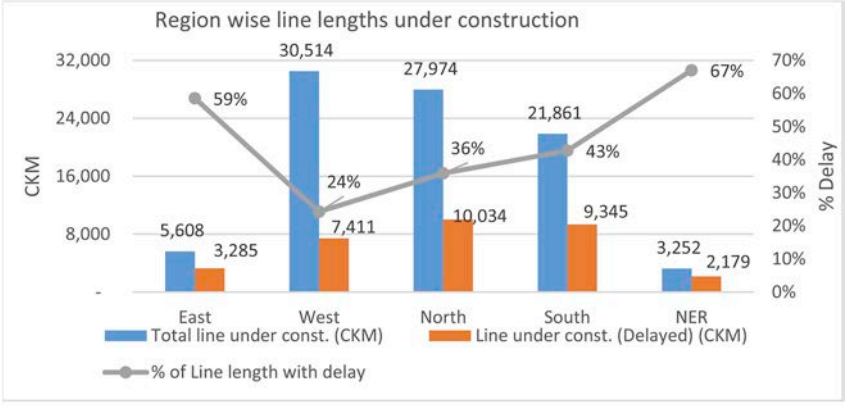

(a)

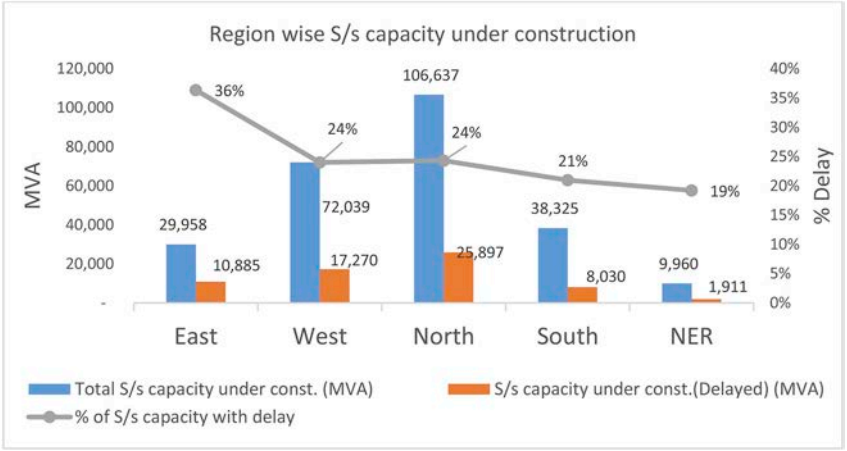

(b)

Fig. 7. (a): Percentage delay in Transmission line projects (Source: MOP, 2017a,b). **(b)**: Percentage delay in Substation projects (Source: MOP, 2017a,b).

Table 3
Conventional Conductor Vs High Performance Conductor for new line.
Source: Singh (2013).

Items	% of project cost	Cost-New *ACSR in USD million	Cost-New *HPC	Differential (%)
Tower Cost	20%	6.764	5.862	−13.3%
Conductor Cost	38%	12.626	37.203	195%
Erection and Foundation	15%	4.96	4.81	−3%
Other costs	27%	8.718	8.267	−5%
Total Cost (100 kM Line)	**100%**	**33.06**	**56.142**	
Transfer Capacity		**3400 MW**	**6800 MW**	**100%**
Cost in USD/MW/kM		**972.38**	**828.229**	**−15%**

*ACSR is Aluminum Conductor Steel Reinforced.
*HPC is High Performance Conductor.

Developers do not have sufficient incentives for innovation and new ways of working. For this reason, policies should focus on output parameters rather than input parameters. The Central Transmission Utility should leverage all prospects for deploying the best technologies in view of optimizing the existing network and provide power to all by 2019 (Singh, 2013).

2.8. Grid instability due to renewable energy

The share of renewable energy is expected to increase in India by 91% from 2017 to 2022 as the share of thermal generation declines. Bringing higher shares of renewable electricity into the existing energy mix is a fundamental concern due to variability (intermittency) in its nature (Kanase-Patil et al., 2010). The integration of cleaner, green, and reliable sources of energy may have a significant impact on the existing transmission system. Renewable energy sources need to be connected to the main grid but cannot support the entire grid by themselves (Banerjee et al., 2013). Operators and planners of the power system are experiencing major bottlenecks in integrating renewable energy sources into power grids (Smiti, 2017). The technical challenges include power quality, power fluctuations, storage issues, protection issues, constraints to accommodate renewable energy system in existing transmission grids, and non-technical issues such as lack of skilled workers (Sandhu and Thakur, 2014). Fig. 8 depicts the share of renewable energy sources per year.

Thus, power generation from renewable energy sources must be integrated into the grid through control measures (CAC, 2015).

2.9. Poor performance and financial health of utilities

The state utilities of India are experiencing heavy financial losses because of their poor financial performances. The key reasons for poor performances are rising debt to equity ratios (from 10:1 to 20:1) charging non-remunerative tariffs to some consumers, poor collection rates, and an increase in input costs (Bhattacharyya, 1994). The debt of the power sector reached USD 75156.89 million in 2013 (Pandey, 2015).

The poor financial health of utilities, requiring subsidization from the government, accounts for about 1.5% of national GDP (Thakur et al., 2004). This is reflected in a large gap between national average generation costs (currently INR 3.50 per kWh) and the average realization from consumers (currently INR 2.50 per kWh), and this gap is increasing (Thakur et al., 2004). These conditions adversely affect the utility's day-to-day performance due to the lack of adequate revenue generation (Schramm, 1993). They also affect the utility's ability to raise capital investment for system improvement. This is reflected in the low investment in the power sector by the states, particularly in the transmission sector.

3. Methodology and data sources

The Decision Making Trial and Evaluation Laboratory (DEMATEL) method has been successfully used to address various management problems by evaluating the cause and effect relationship among a set of factors (Lin, 2013). This methodology provides a visual representation to show the influence of each factor on another. The key benefit of using this modeling approach is that it allows the conversion of a qualitative problem to quantitative diagnosis. Bacudio et al. (2016)

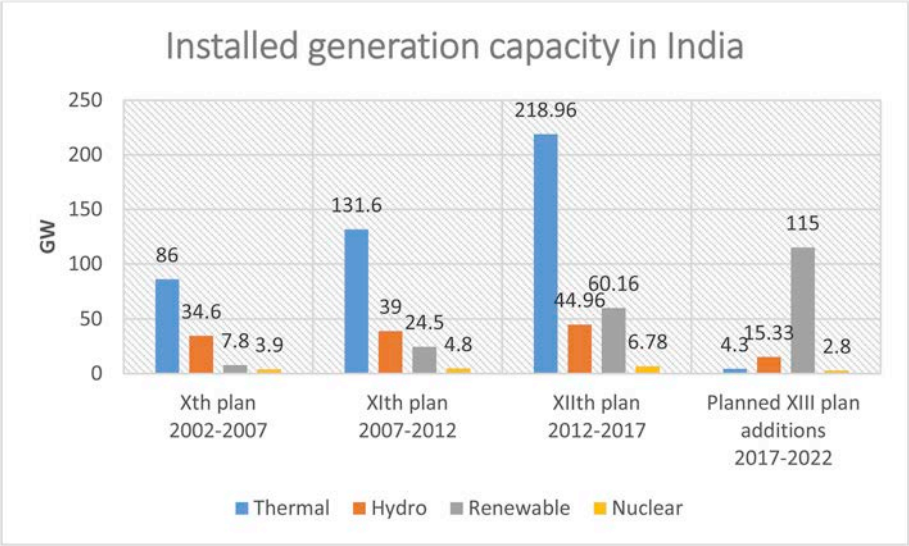

Fig. 8. Share of renewable energy sources per year.

Table 4
Linguistic rating.

Linguistic Grade	Influence Score
No Influence	0
Very Low Influence	1
Low Influence	2
High Influence	3
Very High Influence	4

have implemented DEMATEL to identify the influential factors that impede the evolution of green supply chain management. Similarly, Lee et al. (2011) have analyzed causal factors related to equity investments from a multi-stakeholder perspective. Xia et al. (2015) have analyzed internal factors to improving the productivity of automotive re-manufacturers. The procedures for implementing the DEMATEL methodology here were adopted from Bacudio et al. (2016), Lee et al. (2011), Xia et al. (2015), Ramkumar and Jenamani (2015), Wang et al. (2017), Gigovic et al. (2016) and Debnath et al. (2017). These are outlined as follows:

Step I: Calculation of Initial Average Matrix

In this step, experts were asked to provide their respective opinions on the influence of each factor i on each factor j using DEMATEL scale as provided in Table 4. The matrix of expert opinions is denoted as a_{ij}. Once the expert opinions are gathered an initial average matrix A was formed.

$$A = \begin{bmatrix} a_{11}... & a_{1j}... & a_{1n} \\ a_{i1}... & a_{ij}... & a_{in} \\ a_{n1}... & a_{nj}... & a_{nn} \end{bmatrix}$$

Step II: Calculation of Initial Influence Matrix

The initial average matrix A is normalized to compute the initial influence matrix $X = [x_{ij}]nxn$ using Equation (1). This matrix represents the degree of relationships among various factors existing in the system. The numerical score in the matrix indicates the degree of influence. The normalized matrix is represented as B, where

$$B=[b_{ij}]_{nXn} = \frac{A}{max_{1\le i\le n}\sum_{j=1}^{n} a_{ij}} \quad (1)$$

Step III: Computing the Total Influence Matrix T

The total influence matrix **T** is computed using Equation (2):

$$T=B+B^2 + B^h = B(I-B)^{-1}, \text{when } \lim_{h\to\infty} B^h = [0]_{nXn} \quad (2)$$

I = Identity matrix.B = Normalized overall direct relation matrix.

Step IV: Calculation of prominence and net-cause effect values

Let r_i be the summation of rows of total influence matrix T and s_j be the summation of columns of total influence matrix T such that

$T = [t]_{iXj}$ where, i, j = 1, 2, …, n.

$$r=[r_i]_{nX1} = \left[\sum_{j=1}^{n} t_{ij}\right]_{nX1}$$

$$s=[s_j]_{nX1} = \left[\sum_{j=1}^{n} t_{ij}\right]1Xn, \quad (3)$$

Here, r_i indicates the total of the direct and indirect influence of factor i on the other factors and s_j indicates the total of direct and indirect influence factor j has received from other factors. $(r_i + s_i)$ indicates the total influences provided to or taken by each factor. In other words, it indicates the overall amount of influence each factor has on the given problem. Further, the net effect of each factor on the given problem is indicated by the difference $(r_i - s_i)$. The positive value of $(r_i - s_i)$ prominently indicates the causal nature of the factor, and the negative value of $(r_i - s_i)$ prominently indicates the effect trait of the factor.

Step V: Development of Cause-Effect Diagram

The last step diagrams the structural relationships among factors. The $(r_i + s_i)$ and $(r_i - s_i)$ values are plotted in the graphical diagram, wherein vertical axis represents $(r_i - s_i)$ and horizontal axis represents $(r_i + s_i)$. The entries of the inner dependence matrix are mapped using solid lines representing a two-way significant relationship and broken lines representing a one-way significant relationship.

3.1. Data-collection process

A Multi-Criteria Decision Making (MCDM) approach takes into account the interests of various perspectives in the evaluation of a problem. Fontela and Gabus were the first to apply DEMATEL, an MCDM method in 1971. The methodology uses the opinions of the elite group of identified 'experts' to solve complicated global issues in a subject area (Fontela and Gabus, 1974). One of the advantages of using MCDM techniques is that it includes both quantitative as well as qualitative factors. MCDM techniques like DEMATEL generally do not require a large amount of data (Lin, 2013). Compared to other statistical methods, MCDM techniques are unconstrained by sample size (Tzeng and Huang, 2012; Dehdasht et al., 2017). According to Patton (1990), there exist no strict rules for the sample needed for analysis. The choice depends on the type and purpose of the inquiry and the availability of time and resources. According to Harrison and Qureshi (2000), the sample size is based on selecting representatives from different perspectives. A small sample avoids opinion divergence (Kuo and Lu, 2013). However, the minimum number of respondents should be between three and nine (Büyüközkan, and Güleryüz, 2017; Dehdasht et al., 2017). The literature strongly recommends the involvement of experts when applying the DEMATAL method to managerial and policy problems (Bacudio et al., 2016). See Altuntas and Dereli (2015), Shieh et al. (2010), Hsu and Lee et al. (2014), and Xia et al. (2015).

In this study, we applied the DEMATEL method to address the policy level issues in IPTS. To ensure the overall representation of the transmission sector in this study, the expert panel was constituted from the following stakeholder groups based on their varied knowledge and relevant experience of more than 15 years in the area of policy and decision-making:

a. Transmission EPC group
b. Substation EPC group
c. Power industry association group
d. Power advisors/consultants group
e. Electrical equipment manufacturers group

Out of the 35 experts approached, twenty-one experts agreed to provide their input, which was considered sufficient to conduct the study. Further, expert opinions were sought from the different hierarchies, ranging from managers to the president. This has helped to view diverse perspectives of stakeholders on the interaction and relationship of the identified factors. Table 5 represents the overall composition and characteristics of experts groups participating in this study.

For collecting opinions, as background information, a preliminary set of the perceived factors to improving the transmission system was provided to the experts and explained to them. A structured interview questionnaire was used as a tool to collect data from the experts, where

Table 5
Expert group.

Groups	Name	Affiliation	Age Range	Educational Level	Experience	No. of experts
Expert Group 1	Transmission	1. Central Utilities (2) 2. State Utilities (2) 3. Private Licensee (1)	42–58	Bachelors	≥ 15	5 (24%)
Expert Group 2	Substation	1. Central Utilities (1) 2. State Utilities (2) 3. Private Licensee (1)	42–55	Bachelors	≥ 15	4 (19%)
Expert Group 3	Industry Association	Autonomous	41–56	Masters or above	≥ 20	5 (24%)
Expert Group 4	Power Advisors/Consultants	1. Government Advisory body (2) 2. Private Consultant (2)	45–65	Masters or Above	≥ 20	4 (19%)
Expert Group 5	Electrical Equipment Manufacturers	Private Sector	42–57	Bachelors or above	≥ 15	3 (14%)

Electrical Equipment Manufacturers of experts application to various areasup must be included ng documents etc.).

the response choices were fixed. Further, expert opinions on the interactions and relationship among the factors were sought. Experts were asked to provide grades, as shown in Table 4 to determine interactions among factors. The responses were recorded in groups of 6, 12, 18 and 21. We observed that the opinions of selected experts were not very divergent. In other words, increasing the sample size did not appear to affect the results. Subsequently, the responses provided by the experts were recorded and used for further analysis.

4. Results and discussion

This section provides an outline of our application of the DEMATEL methodology in assessing the challenge to improving the Indian Power Transmission System (IPTS).

***Step* I: Calculation of Initial Average Matrix:** Table 6 presents the resulting Initial Average Matrix (A) that contains the average of expert opinions representing pairwise comparisons among factors in terms of degree of influence.

***Step II:* Calculation of Initial Influence Matrix:** Table 7 shows the normalized matrix of the initial average matrix i.e., total influence matrix (B) of factors calculated using Equation (1).

***Step III:* Computing the Total Influence Matrix (T):** The Total Influence Matrix (T) is calculated using Equation (2) and the results are shown in Table 8.

***Step IV*: Calculation of prominence and net-cause effect values**: Table 9 shows the values of the degree of prominence $(r_i + s_i)$ and net cause/effect $(r_i - s_i)$, which were obtained from Equation (3). In simple terms, $(r_i + s_i)$ indicates the relative importance of each factor and $(r_i - s_i)$ demonstrates the net effect contributed by each factor on the problem. Here, r_i represents the total direct as well as indirect influence of factor i on other factors and s_i represents the total direct as well as indirect influence received by factor i from other factors.

Table 6
Initial average matrix.

Factors	B1	B2	B3	B4	B5	B6	B7	B8	B9
Absence of strategic planning by Govt (B1)	0.0	3.7	3.3	2.6	1.8	0.9	3.8	0.9	1.9
Low investments in Power Transmission (B2)	0.0	0.0	1.4	3.8	1.9	0.7	0.0	0.6	1.8
Fewer private players in Transmission (B3)	0.0	1.3	0.0	3.5	2.7	1.5	0.0	0.8	2.0
Transmission congestion (B4)	0.0	0.0	0.0	0.0	3.7	1.6	0.0	1.1	1.6
Transmission Losses (B5)	0.0	0.0	0.0	0.0	0.0	2.7	0.0	1.5	1.9
Failure to Upgrade Technology (B6)	0.0	0.0	0.0	0.0	0.0	0.0	0.0	3.0	0.0
Delay in project execution (B7)	0.0	0.0	0.0	3.8	2.6	1.3	0.0	1.3	1.8
Grid instability due to Renewable Energy (B8)	0.0	0.0	0.0	0.0	0.0	0.0	0.0	0.0	0.0
Poor performance and financial health of Utilities (B9)	0.0	0.0	0.0	0.0	0.0	0.0	0.0	3.3	0.0

Table 7
Initial influence matrix.

	B1	B2	B3	B4	B5	B6	B7	B8	B9
B1	0.00	0.20	0.17	0.14	0.10	0.05	0.20	0.05	0.10
B2	0.00	0.00	0.07	0.20	0.10	0.04	0.00	0.03	0.10
B3	0.00	0.07	0.00	0.19	0.14	0.08	0.00	0.04	0.11
B4	0.00	0.00	0.00	0.00	0.20	0.08	0.00	0.06	0.08
B5	0.00	0.00	0.00	0.00	0.00	0.14	0.00	0.08	0.10
B6	0.00	0.00	0.00	0.00	0.00	0.00	0.00	0.16	0.00
B7	0.00	0.00	0.00	0.20	0.14	0.07	0.00	0.07	0.10
B8	0.00	0.00	0.00	0.00	0.00	0.00	0.00	0.00	0.00
B9	0.00	0.00	0.00	0.00	0.00	0.00	0.00	0.18	0.00

Table 8
Total influence matrix.

	B1	B2	B3	B4	B5	B6	B7	B8	B9
B1	0.00	0.21	0.18	0.26	0.23	0.14	0.20	0.17	0.20
B2	0.00	0.00	0.07	0.21	0.15	0.09	0.00	0.10	0.14
B3	0.00	0.07	0.00	0.20	0.19	0.13	0.00	0.12	0.15
B4	0.00	0.00	0.00	0.00	0.20	0.11	0.00	0.11	0.10
B5	0.00	0.00	0.00	0.00	0.00	0.14	0.00	0.12	0.10
B6	0.00	0.00	0.00	0.00	0.00	0.00	0.00	0.16	0.00
B7	0.00	0.00	0.00	0.20	0.18	0.11	0.00	0.14	0.13
B8	0.00	0.00	0.00	0.00	0.00	0.00	0.00	0.00	0.00
B9	0.00	0.00	0.00	0.00	0.00	0.00	0.00	0.18	0.00

Fig. 9 shows the prominence value $(r_i + s_i)$ of each factor, organized in decreasing order. Fig. 10 on the other hand, shows the net cause/effect value (R − S) of each factor. A factor with $(r_i - s_i) > 0$ is classified as a cause factor whereas factor with $(r_i - s_i) < 0$ is classified as an effect factor.

Based on the results reported in Fig. 10, "Absence of strategic planning (B1)", "Low investments in Power Transmission (B2)", "Fewer private players (B3)", and "Delays in project execution (B7)" are classified as causal factors. "Absence of strategic planning (B1)", was ranked highest among all factors. This confirms that planning for IPTS is essential to conducting a current assessment, providing a clear visualization of the future, and taking concrete action. Improper planning has a direct impact on costs and timelines. In short, the absence of strategic planning may hinder the evolution of the transmission system. Lack of adequate investments in the IPTS sector (B2) is one of the key hindrances to strengthening and upgrading the transmission infrastructure. The investment deficit has handicapped the sector. Another area of concern is delays in project execution and completion (B7) due to right-of-way issues.

Five factors are identified as "effect" factors. These include "Transmission congestion (B4)", "Transmission losses (B5)", "Failure to

Table 9
Degree of prominence ($r_i + s_i$) and net cause/effect ($r_i - s_i$).

Factors	r_i (Total direct and indirect influence of Factor i on other Factors)	s_i (Total direct and indirect influence Factor i has received from other Factors	$r_i + s_i$ (Degree of Prominence)	$r_i - s_i$(Net cause/effect)
B1	1.59	0.00	1.59	1.59
B2	0.77	0.29	1.05	0.48
B3	0.86	0.26	1.12	0.61
B4	0.52	0.88	1.40	−0.36
B5	0.36	0.95	1.31	−0.59
B6	0.16	0.71	0.87	−0.55
B7	0.76	0.20	0.96	0.56
B8	0.00	1.10	1.10	−1.10
B9	0.18	0.83	1.01	−0.65

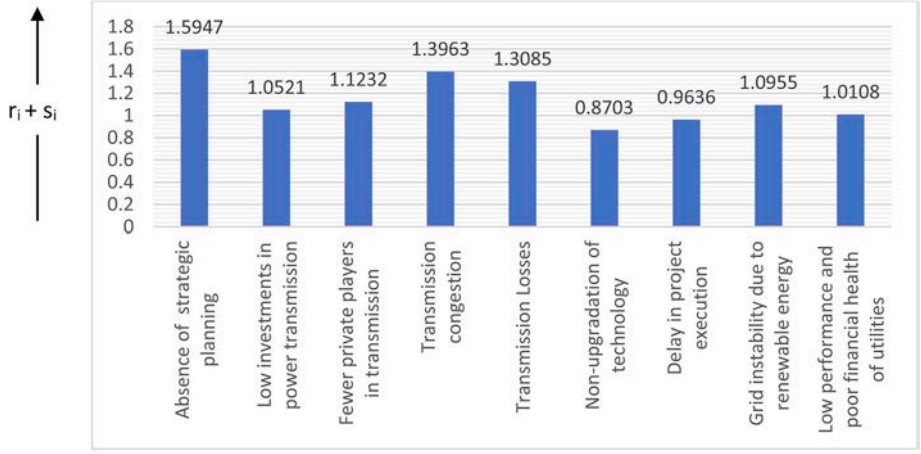

Fig. 9. Prominence graph.

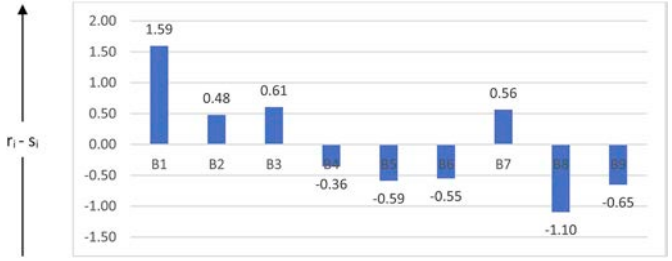

Fig. 10. Net cause/effect graph. Note: Positive value of ($r_i - s_i$) for Factor i indicates that Factor i affects other Factors and negative value of ($r_i - s_i$) for Factor i indicates that Factor i is influenced by other Factors.

Table 10
Inner dependence matrix.

	B1	B2	B3	B4	B5	B6	B7	B8	B9
B1		0.21	0.18	0.26	0.23	0.14	0.20	0.17	0.20
B2			0.07	0.21	0.15	0.09		0.10	0.14
B3		0.07		0.20	0.19	0.13		0.12	0.15
B4					0.20	0.11		0.11	0.10
B5						0.14		0.12	0.10
B6								0.16	
B7				0.20	0.18	0.11		0.14	0.13
B8									
B9								0.18	

upgrade technology (B6)", "Grid instability due to Renewable Energy (B8)", and "Poor performance and financial health of utilities (B9)". These factors are influenced by the causal factors, which lower the overall performance of the transmission system. Among the effect factors, "Grid instability due to renewable energy (B8) is the least priority concern for the policymakers while eliminating factors as it has the lowest R-S value of −1.10.

While generating the Inner dependency matrix, only factors with higher prominence are considered. The factor with the highest prominence is "Absence of strategic planning (B1)" with r+s value 1.5947. The entries in the Total Influence Matrix (T) is aggregated by taking their average to compute the threshold value. Thus, the inner dependency matrix is derived from the total influence matrix by eliminating entries having values that are lower than the threshold value. In this study, the threshold value is calculated to be 0.064 and accordingly Inner dependency matrix is formed as shown in Table 10. The significance of the inner dependence matrix is that it only retains the substantial relationships. Based on the table, "Absence of strategic planning (B1)" has significant relationships with all other factors and has the highest influence on "Transmission congestion (B4)" with a value of 0.26. This suggests that inadequate planning can lead to significant delays in transmission capacity addition and upgrades to the network leading to transmission congestion. "Failure to upgrade technology (B6)" only has a significant relationship with "Grid instability due to renewable energy (B8)". This can be attributed to the fact that to integrate renewable energy into the conventional grid requires new and upgraded technologies. Among all factors, B8 is the only factor that does not appear to cause any other factors. Hence, policymakers may give it the lowest priority factor.

Fig. 11 shows the overall prominence-causal relationship (PCR) diagram that was generated to indicate general patterns and a significant relationship among factors. In this cause-effect diagram, the causal factors are in the upper half of the diagram while the effect factors lie in the lower half. The factors with the highest correlation are at the rightmost side of the PCR diagram whereas the factor with the lowest correlation lies at the leftmost side of the PCR diagram. The key

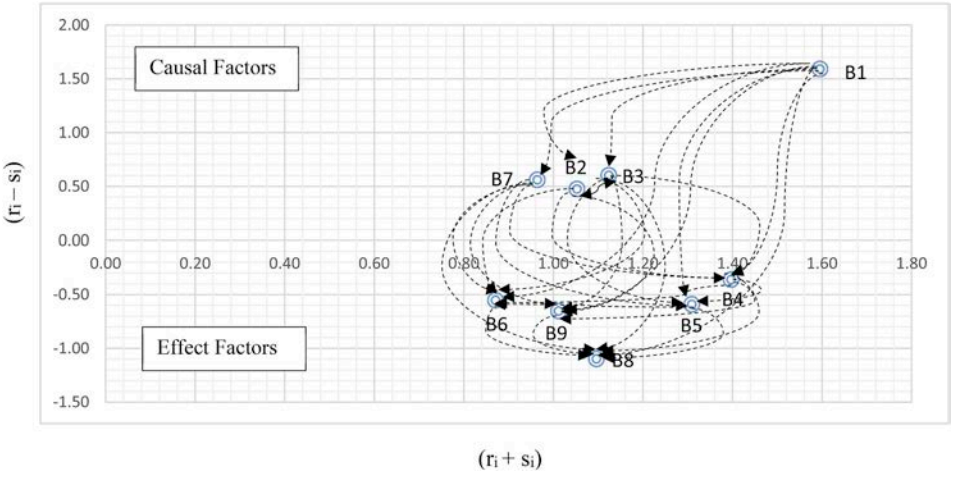

Fig. 11. Prominence–causal relationship diagram- DEMATEL. *Note: The prominence-causal relationship diagram categorizes the Factors of IPTS into causal Factors and effect Factors. Factors that have positive (r_i - s_i) are categorized as a 'causal Factors'. Such Factors also have higher (r_i + s_i) indicating higher relative importance that impacts the whole system. Factors that have negative (r_i - s_i) are categorized as 'effect Factors'. Dotted lines in the diagram indicate uni-directional relationship and bold line indicates bidirectional relationship.
Causal Factors (upper half): B1 (Absence of strategic planning by Government): B2 (Low investments in Power Transmissions): B3 (Fewer private players in Transmission): B7 (Delays in project execution).
Effect Factors (lower half): B4 (Transmission congestion): B5 (Transmission Losses): B6 (Failure to Upgrade Technology): B8 (Grid instability due to Renewable Energy): B9 (Poor performance and financial health of Utilities).
Primary causal Factor: B1 (Absence of strategic planning by Government): Most correlated Factor: B1 (Absence of strategic planning by Government).

causal factor is located at the top and the least influencing factor located at the bottom. Entries in Inner dependence matrix with a higher value than the threshold value are plotted while generating PCR diagram. The arrows show the inter-relationship among factors of IPTS system, where the solid arrow indicates a bi-directional relationship and dotted arrow indicate a unidirectional relationship. Most of the factors exhibit unidirectional relationships except "Low investments in power transmission (B2)" and "Fewer private players (B3)", which are exhibiting bi-directional relationship. "Absence of strategic planning (B1)" located at the uppermost of the PCR diagram is considered as the fundamental causal factor of IPTS system. This implies that adequate strategic planning by policymakers of the transmission sector will significantly influence other factors and the system as a whole. Policymakers should create procedures and policies to positively support the IPTS. Appropriate allocation of funds and private player participation are also considered necessary to an improved IPTS system. Streamlined processes from improved planning may also help address the delays in project execution and facilitate the integration of power generated from renewable resources in the transmission network. The results further suggest that targeting other factors may not significantly impact "Absence of strategic planning (B1)". These results confirm that a key focus must be given to strategic planning that impacts all other factors to improving IPTS.

5. Conclusion and policy implications

The IPTS is experiencing a revolutionary transformation from a conventional centralized grid to a more consumer interactive grid. If serious and timely reforms addressing the transmission system are not undertaken, the country may experience cascading risks on the power sector and the economy as a whole. A robust IPTS is needed to ensure "24X7 Power to all". We identified key challenges to the development of IPTS and applied DEMATEL in categorizing causal factor and effect factors to IPTS improvement. Accordingly, "Absence of strategic planning" emerged out as the primary causal factor.

These findings indicate that more policy interventions are needed. In the recent past, policymakers initiated various steps toward increasing power generation capacity (including from renewable resources), expanding privatization and competition, and encouraging the use of new technologies. However, these measures have not addressed the problems of power system because of the skewed focus on generation, which has resulted in relatively low transmission investments by the government. Certainly, policy reforms that enable adequate and timely investment can act as a key catalyst to increase the transmission capacity. A first step to revitalizing the sector is to augment transmission capacity ahead of generation capacity. These investments can be further supported by synchronizing the policy framework with the new reality of private player participation. Policies can be framed to provide equal stature to the experienced private players when awarding and executing power transmission projects. A well-coordinated regulatory framework should also be designed to align central and state government planning within the sector to facilitate interstate links.

During the planning stage, policymakers should involve all stakeholders from the various sectors of the economy. India should establish a nodal agency whose key function is the coordination with stakeholders to improve the understanding of overall power requirements as well as coordinate monitoring and planning. The nodal agency would also facilitate the collation and dissemination of the information on state-level power transmission infrastructure and investment needs. It would serve as a single authoritative system, where generation, transmission, and distribution sectors would integrate.

Optimal project planning could accelerate the development of the transmission sector. The formation of an empowered panel for advanced approvals and spot decisions could boost the progress of the sector. Human resource development, skills training, research and development, and technology adoption can also be encouraged. All stakeholders (such as manufacturers, policymakers, contractors, financial agencies, consumers, and the central and state utilities) must contribute long-term effort to improving the system.

The landscape of power transmission in India is expected to change at a fast pace. The entire power sector in India and its ability to meet growing demand depends on a robust and sustainable transmission network. Our findings recommend policy interventions to ensure adequate strategic planning and infrastructure investment in the transmission sector.

Appendix

1. Structure of Indian Power Transmission System

1.1. The Inter-State Transmission System (ISTS) serves the following purpose:

a. Power evacuation from inter-state generation stations which have beneficiaries in more than one state.
b. Delivery of power from inter-state generation stations up to the delivery point of the state grid.

c. Transfer of operational surpluses from surplus state(s) to deficit state(s) or from surplus region(s) to deficit region(s).
d. Economic dispatch and procurement of power as a competition enabler.

1.2. The Intra-State Transmission System (InSTS) serves the following purpose:

a. Evacuation of power from the generating stations having beneficiaries in that State.
b. Delivery of power within the State from ISTS boundary up to the various substations of the state grid network.
c. Transmission within the state grid for delivery of power to the load centers within the state.

2. Types of Open Access (OA) in Indian Power Transmission System

Open Access (OA) is further categorized according to the location of the buyer and seller:

1. Inter-State Open Access: In this case, the buyer and seller are located in different states and thus follow CERC regulations. It is further divided into three categories:
   a. Short Term Open Access (STOA): OA is permitted for the duration of less than one month.
   b. Medium Term Open Access (MTOA): OA is permitted for the duration of 3 months to 3 years.
   c. Long Term Open Access (LTOA): OA is permitted for the duration of 12 years–25 years.

Intra State Open Access: In this case, buyer and seller belong to the same state and thus, SERC regulations are followed. It is also categorized into STOA, MTOA, and LTOA as per the duration for which OA is permitted.

3. Recent examples of the impact of power transmission sectoral inefficiencies.

- In 2015, the state of Karnataka in India, required about 185×10^6 kWh of electricity a day, but only 135×10^6 kWh were available. The demand-supply situation also could not be bridged owing to a weak monsoon. Due to unavailability of transmission corridors, the states like Karnataka remains a power deficit region (Krishnan, 2015).
- Another resource-rich Indian state Chhattisgarh had expected power generation capacity in excess of 30,000 MW by the end of the fiscal year (FY) 2017 with the state peak demand of only 3300 MW, whereas, transmission capacity to evacuate power was only 7000 MW (IBEF Report 2013).
- Till FY 2016, there was no transmission corridor available in WR-SR, ER - SR and ER – WR route in advance basis for STOA and MTOA for import of power from the grid (CEA, 2016). North-East Route (NER) states of the country are also facing congestion during winter months.

The developments in IPTS are generally at the central level, whereas state-level developments still require due focus. There are instances wherein the available power at ISTS is not being transmitted at InSTS due to the unavailability of the transmission corridor (Gupta et al., 2012).

Appendix A. Supplementary data

Supplementary data to this article can be found online at https://doi.org/10.1016/j.jup.2018.10.002.

References

Altuntas, S., Dereli, T., 2015. A novel approach based on DEMATEL method and patent citation analysis for prioritizing a portfolio of investment projects. Expert Syst. Appl. 42 (3), 1003–1012.

Bacudio, L.R., Benjamin, M.F.D., Eusebio, R.C.P., Holaysan, S.A.K., Promentilla, M.A.B., Yu, K.D.S., Aviso, K.B., 2016. Analyzing challenges to implementing industrial symbiosis networks using DEMATEL. Sustain. Prod. Consum. 7, 57–65.

Bahuguna, K., 2015. India loses 3.1 billion units of electricity to transmission congestion in 2014-15, June 2015. Retrieved from. http://economictimes.indiatimes.com/industry/energy/power/india-loses-3-1-billion-units-of-electricity-to-transmission-congestion-in-2014-15/articleshow/47880267.cms.

Banerjee, S., Meshram, A., Swamy, N.K., 2013. Integration of renewable energy sources in smart grid. Int. J. Sci. Res. 4 (3), 247–250.

Bhattacharyya, S.C., 2007. Sustainability of power sector reform in India: what does recent experience suggest? J. Clean. Prod. 15, 235–246.

Bhattacharyya, S.C., 1994. An overview of problems and prospects for the Indian power sector. Energy 19 (7), 795–803.

Brunekreeft, G., Neuhoff, K., Newbery, D., 2005. Electricity transmission: an overview of the current debate. Util. Pol. 13 (2), 73–93.

Büyüközkan, G., Güleryüz, S., 2017. Evaluation of Renewable Energy Resources in Turkey using an integrated MCDM approach with linguistic interval fuzzy preference relations. Energy 123, 149–163.

CAC, 2015. Report on CAC sub-committee on congestion transmission, June 2015. Retrieved from. cercind.gov.in.

CEA, 2014. Report (Part-A) on national transmission plan for 2021-22, 29th August, 2014. Retrieved from. cea.nic.in/reports.

CEA, 2016. Report (Part-A) on advance national transmission plan for 2021-22, 29th February, 2016. Retrieved from. cea.nic.in/reports.

CEA, 2017. Growth of electricity sector in India from 1947-2017, may 2017. Retrieved from. http://www.cea.nic.in/reports/others/planning/pdm/growth_2017.pdf.

Daruka, 2015. Changing the rules of indian power sector: empowering economy, PWC. Retrieved from. www.pwc.in.

Debnath, A., Roy, J., Kar, S., Zavadskas, E.K., Antucheviciene, J., 2017. A hybrid MCDM approach for strategic project portfolio selection of agro by-products. Sustainability 9 (8), 1302.

Dehdasht, G., Mohamad Zin, R., Ferwati, M.S., Mohammed Abdullahi, M.A., Keyvanfar, A., McCaffer, R., 2017. DEMATEL-ANP risk assessment in oil and gas construction projects. Sustainability 9 (8), 1420.

Fontela, E., Gabus, A., 1974. DEMATEL, innovative methods (2), 67–69 (Report).

Gigović, L., Pamučar, D., Bajić, Z., Milićević, M., 2016. The combination of expert judgment and GIS-MAIRCA analysis for the selection of sites for ammunition depots. Sustainability 8 (4), 372.

Gupta, J.P., Sravat, A.K., 1998. Development and project financing of private power projects in developing countries: a case study of India. Int. J. Proj. Manag. 16 (2), 99–105.

Gupta, N., Shekhar, R., Kalra, P.K., 2012. Congestion management based roulette wheel simulation for optimal capacity selection: probabilistic Transmission expansion planning. Int. J. Electr. Power Energy Syst. 43 (1), 1259–1266.

Harrison, S.R., Qureshi, M.E., 2000. February). Choice of stakeholder groups and members in multi-criteria decision models. In Nat. Resour. Forum 24 (1), 11–19.

Hsu, C.C., Lee, Y.S., 2014. Exploring the critical factors influencing the quality of blog interfaces using the decision-making trial and evaluation laboratory (DEMATEL) method. Behav. Inf. Technol. 33 (2), 184–194.

IBEF, 2013. Power Sector in India- Solar. Renewable & Wind Energy Sectors Retrieved from. http://www.ibef.org/industry/power-sector-india.aspx.

IEX, 2014. Indian Power Market: journey so far and way forward. Retrieved from. https://www.iexindia.com/Uploads/Reports/14_01_2015IEX_India_IPM_Report.pdf.

Jai, S., 2016. One nation, one grid & now, one price. Retrieved from. http://www.business-standard.com/article/economy-policy/one-nation-one-grid-now-one-price-116010100010_1.html.

Joseph, K.L., 2010. The politics of power: electricity reform in India. Energy Pol. 38 (1), 503–511.

Kanase-Patil, A.B., Saini, R.P., Sharma, M.P., 2010. Integrated renewable energy systems for off grid rural electrification of remote area. Renew. Energy 35 (6), 1342–1349.

Kovendan, A.K.P., Sridharan, D., 2017. Development of smart grid system in India: a survey. In: Proceedings of the International Conference on Nano-electronics, Circuits & Communication Systems. Springer, Singapore, pp. 275–285.

Krishnan, R., 2015, September 28. Karnatka's Problems Get Worse. Business Standard Retrieved from. http://www.business-standard.com/article/economy-policy/karnataka-s-power-problems-get-worse-115092801288_1.html.

Kumar, A., Srivastava, S.C., Singh, S.N., 2004. A zonal congestion management approach using real and reactive power rescheduling. IEEE Trans. Power Syst. 19 (1), 554–562.

Kuo, Y.C., Lu, S.T., 2013. Using fuzzy multiple criteria decision making approach to enhance risk assessment for metropolitan construction projects. Int. J. Proj. Manag. 31 (4), 602–614.

Lee, W.S., Huang, A.Y., Chang, Y.Y., Cheng, C.M., 2011. Analysis of decision making factors for equity investment by DEMATEL and Analytic Network Process. Expert Syst. Appl. 38 (7), 8375–8383.

Lin, R.J., 2013. Using fuzzy DEMATEL to evaluate the green supply chain management practices. J. Clean. Prod. 40, 32–39.

Min, B., Golden, M., 2014. Electoral cycles in electricity losses in India. Energy Pol. 65, 619–625.

Moazzam Jazi, Z., Maryam, H., Esmaeilian, G., 2015. Identification, assessment and ranking risks of overhead power lines projects using TOPSIS method. Eur. J. Acad.

Essay 1 (12), 1–7.
MOP, 2005. National Electricity Policy. Ministry of Power (MOP), Government of India, New Delhi, India 2005 (available on. www.powermin.nic.in.
MOP, 2012. National Electricity Policy. Ministry of Power (MOP), Government of India, New Delhi, India 2012 (available on. www.powermin.nic.in.
MOP, 2017a. Transmission app for real time monitoring and growth: Ministry of power (MOP). 2017 (available on. http://www.tarang.website/home.
MOP, 2017b. Growth in Transmission Sector: Ministry of Power (MOP). Government of India 2017 (available on. www.powermin.nic.in.
MOP, 2018. Growth in Transmission Sector: Ministry of Power (MOP). Government of India 2018 (available on. www.powermin.nic.in.
Nappu, M.B., Arief, A., Bansal, R.C., 2014. Transmission management for congested power system: a review of concepts, technical challenges and development of a new methodology. Renew. Sustain. Energy Rev. 38, 572–580.
Omer, A., Ghosh, S., Kaushik, R., 2013. Indian power system: issues and opportunities. Int. J. Adv. Res. Electr. Electron. Instrum. Eng. 2 (3), 1089–1094.
Pandey, 2015. India's Power Sector Suffered Loss of INR 2.9 Lakh Crore in 2013. World Bank Retrieved from. www.downtoearth.org.in.
Patton, M.G., 1990. Qualitative Evaluation and Research Methods, second ed. Sage Publications, Newbury Park, USA.
Planning Commission, 2014. Annual report on working of state power utilities & electricity departments. Retrieved from. planningcommission.gov.in/reports/genrep/rep_arpower1305.pdf.
Rahman, H., Khan, B.H., 2007. Power upgrading of transmission line by combining AC–DC transmission. Power Syst. IEEE Trans. 22 (1), 459–466.
Ramkumar, M., Jenamani, M., 2015. Sustainability in supply chain through E-procurement—an assessment framework based on DANP and liberatore score. IEEE Syst. J. 9 (4), 1554–1564.
Sachchidanand, 1999. Automation in Power Distribution. Indian Institute of Technology Kanpur Retrieved from. http://www.iitk.ac.in/infocell/Archive/dirmar1/power_distribution.html.
Samantaray, S.R., 2014. Letter to the editor: smart grid initiatives in India. Elec. Power Compon. Syst. 42 (3–4), 262–266.
Sandhu, M., Thakur, T., 2014. Issues, challenges, causes, impacts and utilization of renewable energy sources - grid integration. Int. J. Eng. Res. Appl. 4 (3), 636–643.
Sanghvi, A.P., 1991. Power shortages in developing countries: impacts and policy implications. Energy Pol. 19 (5), 425–440.
Sasi, A., 2015, September 9. Power Transmission: a Towering Problem. The Indian Express Retrieved from. http://indianexpress.com/article/india/india-others/power-Transmission-a-towering-problem/.
Schmidt, P., Lilliestam, J., 2015. Reducing or fostering public opposition? A critical reflection on the neutrality of pan-European cost–benefit analysis in electricity transmission planning. Energy Res. Soc. Sci. 10, 114–122.
Schramm, G., 1993. Issues and problems in the power sectors of developing countries. Energy Pol. 735–747.
Smiti, 2017. Germany to help India with grid integration of renewable energy 8th september, 2017. Retrieved from. https://cleantechnica.com/2017/09/08/germany-help-india-grid-integration-renewable-energy/.
Sharma, D.P., Nair, P.S.C., Balasubramanian, R., 2005. Performance of Indian power sector during a decade under restructuring: a critique. Energy Pol. 33, 563–576.
Shieh, J.I., Wu, H.H., Huang, K.K., 2010. A DEMATEL method in identifying key success factors of hospital service quality. Knowl. Base Syst. 23 (3), 277–282.
Shukla, U.K., Thampy, A., 2011. Analysis of competition and market power in the wholesale electricity market in India. Energy Pol. 39 (5), 2699–2710.
Singh, 2013. Power transmission the real bottleneck, FICCI. Retrieved from. ficci.in/spdocument/20311/power-Transmission-report_270913.pdf.
Singh, A., 2006. Power sector reform in India: current issues and prospects. Energy Pol. 34 (16), 2480–2490.
Sinha, A., Neogi, S., Lahiri, R.N., Chowdhury, S., Chowdhury, S.P., Chakraborty, N., 2011, July. Smart grid initiative for power distribution utility in India. In: Power and Energy Society General Meeting, 2011 IEEE. IEEE, pp. 1–8.
Swami, A., 2013. Transmission congestion impacts on electricity market: an overview. Int. J. Emerg. Technol. Adv. Eng. 3 (8), 460–462.
Thakur, T., Deshmukh, S.G., Kaushik, S.C., Kulshrestha, M., 2005. Impact assessment of the electricity act 2003 on the indian power sector. Energy Pol. 33 (9), 1187–1198.
Thakur, T., Kaushik, S.C., Deshmukh, S.G., Tripathi, S.C., 2004. April). Indian electricity act 2003: implications for the generation, transmission and distribution sectors. In: Electric Utility Deregulation, Restructuring and Power Technologies, 2004.(DRPT 2004). Proceedings of the 2004 IEEE International Conference on, vol. 1. IEEE, pp. 54–58.
Tzeng, G.H., Huang, C.Y., 2012. Combined DEMATEL technique with hybrid MCDM methods for creating the aspired intelligent global manufacturing & logistics systems. Ann. Oper. Res. 197 (1), 159–190.
Verma, R., 2016. Analysis of electricity transmission congestion management in India with reference to IEX. Int. J. All Res. Educ. Sci. Meth. 4 (6), 6–13.
Wang, W., Tian, Y., Zhu, Q., Zhong, Y., 2017. Barriers for household e-waste collection in China: perspectives from formal collecting enterprises in Liaoning Province. J. Clean. Prod. 153, 299–308.
World Bank, 2016a. Private participation in infrastructure database. Retrieved from https://ppi.worldbank.org/ .
World Bank, 2016b. Power sector inefficiency. Retrieved from. http://data.worldbank.org.
Xia, X., Govindan, K., Zhu, Q., 2015. Analyzing internal barrier for automotive parts remanufacturers in China using grey-DEMATEL approach. J. Clean. Prod. 87, 811–825.
Xue, Y., Xiao, S., 2013. Generalized congestion of power systems: insights from the massive blackouts in India. J. Mod. Power Syst. Clean Energy 1 (2), 91–100.

Modified Algorithm for Fault Detection on AC Electrical Traction Line: An Indian Climate Case Study

Devender Kumar Saini, *Member, IEEE*, Ravikumaran Nair, Monika Yadav, *Member, IEEE*, and Rajendra Prasad

***Abstract*— Almost all the developing countries are electrifying more and more rail routes with high-voltage ac electric power, mostly with 25 kV, 50 Hz, or 60 Hz. However, electrified nonsuburban areas of tracks are prone to the risk of railway systems' reliability. Deviation of 1 km in the informed fault location from the actual shall consume 40–50 min in excess to clear those faults off. This paper made intensive study at the sampling region in India revealed that the variation happened in the parasite capacitance is primarily responsible for the erratic pinpointing of the persisting earth fault position on the electrified railway system. The experimental studies conducted with the help of table top as well as prototype models of high-voltage ac traction lines for the identification and quantification of those vulnerabilities causing the changes in the parasite capacitance on ac electric traction system and the subsequent remodeling of it are detailed in this paper. Furthermore, this paper suggests the feasible algorithm to mitigate railways' risk in pinpointing the persisting earth fault on high-voltage ac power traction lines with the dynamically modeled high-voltage ac electric railway traction line. The proposed algorithm has been tested on trial basis after approval from Indian Railways.**

***Index Terms*— Capacitance, electric variables, fault location, rail transportation power systems, rail transportation reliability.**

I. Introduction

IN THE context of developing countries, electric traction power networks act as the booster of the rail transportation system. The statistics [1] on the electrified rail routes of various countries substantiate it. India has already electrified 44 950-km railway track out of 115 000 km and continues to electrify 3000 km of railway tracks in every year.

Evidently, in India, railway traffic dealt on electrified routes is around 68% of the total, whereas the length of the electrified track is only 35% of the total [2]. Unlike highways, rail routes are mostly laid on countrysides, where topographical features like tunnels, earth excavated portion to lay tracks (termed as earth cuttings) is available abundant in the vicinity of railway track. In such areas, the electric traction lines (bare conductors) erected over railway track would be very close to earth potential; hence, the chances of occurring earth faults are also very high. Such vulnerabilities will affect the reliability of the electrified railway system to a large extent. A small interruption in electric traction supply will cause the total stalling of train services at those regions. Its impact on monetary terms would be very huge if the electric traction supply interruption period is longer. Obviously, traffic interruption in electrified rail routes can give enormous setback on the gross domestic product of the developing countries.

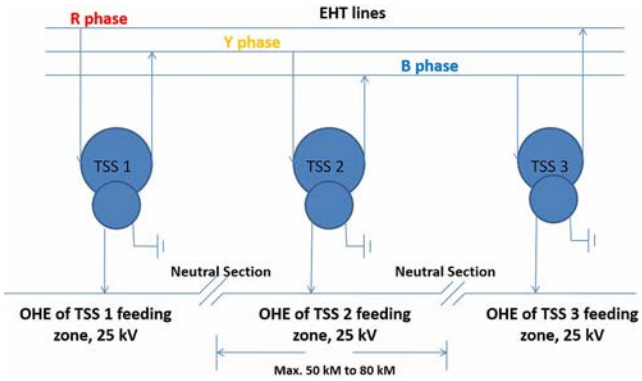

Fig. 1. Layout of single-line electric traction system.

Railway electrification system is the integral form of various facilities that are made to transit electrical energy from a high-tension electric power network to the electric locomotive (load). It has many similarities with the transmission and distribution system of the electric power sector. The main differences between the electrified railway system and the general electric power system lie on the arrangement of feeding the electric power to the load. Unlike the electric power transmission and distribution system, railway electrification system feeds power to the moving load (electric locomotives) and there exists many general safety as well as reliability aspects that are not able to be complied as it is the case of general power transmission systems. However, railway electrification networks are constructed at the overhead of the railway tracks, which are considered to be the isolated system from the remaining power networks, as well as from the public. Railway electrification system shall ordinarily be linear in general layout, as shown in Fig. 1.

Traction power distribution lines are also termed as overhead equipment (OHE) since it is deployed exactly at the overhead of the railway tracks (Fig. 2). OHE is fed at

Manuscript received April 1, 2018; revised June 6, 2018; accepted July 12, 2018. Date of publication July 25, 2018; date of current version December 18, 2018. *(Corresponding author: Devender Kumar Saini.)*

D. K. Saini and M. Yadav are with the Department of Electrical, Power and Energy, University of Petroleum and Energy Studies, Dehradun 248007, India (e-mail: dev.iit.roorkee@gmail.com; monika.yadav022@gmail.com).

R. Nair is with Indian Railways, Thiruvananthapuram 695014, India (e-mail: nair.ravikumar@rediffmail.com).

R. Prasad is with IIT Roorkee, Roorkee 247667, India (e-mail: rpdeefee@iitr.ernet.in).

Digital Object Identifier 10.1109/TTE.2018.2859379

2332-7782 © 2018 IEEE. Personal use is permitted, but republication/redistribution requires IEEE permission.
See http://www.ieee.org/publications_standards/publications/rights/index.html for more information.

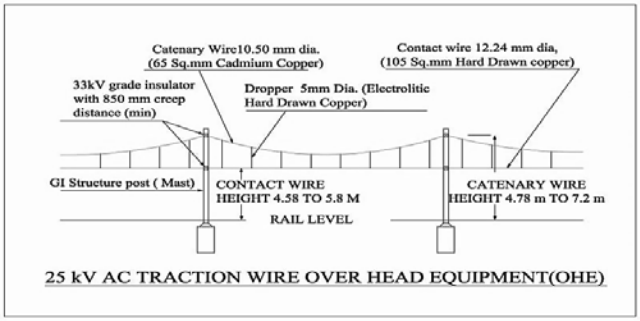

Fig. 2. Dimensional details of conventional high-voltage OHE.

a single point with the high-voltage electric power from traction subsystem (TSS) (most probably at the endpoint of the feeding sector). It consists of the catenary system, along with track feeder system, intermediate auxiliary transformer stations (ATSs), and sectioning posts. The maximum length of the OHE fed with electric supply through switchgear associated with protective relays usually shall be 30–40 km, and the working voltage should be below 27.5 kV.

A. Challenges Faced by the Electric Traction System

Persisting traction supply failure happens due to miscreant actions on the electric traction lines, or earth faults happen on it due to the making of continuity with earth by foreign bodies such as tree branches, birds, animals, and human will lead to the train traffic interruption for a prolonged period.

Occurrences of the faults persist on railway electric traction lines will automatically interrupt the traction supply, which could not be restored until those faults are cleared off. Recently, Serrano [3], [4] proposed a method to identify faulty subsection between ATS and conductor based on angle comparison of voltage and current. This technique is already in practice. Furthermore, Serrano [3], [4] suggested to remove the identified subsection and claim that the length of isolation of the earth faulty section will be small but this could not be made practical unless switchgears are provided at more intermediate stations. At present, the isolation of faulty section in tune of 10 km is possible in railway electric traction. There is no meaning to say that the faulty section is minimized, and hence, the train traffic is affected least, because, the train service could not be diverted through other routes easily, even if the faulty section is very small. Hence, it is very essential to correctly locate the position of the persisting fault(s), and to remove it as quick as possible, even if the affected subsection is very short. Even though the physical appearance of high-voltage ac power line of railway traction has no similarity with the short electric power transmission line, its modeling is done at par with the short length ac power transmission line (Fig. 3) [5]–[9] as, the length of high-voltage ac electric traction lines will be less than 50 km, and the working voltage would not go beyond 27.5 kV.

Presence of earth or earthed structures shall not be there at the proximity of electric power transmission lines. Hence, the effect of line capacitance is neglected in short transmission lines.

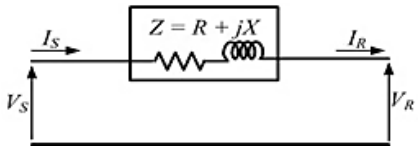

Fig. 3. Generalized model of short length transmission line.

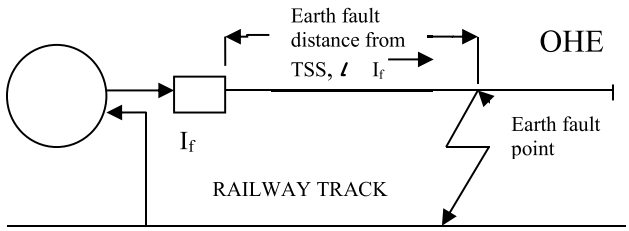

Fig. 4. Model of an earth fault persisting traction system.

The same concept is adopted in ac electric traction line model but unlike in power transmission lines, ac traction line often drew closer to earth potential surface to a considerable length. As the capacitance of a power line varies inversely with its distance from the earth/earthed surface, the effect of the capacitance of ac traction lines will be many times higher. As such, the generalized model (Fig. 3) cannot be fit as it is on high-voltage ac electric traction lines, and for developing the algorithm for its protection scheme, despite the working voltage and the length of high-voltage ac traction line is far below the levels stipulated for short transmission lines. Wei [10] proposed a distributed parameter line model for electric traction line and also considers the effect of capacitance to locate the fault position. However, the authors have assumed the line parameters are distributed and linear. This paper found out that the capacitance of the electric traction lines is not linearly distributed. Its effects at some area are negligible but significantly high at the vicinity of some topographical features. Hence, the proposed model in [10], of short length power lines is also not fit for the ac traction power line.

B. Fault Location on Electric Traction Lines

From the theories available [11]–[14] for pinpointing the persisting fault location (methods for fault location) on electric power lines, it is learned that those were made on the loop impedance theory for electric traction power network. Fig. 4 shows the model of an OHE with zero impedance persisting earth fault on it. The scheme of locating the fault is clubbed with the impedance relay (or MHO relay) developed based on the principle of loop impedance of the ac railway electric traction line [5].

l is the distance of the earth fault from the TSS, and "I_f" is the earth fault current. The traction line parameters are assumed to be uniformly distributed, where the per unit length resistance, inductance, and capacitance are R_0, L_0, and C_0, respectively, where R_0 is 0.1–0.3 Ω/km, L_0 is 1.4–2.4 mH/km, and C_0 is 10–14 nF/km [5].

There were many experiments conducted to precisely determine the location of persisting earth fault on electric traction

TABLE I
IMPEDANCES OF OHE FOR DIFFERENT LAYOUTS OF RAILWAY TRACKS

Sl. No.	Type of track & OHE	Impedance / km
1	Single line track OHE with return conductor	$0.70 \angle 70^0\ \Omega$
2	Single line track OHE without return conductor	$0.41 \angle 70^0\ \Omega$
3	Double line track OHE with return conductor	$0.43 \angle 70^0\ \Omega$
4	Double line track OHE without return conductor	$0.24 \angle 70^0\ \Omega$

line, using the traveling wave method [15]–[18]. However, none of them was found feasible, simply because, there are parallel lines at some area (loop lines at stations), and auxiliary transformers are connected to electric traction lines at every station for providing power supply to signaling equipment. The detachments of branch lines are not practical for applying the "fault pinpointing" methodology based on fault transient resistance [19]. The transients during fault analysis are mainly due to the auxiliary transformers connected to the traction line. Those transformers cannot be disconnected from traction lines until the railway staff arrived at the transformers sites. Its numbers will be many tens, and not uniform for all the feeding sections. Hence, the disconnection of all such auxiliary transformers from electric traction line requires huge manpower and longer time. Therefore, any algorithm, which does not address those types of "special features" of the actual traction lines are useless. The success rate of it on laboratory model or on computer-simulated models will not be repeated when used on actual traction system.

The theories [6], [10], [19]–[25] used to make prevailing algorithms for locating the fault distance measurement by the distance protection relay (DPR) are based on the measurement of loop impedance under different types of a fault condition of electric traction lines. The assumption is made that the impedance angle of OHE is constant in all fault conditions, duly considering the line parameters are uniformly distributed [22] in all models, despite the impedances of traction line are different (Table I) for different layouts of railway tracks.

The distance of fault "L" occurs on OHE is calculated using the general formula

$$L = Z_f/z \text{ km} \tag{1}$$

where "Z_f" is the total loop impedance in Ω up to the point of persisting earth fault on OHE, and "z" is the unit impedance of the OHE per unit length, in Ω/km.

The relay characteristic angle (RCA) (Fig. 5) plays the crucial role in differentiating a fault current in high-voltage ac electric traction lines, and the load current contributed by the electric locomotives. It shows how the resistive reach settings arrived. The impedance relay is also called DPR, which works on the principle of overshooting the impedance parallelogram by the traction current vector.

The phase angle of the load current of the locomotive will be around 40° lagging, and the angle of the earth fault current would be around 72.5° lagging for all fault distance calculations [26].

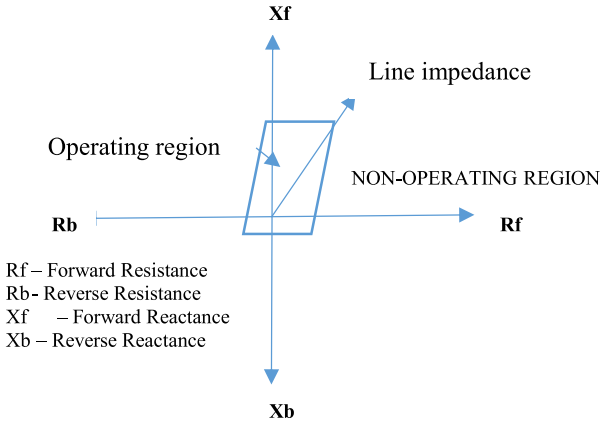

Fig. 5. Solid-state impedance relay's characteristic curve, when used as DPR.

The RCA is so determined that the relay does not actuate at the higher traction load current contributed by the electric locomotives and will act when earth fault current occurs even with lesser magnitude. The angle of the earth faults current, which is determined by the angle of loop impedance of OHE, if varies; the magnitude of the minimum current required to actuate the DPR will also vary. The distance between dead earth fault point/area and the source of supply is being arrived from the loop impedance, which is derived from the magnitude of the fault current and the instantaneous voltage of the OHE. The prevailing method, which was developed based on the existing theories of locating the fault position on electric traction lines shall succeed only if the two conditions are satisfied. One is the fault on OHE should be stationary and is having continuous earth contact, and the other is, the impedance of OHE is uniform throughout its length.

Documents on persisting earth faults kept by electric traction department of railway organization [27] highlight significant variations in the fault distances indicated by the relay from the distance of actual fault occurred. Variations in the data happened in an irregular manner on railway track laid at the hilly area where a lot of earth cuttings and tunnels are present. Single optimized value of capacitance of OHE for the fault distance calculation defies the chances of significant variations in the capacitance with the variations in topography.

On reviewing the available studies on the railway electric traction, it is noticed that no specific attention is given for modeling the railway traction lines. All the analysis is made by considering the railway electric traction lines at par with short length transmission line only. The aim of this paper is to model the electric traction line, duly including all those features and to quantify the variations in the parasite capacitance of electric traction lines at geographically challenged areas, formulate the variations empirically, and incorporate them to the existing model. The prevailing concept of the railway electric traction line parameters, i.e., all the three parameters are constant and are uniformly distributed throughout its length, is now modified as; "the capacitance is varying," and established that the pinpointing of persisting earth fault will also vary with the variation in traction line parameters.

TABLE II
ACTUAL EARTH FAULT DISTANCE AND THE FAULT DISTANCE INDICATED BY DPR FOR THE TWO EXTREMELY DIFFERENT TERRAINS

Actual fault distance and fault distance indicated by DPR Distance					
At plane area			At terrain with earth cuttings & tunnels		
Trial Date	Actual fault distance	Indicated Fault distance	Date	Actual fault distance	Indicated Fault distance
02/10/2016	35 km	40 km	14/06/2017	34 km	31 km
29/10/2016	20 km	23 km	27/06/2017	16 km	19 km
06/02/2017	14 km	16 km	30/06/2017	37 km	36 km
26/03/2017	20 km	23 km	22/08/2017	19 km	19 km
02/07/2017	19 km	22 km			
12/10/2017	9 km	10 km			

II. EXPERIMENTAL STUDY CONDUCTED TO DETERMINE THE INFLUENCING FACTORS

Persisting earth faults on high-voltage ac electric traction line were created with zero impedance at two different places where the difference in topographies is extreme to determine the factors influencing the impedance of the ac high-voltage electric traction lines.

A. Sections Selected for Experimentation

Two distinct sections with the two extreme topographical features, where high-voltage ac railway traction lines erected, are selected for conducting experimentation. One was at the railway section between Eraniel and Thovala in Tamilnadu state of India (8° 12′ 9.00″ N, 77° 18′ 55.37″ E), where railway tracks are laid on the level ground. The other was the railway section between Eraniel and Balaramapuram (8.4295° N, 77.0478° E), where railway tracks are laid through steep earth cuttings and tunnels made through the valley of Western Ghats, in India.

B. Test Conditions

Experiments were conducted only on nonrainy days duly ensuring no rolling stocks or trains were present in the entire zone of experiments, i.e., from the supply point to the farthest point of OHE, and all other power lines run in parallel and across at the vicinity of OHE (owned by other organizations) were switched OFF.

Ten trials were conducted, by creating the earth faults on OHE. Table II shows the actual distance of persisting earth fault locations, and distance of location indicated by the distant protection relay for two different places.

C. Analysis of the Outcome of Field Experimentations

The variations in the fault distance are observed to be more or less linear with progressing offset value in the section where tracks are laid on plane areas. The continuous consistent positive diversion is contributed by the uniformly distributed shunt admittance present in the entire length of OHE and the ground.

The least variations, but in highly irregular manner, were observed at the sections where railway tracks are laid at terrain where steep slope earth profiles and tunnels are present at the proximity of OHE. The earth fault distance indicated by the DPR for the OHE at terrain, where steep earth cuttings and tunnels are present, is almost linear with cumulative offset from the actual at its initial 15-km-long stretch due to the reason that the topography at those stretch is generally plane ground with some minor gradual slope profiling's of short lengths and a short length tunnel. A sudden shift toward the theoretical value is observed at 15–19 km due to the reason that many steep earth cuttings of high altitude and length, and two lengthy tunnels are available in this stretch. In the remaining stretches up to 37 km, combinations of plane grounds, few minor slope earth cuttings, the large number of steep earth cuttings, and one tunnel of length 201 m are available en route.

From Table II, it can be presumed that the shut admittance between the electric traction lines and the surrounding geographical features gave significant influence on the fault distance locating algorithm of the DPR. Hence, it is hypothetically accepted that the parasite capacitance of high-voltage ac railway traction line/overhead equipment (OHE) varies with the presence of surrounding earth, and earthed structures; and the variations are decided by various physical measurements such as area of earth/earthed structure, its clearances from OHE, angle of slope, and alignment of track. It is inevitable to model the variation of parasite capacitance to find the exact location of earth fault on ac traction line. Hence, the subsequent section dedicated to model the dynamism of parasite capacitance with respect to the height of OHE on the plane ground, height and width of earth cuttings, the angle of earth cuttings, and inside railway tunnel. Furthermore, the obtained results are used to develop the new segregated model for electrified railway track and the modified algorithm for fault location on OHE.

III. MODELING THE RELATION OF PARASITE CAPACITANCE OF 25-KV ELECTRIC TRACTION LINES

In practice, with the many unique features of OHE, the theoretically calculated parasite capacitance using the mirror imaging principle [28] is found mismatched with the actual. It is so happens with some of the special features in railway systems which influence the line parameters of OHE.

A. Modeling Parasite Capacitance With the Height of Railway Track on Plane Ground

Altitude of the bottom conductor (contact wire) of OHE varies between 4.58 and 5.8 m, and the top conductor (catenary wire) varies between 4.78 and 7.0 m from the ground (rail level). Also, there present earthed structure (metallic structure holding the cantilever assembly of the OHE) just at a distance of 0.3 m apart from the live part of OHE. There shall be such 20 metallic supports (OHE masts) on an average in every kilometer length. In addition, the catenary wire is strung in parallel to the center line of the railway track, but the contact wire is strung in a horizontally staggered manner with a maximum from $+0.3$ to -0.3-M deviation from the center line of the railway track at alternate supporting masts (Fig. 6).

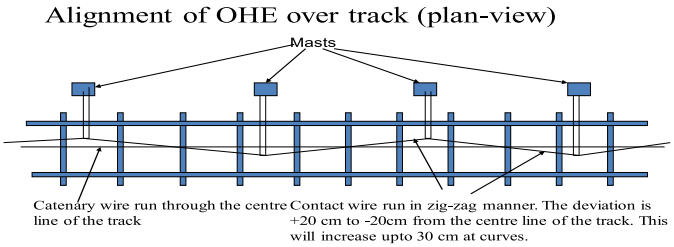

Fig. 6. Horizontal alignment of contact wire and catenary wire of OHE.

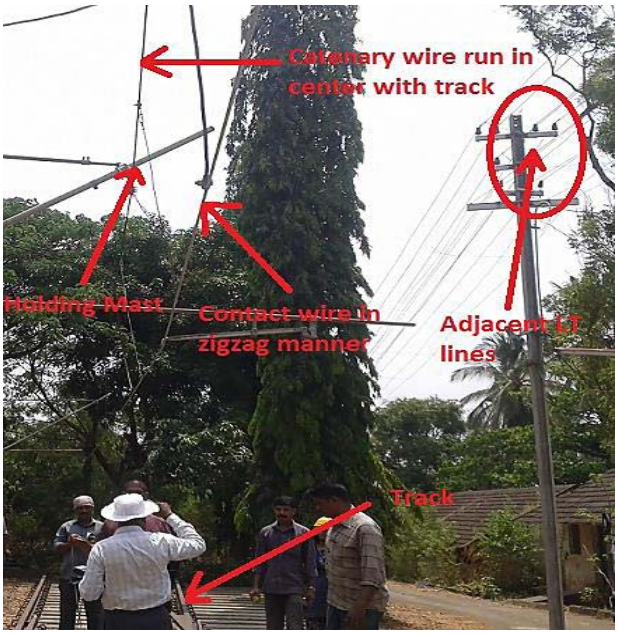

Fig. 7. Experiment conducted on a 50-m-long prototype of conventional OHE.

Since the OHE is considered to be a single conductor, the formula for capacitance by the mirror imaging method [28] is used for calculating the theoretical value of the parasite capacitance of it. Capacitance for single conductor power line with the earth in mirror imaging method is shown in the following equation:

$$C = 10^{-9}/(18 * \ln(2h/r)) \text{ F/m} \quad (2)$$

where "h" is the height of conductor from earth, "r" is the radius of the conductor, and "ln" is the natural logarithm. It is obvious that the (2) is not suitable to precisely calculate the capacitance between OHE and the earth due to the several unique features associated with the OHE.

1) Data Collection and Formulation of Parasite Capacitance: A 50-m-long specimen of OHE with its actual components was setup (Fig. 7) for the measurement of capacitances for various heights of OHE.

Data collected (Fig. 7) at outdoor area, which is subject to all kinds of stray nuisances produced by nearby power lines, telecommunication towers, high-frequency equipment and so on, similar to that of the actual electrical traction lines in use. The experiments were repeated for various heights of OHE ranging from 3.00 to 5.50 m on the level ground. Readings are shown in Table III.

TABLE III
PARASITE CAPACITANCES OF CONVENTIONAL OHE AT ITS VARIOUS HEIGHTS FROM RAILWAY TRACK ON LEVEL GROUND

Height of contact wire of OHE from rail level, in m	Parasite capacitance of 50 m long OHE, in nF
3.00	0.990
3.25	0.902
3.50	0.860
3.75	0.831
4.00	0.809
4.25	0.786
4.50	0.768
4.75	0.754
5.00	0.739
5.25	0.727
5.50	0.718

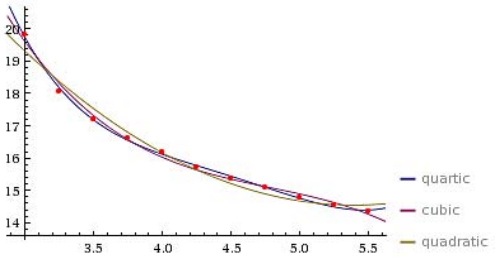

Fig. 8. Parasite capacitances for different heights of OHE at the level surface.

TABLE IV
COMPARISON OF THEORETICALLY CALCULATED PARASITE CAPACITANCE AND THE VALUE MEASURED FROM THE SPECIMEN OHE

Height of contact wire, in m	Capacitance of OHE as per mirror imaging formula, in nF/km [5, 28]	Capacitance measured directly from the proto type of OHE, nF/km	Variations in theoretical value from the actual
3.00	15.858	19.80	- 19.91 %
3.25	14.84	18.04	- 17.71 %
3.50	14.479	17.20	- 15.82 %
3.75	14.3032	16.62	- 13.94 %
4.00	14.232	16.18	- 12.04 %
4.25	14.1245	15.72	- 10.15 %
4.50	14.0913	15.36	- 8.26 %
4.75	14.1195	15.08	- 6.37 %
5.00	14.1171	14.78	- 4.48 %
5.25	14.1635	14.54	- 2.59 %
5.50	14.20	14.36	- 0.7 %

2) Curve Fitting: Fig. 8 shows the plots obtained through the regression analysis made on the parasite capacitances of 25-kV ac traction line with the earth at a varying height of OHE, at level ground with the help of a curve fitting and analyzing tool [29]. OHE heights in meters (m) are on the abscissa and parasite capacitances are on the ordinate in nF/km.

Percentage variations of the theoretical value of parasite capacitance from the value obtained in the experimental setup are given in Table IV.

Quadratic equation (3) for the parasite capacitance is also obtained with the equation generating tool [29] for different

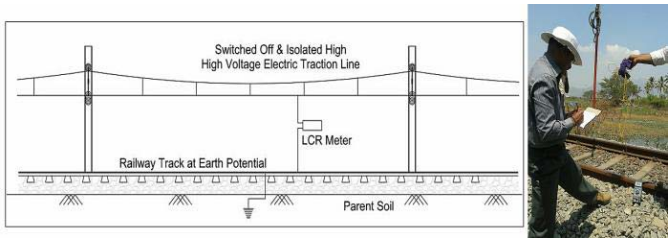

Fig. 9. Validation test conducted on an actual 25-kV electric traction system laid through the plane ground.

TABLE V
COMPARISON OF ACTUAL VALUE MEASURED AND THE VALUE ARRIVED USING NEW EMPIRICAL EQUATION (4) FOR THE PARASITE CAPACITANCE OF OHE

Height of Contact wire, in m	Length of OHE, in m	Parasite capacitance measured, in nF	Parasite capacitance of ONE km, in nF	Parasite capacitance calculated (Eqn. 4)	
				Value, in nF/km	% variation from actual
5.6	1234	17.81	14.43	14.16	- 1.9 %
5.3	1410	20.95	14.85	14.61	- 1.7 %
5.0	1081	16.21	14.99	14.75	- 1.6 %

heights of OHE from rail level to ground level

$$Y = 0.83333X^2 - 8.999X + 38.33 \text{ nF/km.} \quad (3)$$

An empirical equation for the parasite capacitance of OHE (Cp) duly incorporating the length of OHE in quadratic form (4) is framed.

Parasite capacitance of OHE at the plane level geographical area

$$\text{Cp} = \frac{L}{3} * 10^{-12}(2.5H^2 - 27H + 115) \text{ Farads} \quad (4)$$

where "*Cp*" is the parasite capacitance of conventional OHE on the plane geographical area, "*L*" is the length of OHE in meters, and "*H*" is the height of contact wire of OHE from the ground in meters.

3) Validation Test: Validation test for verifying the level of acceptance of the newly generated formula for the parasite capacitance of the actual 25-kV ac OHE of railway system, where the track is laid on the level ground, was also conducted at Thovala–Nagerkoil Section of Indian Railways (8.1833° N, 77.4119° E) by isolating three segments of OHE with different length and heights (Fig. 9).

Contact wire heights were 5.6, 5.3, and 5.0 m, for the lengths of OHE 1234.2, 1410, and 1081 m, respectively, and the parasite capacitances measured are 17.81, 20.616, and 16.21 nF, respectively, for those three segments of OHE. The experimentation on real traction line was conducted after switching OFF them and then capacitance values were measured by using certified calibrated inductance–capacitance–resistance meter. The readings obtained in the validation tests and the theoretical values arrived through the new empirical equation (4) are given in Table V.

The calculated values show the variation in between −1.6% and −1.9% only from the actual values obtained in validation tests. It is noted that a very thin layer of dust deposited on supporting insulators of actual OHE system is the reason for the higher value of capacitance obtained in the validation test.

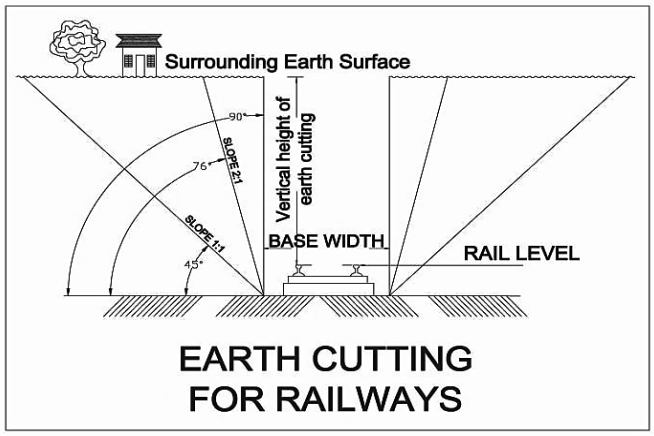

Fig. 10. Theoretical earth cutting for railways.

B. Modeling Parasite Capacitance at Earth Cuttings for Its Various Widths and Angles

Experiments conducted with a 50-m-long similitude model of OHE at various earth cuttings with varying base width and angles for collecting data for formulating the parasite capacitance of OHE. Earth cuttings made for railways have many unique features. Since the trains have snakelike shape, the cross section of the earth cutting (Fig. 10) should not be wide as much as those made for inland roadways.

The area of the earth cuttings available at the proximity of the OHE depends on the base width of the earth cuttings. The area, horizontal distance of OHE from the earth, the angle of the cuttings, and so on, will also quantitatively influence the parasite capacitance of OHE. Equation (4) is capable to formulate the parasite capacitance of OHE, where the earth is at the bottom of OHE with the infinite plane area only. It is found inadequate to precisely calculate the parasite capacitance of the OHE at earth cuttings of random variations in their dimensions. Actual earth cuttings (Fig. 11) are made to lay the railway track where the geography in undulating.

Railway organizations usually maintain the earth cuttings at some specific angles only. Cuttings with slopes 1/1 (45° cutting) and 2/1 (76° cutting) are generally available at laterite and at hard rock areas, respectively. Vertical cuttings (cutting with 90°) are found strengthened by a concrete wall. The maximum heights of earth cuttings were found permitted up to 18 m only.

1) Data Collection From Table Top Model: Experiments conducted on the similitude model of OHE set up at laboratory (Fig. 11) for data collection on the parasite capacitance exists between OHE and earth cuttings, for different angles and different base widths of it at the proximity of OHE, keeping the height of OHE and earth cutting controlled.

The model is setup using two hardboard sheets hinged on a base wooden sheet, pasted with metal foil inside, connected to an earth pit to create uniform electrical potential surface

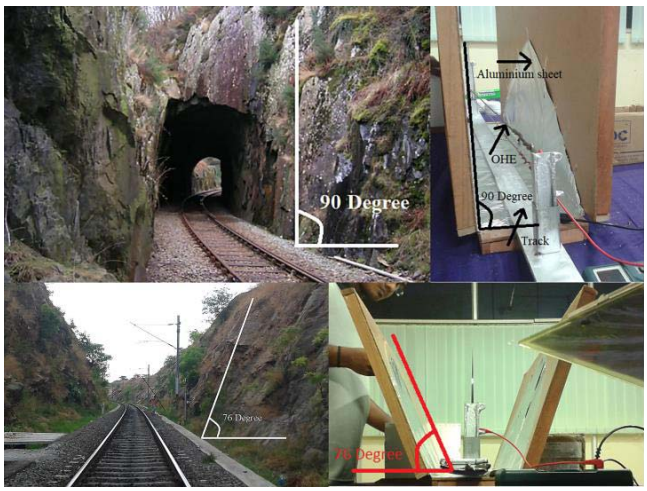

Fig. 11. Experiment on the model of OHE at the laboratory at different angles and different base widths.

TABLE VI
PARASITE CAPACITANCES OF TRACTION WIRE MODEL WITH THE SAME POTENTIAL SURFACE, AT ITS DIFFERENT ANGLES

Ht. of wire in m	Parasite capacitance of the model traction wire measured for different angles of the same potential surface, in pF/m						
	0^0	10^0	30^0	40^0	60^0	70^0	90^0
0.10	37.93	38.09	38.51	38.83	39.72	40.48	42.77
0.11	37.84	37.99	38.42	38.74	39.63	40.39	42.67
0.12	37.76	37.91	38.33	38.65	39.54	40.30	42.58
0.13	37.67	37.83	38.24	38.56	39.44	40.21	42.48
0.14	37.58	37.74	38.15	38.47	39.35	40.11	42.38

analogous to earth surface, and by placing a miniature size of OHE inside the experimental setup (Fig. 11). Length of the model is 1 m. Parasite capacitances in between the earth and the OHE of 1 m length, for different angles of the uniform electrical potential surfaces, were measured, in six trials. Average readings of the trials obtained for different angles for different heights of the model traction wires are shown in Table VI.

On analyzing those readings statistically [29], the relation of the angle of cutting surfaces and the parasite capacitance for OHE of height 0.1 m is obtained as

$$C = 0.00068x^2 0.01x + 38.09 \text{ pF/m} \tag{5}$$

where "x" is the angle of cutting in degree (Fig. 12).

The Akaike information criterion (AIC) and Bayesian information criterion (BIC) [30], R^2 and adjusted R^2 are -4.63, -3.42, 0.993, and 0.991, respectively. The AIC is a way of estimation of the relative correctness of models made out of a given set of data. AIC approximates the quality of each model with a collection of standard models for the data. Thus, AIC provides the level of confidence for model selection. Its value will be negative if the model selection is very close to the standard model.

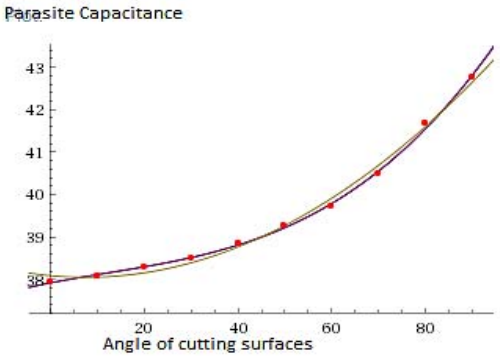

Fig. 12. Characteristic curve of capacitance of traction wire at earth cuttings.

The BIC is a criterion for selection of model among a finite set of models. The model with the lowest BIC (including negative) is preferred. BIC is advocated to be suitable for selecting the true model that generated the data from the set of presented models.

R is the correlation coefficient of the mathematical model made out of a set of data, whose value will be 1 if the mathematical model has the perfect fitness with the given data set. If the value of R is more than 0.9, the model so obtained can be accepted statistically. R^2 will give more clarity on the correlation coefficient, as the variations of the value of R from the perfect value 1, can be seen in magnified version if the square of the R is used. It is revealed that the variations in the parasite capacitance of OHE at earth cuttings in accordance with variations in the slopes of earth cuttings are nonlinear. However, the outcome of the laboratory experiments are not sufficient to formulate the variation of parasite capacitance of the actual railway traction line, since the effect of many other factors such as dust accumulation on the insulators of traction line and humidity in the surrounding air, which are present in actual lines were not present in laboratory experiments.

2) Data Collection From Actual High-Voltage Traction System: The capacitance of the traction wire varies inversely proportional to the height of it from the ground (rail level) in accordance with the newly established relation (4). However, it is unable to calculate the parasite capacitance of the OHE at earth cuttings, since they do not have common profiles, except in the cases of their slopes. Hence, further data collection for different base widths of the earth cuttings are done by conducting the experiments at various locations (Fig. 13) of earth cuttings with various base widths with the aid of a 50-m-long model of high-voltage ac railway traction wire.

Averages of the readings obtained in the experiments' trials conducted at earth cuttings of various widths are shown in Table VII. Standard angles of earth cuttings available in railway systems are 30° for ordinary soil, 45° for laterite, 76° for rocks, and 90° for concrete walls. In all the cases, the vertical height of earth cutting is kept more or less 7.8 m and height of lower conductor OHE (contact wire) 5.6 m, as controlled variables.

3) Curve Fitting: All the data collected from the experiments conducted at the actual high-voltage ac traction lines at different earth cuttings of different base widths are subjected to

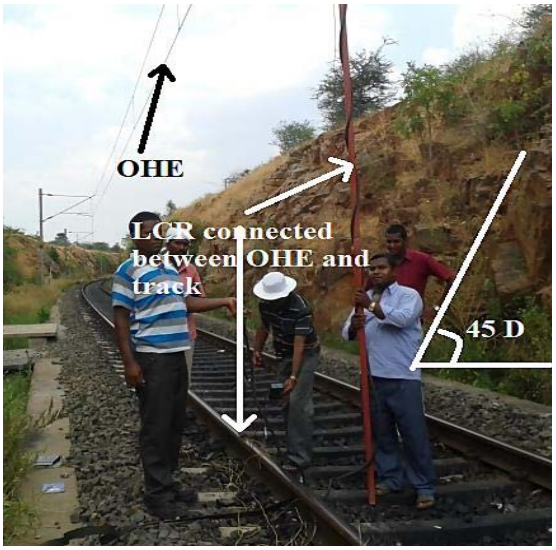

Fig. 13. Data collection from the actual high-voltage traction line at railway earth cutting.

TABLE VII
PARASITE CAPACITANCE BETWEEN OHE AND EARTH AT CUTTINGS

Angle of cutting	Average of parasite cap. in nF/km at , measured in 6 trials at earth cuttings for its various base widths				
	Base width	Base width	Base width	Base width	Base width
	6.72 m	7.28 m	7.84 m	8.40 m	8.96 m
30^0	14.59	14.55	14.53	14.51	14.50
45^0	14.77	14.74	14.70	14.65	14.60
76^0	15.45	15.34	15.23	15.10	14.95

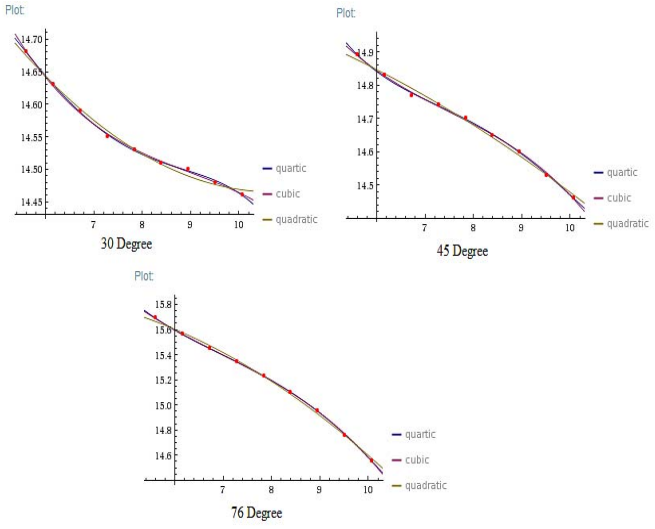

Fig. 14. Plot on the parasite capacitances of OHE run through at a 30°, 45°, and 76° earth cutting, for different widths of it, at the controlled height of earth cutting height & OHE.

the curve fitting process and statistical analysis. Fig. 14 shows the plots obtained from the statistical analysis made on the parasite capacitances of 25-kV ac traction line with the varying

TABLE VIII
QUARTIC EQUATIONS GENERATED FOR VARIOUS ANGLES OF EARTH CUTTINGS

Angle of cut	Coefficient of w^4, a	Coefficient of w^3, b	Coefficient of w^2, c	Coefficient of w, d	Constant term, k
30^0	- 0.0008	+0.218	-0.216	+0.816	+13.8
45^0	+0.0011	-0.039	+0.506	-2.88	-20.9
76^0	+0.001	-0.039	+0.536	-3.235	+22.9

TABLE IX
CUBIC EQUATIONS GENERATED FOR VARIOUS ANGLES OF EARTH CUTTINGS

Angle of cut	Coefficient of w^3, a	Coefficient of w^2, b	Coefficient of w, c	Constant term, k
30^0	-0.0024	+0.0645	-0.606	+16.476
45^0	-0.0043	+0.097	-0.801	+17.09
76^0	-0.0032	+0.0633	-0.541	+16.767

TABLE X
QUADRATIC EQUATIONS GENERATED FOR VARIOUS ANGLES OF EARTH CUTTINGS

Angle of cut	Coefficient of w^2, a	Coefficient of w, b	Constant term, k
30^0	+0.0081	-0.173	+15.391
45^0	-0.0044	-0.022	+15.137
76^0	-0.0218	+0.0979	+15.799

profiles (base widths) of earth cuttings at different angles of cuttings, i.e., 30°, 45°, and 76°, respectively.

Ordinate represents the parasite capacitance measured, in nanofarad/kilometers, and the abscissa represents the base width of earth cutting, in meters (m).

As the results of the statistical analysis, three nonlinear forms of equations, namely, quartic, cubic, and quadratic with approximate fit to the curves are also generated for different angles of earth cuttings, namely, 30°, 45°, and 76° whose base widths varies from 5.6 to 8.96 m.

The height of earth cutting and the height of the lower conductor of OHE were kept controlled at 7.8 and 5.6 m, respectively. Equations thus generated in quartic, cubic, and quadratic forms are given in tabular form in Tables VIII–X, respectively, where "w" is the width of earth cutting in meters.

4) Statistical Analysis of Data: The AIC and BIC [32], R^2 and the adjusted R^2 calculated for all those three equations given separately in Tables XI to XIII. In the statistical analysis of all sets of data of all the different angles of earth cuttings, the coefficient of determination R^2 and the adjusted R^2 are found more than 0.9, which are above the minimum acceptance level in curve fittings. In addition, the AIC and BIC are negative for all those equations, which further enhance the degree of acceptance level of those empirical formulae. Hence, the empirical formulae generated in quartic, cubic, and quadratic forms of equations (Tables VIII–X) are statistically significant.

The highest R^2 is obtained in the quartic equations, which will give the highest accuracy if utilized in creating the fault

TABLE XI

AIC, BIC, R^2, AND ADJUSTED R^2 FOR QUARTIC EQUATIONS

Angle of cut	AIC	BIC	R^2	(adj.R^2)
30^0	-74.49	-73.30	0.999	0.998
45^0	-64.40	-63.21	0.999	0.998
76^0	-74.31	-73.12	0.999	0.999

TABLE XII

AIC, BIC, R^2, AND ADJUSTED R^2 FOR CUBIC EQUATIONS

Angle of cut	AIC	BIC	R^2	(adj.R^2)
30^0	-70.45	-69.47	0.998	0.997
45^0	-61.81	-60.83	0.999	0.998
76^0	-67.70	-66.71	0.999	0.999

TABLE XIII

AIC, BIC, R^2, AND ADJUSTED R^2 FOR QUADRATIC EQUATIONS

Angle of cut	AIC	BIC	R^2	(adj.R^2)
30^0	-58.61	-57.82	0.992	0.989
45^0	-48.42	-47.63	0.993	0.991
76^0	-38.48	-37.69	0.997	0.996

locating algorithm. However, the quadratic equations are also having very high R^2 value, on the order of 0.99 and above.

C. Modeling Parasite capacitance at Earth Cuttings for Its Various Heights and Angles

Not all the earth cuttings [soil removed from the hillocks to lay railway tracks (Fig. 11)] are having the similar profiles. Its base width, the angle of cuttings, and the height vary from place to place in tune with various factors such as drainage arrangement at water stagnate areas, the stability of soil in accordance with its bearing capacity, and water table at the place from where the soil is to be removed for laying tangent railway track.

Data published by the Research Design and Standard Organization of Indian Railways [31] for making of earth cuttings prescribes to adopt 1:1 slope at laterite soil area, and 2:1 slope for hard rock area for its better stability. Those two slopes are having angles 450 and 760, respectively. Construction of vertical concrete walls is also suggested for the places where space constraints are experienced. It is specifically described that the maximum height of any earth cuttings shall not exceed 18 m.

Since the data collection from the laboratory model cannot exactly replicate the actual effects of the earth cuttings on the parasite capacitance of OHE due to the irregular surfaces of earth cuttings at hard rock area, experiment conducted with a 50-m similitude model of OHE (Fig. 7) by placing it at actual railway earth cuttings of various heights and slopes is adopted as the methodology for data collection, and to formulate the parasite capacitance of OHE at different vertical heights and angles of earth cuttings, by keeping base width and OHE height are controlled variables.

TABLE XIV

PARASITE CAPACITANCE BETWEEN OHE AT VARIOUS HEIGHTS OF EARTH CUTTINGS, AT STANDARD SLOPES (KEEPING OHE HEIGHT AT 5.6 m AND BASE WIDTH OF CUTTING AT 5.6 m)

Height of earth cutting, in m	Capacitance of OHE at 30^0 slope, in nF/km	Capacitance of OHE at 45^0 slope, in nF/km	Capacitance of OHE at 76^0slope, in nF/km
5.60	14.41	14.42	14.54
6.16	14.49	14.52	14,84
6.72	14.58	14.68	15.23
7.28	14.66	14.80	15.53
7.84	14.70	14.85	15.74
8.40	14.76	14.96	15.90
8.96	NA	15.03	16.04
9.52	NA	15.08	16.14
10.08	NA	15.11	16.22
10.64	NA	NA	16.28
11.20	NA	NA	16.32
11.76	NA	NA	16.36
12.32	NA	NA	16.38
12.88	NA	NA	16.40
13.44	NA	NA	16.41
14.00	NA	NA	16.41
14.56	NA	NA	16.41
15.12	NA	NA	16.41

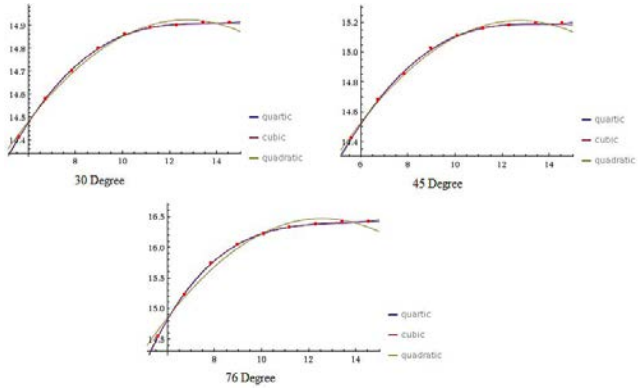

Fig. 15. Plot on parasite capacitance for different heights of earth cuttings at 30°, 45°, and 76°.

1) Data Collection: Series of experiments were conducted on similitude models of OHE set up at the railway tracks laid through the earth cuttings of different angles, namely, 30°, 45°, 76° and for various heights of it, which vary from 5.6 to 15.12 m, by keeping the base width 5.6 m and contact wire height of OHE 5.6 m as controlled variables.

Averages of the readings obtained in the trials are arranged in Table XIV.

2) Curve Fitting and Statistical Analysis: Fig. 15 shows the plots obtained through statistical analysis for curve fittings made on the parasite capacitances of 25-kV ac traction line with the earth at varying heights of cuttings at slopes 30°, 45°, and 76°. Earth cutting's heights in meters are shown on the abscissa (m), and the corresponding parasite capacitances are on the ordinate in nF/km.

Nonlinear equations of the forms quartic, cubic, and quadratic are also generated with the aid of the statistical tool [29] for different slopes of cuttings, namely, 30°, 45°, and 76° whose heights vary from 5.6 to 15.12 m.

TABLE XV

EQUATIONS GENERATED IN QUADRATIC FORM FOR VARIOUS SLOPES OF EARTH CUTTING AT ITS DIFFERENT HEIGHTS

Slope of earth cutting	Coefficient of h^2	Coefficient of h	Constant term, K
30 degree	-0.00978	+0.249	+13.3391
45 degree	-0.01509	+0.3847	+12.7611
76 degree	-0.03744	+0.94207	+10.5427

TABLE XVI

AIC, BIC, R^2, AND ADJUSTED R^2 FOR CUBIC EQUATIONS FOR VARIOUS SLOPES OF EARTH CUTTING

Angle of earth cutting	AIC	BIC	R^2	(adj.R^2)
30 degree	-65.93	-64.95	0.999	0.999
45 degree	-47.19	-46.21	0.998	0.997
76 degree	-43.67	-42.68	0.999	0.999

TABLE XVII

AIC, BIC, R^2, AND ADJUSTED R^2 FOR QUADRATIC EQUATIONS FOR VARIOUS SLOPES OF EARTH CUTTINGS

Angle of earth cutting	AIC	BIC	R^2	(adj.R^2)
30 degree	-43.27	-42.48	0.993	0.990
45 degree	-35.90	-35.12	0.993	0.991
76 degree	-12.84	-12.06	0.985	0.979

Since the shapes of the quartic equation and cubic equations in all the graphs (Fig. 15) almost resemble each other for all the standard slopes of earth cuttings, the analysis of quartic equation is omitted from the scope the analysis. The cubic equation for finding the parasite capacitance (C) of OHE at earth cuttings with angles (slopes) of walls 30°, 45°, and 76°, respectively, are presented in (6)–(8), and quadratic equations generated are shown in Table XV. Where "h" is the height of the earth cuttings in meters

$$C = 8 * 10^{-4}h^3 - 3.3 * 10^{-2}h^2 + 4.74 * 10^{-1}h + 12.668 \text{ nF/km} \quad (6)$$

$$C = 1.1 * 10^{-3}h^3 - 4.7 * 10^{-2}h^2 + 6.69 * 10^{-1}h + 11.844 \text{ nF/km} \quad (7)$$

$$C = 4.3 * 10^{-3}h^3 - 1.67 * 10^{-1}h^2 + 2.1723h + 6.831 \text{ nF/km}. \quad (8)$$

The AIC and BIC [30], the R^2, and the adjusted R^2 (adj.R^2) are also calculated for all those equations and shown in Tables XVI and XVII.

In the analysis, R^2 and the adjusted R^2 are found above 0.9 for the two forms of equations, which imply that both the forms of equations generated are statistically significant. The highest R^2 is obtained in the cubic form of equations. This form of equations will give the highest accuracy in calculating the parasite capacitance of OHE at earth cuttings. However, the quadratic equations also give very good R^2 value, on the order of 0.97 at the minimum.However, it is noted from the graphs (Fig. 15) that the quadratic equations have significant variations from the actual trace of the curve at heights of cuttings above 10 m. Hence, using quadratic equations (Table XV) for finding the parasite capacitance of OHE at earth cuttings of height lesser than 10 m is acceptable. Cubic form of equations (6)–(8) is recommended for the height of earth cuttings above 10 m.

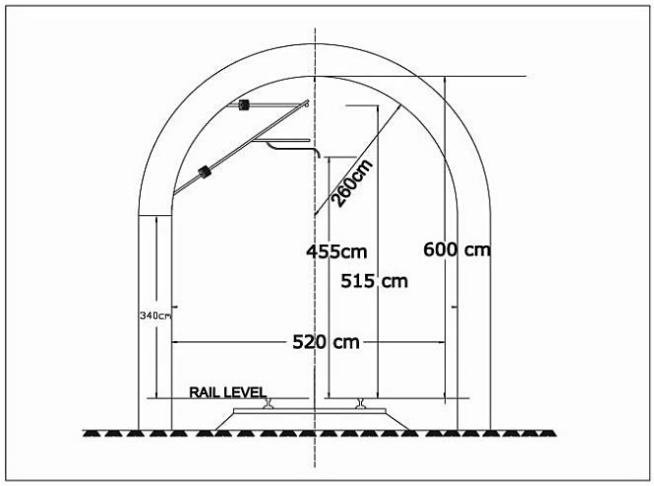

Fig. 16. Broad gauge railway tunnel equipped with standard.

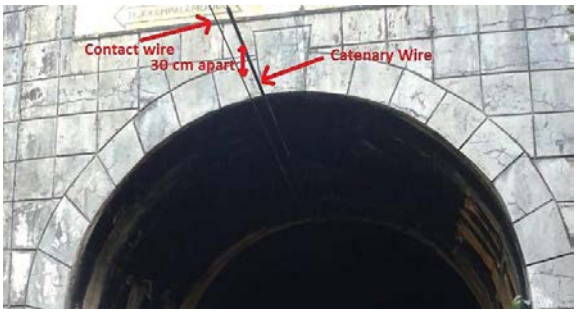

Fig. 17. Uninsulated traction conductor drawn very close to the earth potential surface.

D. Modeling Parasite Capacitance Inside Railway Tunnel

Railway tunnel can be imagined as an earth cutting of vertical walls (90° slopes) covered with a semicircular roof for its entire length (Fig. 16).

In practice, there shall not be various base widths and heights due to standardization of its cross section dimensions of the broad gauge (BG) tunnels.

1) Features of High-Voltage AC Traction Wires Inside Railway Tunnels: BG railway tunnels shall have the standard height of 6 m. Top conductor of high-voltage ac traction wire (catenary wire) is strung at the maximum height of 5.5 m from the ground, and the bottom conductor (contact wire) is strung further at 0.3 m below to it (Fig. 17). Heights of the traction wires inside the tunnel shall vary in accordance with the presence of other over line structures such as bridges, pipelines, aqua ducts, and power lines crossing the railway track at either ends of the tunnels.

There shall not be such an arrangement to run a high-tension ac power electric bare conductor very close to the

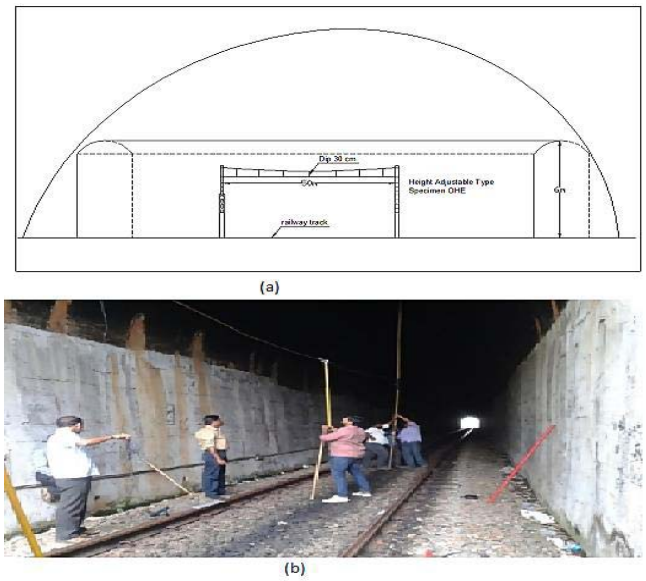

Fig. 18. Measurement of parasite capacitance of OHE within railway tunnel. (a) Graphical representation of similitude OHE inside railway tunnel. (b) Actual OHE placed inside railway tunnel.

earth potential surface anywhere else in electric power transmission or distribution sectors.

2) Data Collection: OHE in the tunnels has many unique features, which make the assessment of parasite capacitance of OHE within the tunnel very complex. A standard similitude model of conventional OHE with 50 m length, and with dip (vertical distance between the catenary and contact wire) 0.3 m is made for data collection, and placed inside a BG railway tunnel which is shown in Fig. 18(a) and (b). Fig. 18(a) shows the physical dimension and OHE parameters of the BG tunnel for experimentation. Fig. 18(b) shows the actual photograph inside the BG tunnel with similitude model of OHE, with created dip for experimentation.

Arrangements to adjust the height of the model OHE in 0.25-m steps were also incorporated to the model. The model is placed inside a BG railway tunnel of length 200 m, in the research region. Readings of parasite capacitances for every 0.25-M steps in its heights are measured, each in six trials. Average of the measurements obtained through the experiment trials are shown in Table XVIII.

3) Curve Fitting and Statistical Analysis: The plots (Fig. 19) obtained through the analysis made on the parasite capacitances of 25-kV ac traction line for the varying heights of the OHE inside a standard dimensioned railway BG tunnel with the help of the curve fitting and analyzing tool. OHE heights in meters are shown on the abscissa in meters (m), and the corresponding parasite capacitances are on the ordinate in nF/km.

Three types of equations, namely, quartic, cubic, and quadratic forms were also generated as the result of the statistical analysis (Table XIX), where H_t is the height of the bottom conductor of conventional OHE from the rail level in meters.

The statistical indices, namely, AIC, BIC, R^2, and adjusted R^2 were also determined for all the three types of the equations (Table XX).

TABLE XVIII

PARASITE CAPACITANCES OF SIMILITUDE MODEL OF OHE OF LENGTH 50 m, INSIDE A RAILWAY TUNNEL HAVING STANDARD DIMENSIONS

Height of Contact (H_t) wire, in m	Height of Catenary wire, in m	Capacitance (Cp) of 50 m long conventional OHE in nF, with fixed dip 0.3 m	Cp, made out of 1000 m long OHE, in nF
0.50	0.80	1.905	38.1
0.75	1.05	1.757	35.94
1.00	1.30	1.71	34.2
1.25	1.55	1.659	33.18
1.50	1.80	1.595	31.9
1.75	2.05	1.565	31.3
2.00	2.30	1.525	30.5
2.25	2.55	1.517	30.34
2.50	2.80	1.495	29.9
2.75	3.05	1.513	30.26
3.00	3.30	1.53	30.6
3.25	3.55	1.553	31.06
3.50	3.80	1.605	32.1
3.75	4.05	1.638	32.76
4.00	4.30	1.705	34.1
4.25	4.55	1.768	35.36
4.50	4.80	1.86	37.2
4.75	5.05	1.943	38.86
5.00	5.30	2.055	41.1
5.25	5.55	2.163	43.25
5.50	5.80	2.271	45.42

TABLE XIX

THREE FORMS OF EQUATIONS GENERATED FOR THE PARASITE CAPACITANCE OF OHE WITHIN RAILWAY TUNNEL OF STANDARD DIMENSIONS

Form of equations	*Coef.of H_t^4	Coef. of H_t^3	Coef. of H_t^2	Coef. of H_t	Constant term, K
Quartic	0.007459	-0.17125	2.8802	-11.4737	43.09
Cubic		-0.08174	2.524	-10.9479	42.87
Quadratic			1.79	-9.1	41.75

*Coef. = Coefficient.

TABLE XX

STATISTICAL INDICES OF EQUATIONS GENERATED FOR THE PARASITE CAPACITANCES OF CONVENTIONAL OHE INSIDE A RAILWAY TUNNEL

Form of equations	AIC	BIC	R^2	adj.R^2
Quartic	-9.04072	-6.65335	0.9996	0.9994
Cubic	-10.0513	-8.06182	0.9998	0.9994
Quadratic	0.66045	0.11252	0.9969	0.9962

From the plots (Fig. 19) of all the three types of the equations (Table XIV), it is understood that curves generated are almost resembled one another.

In the statistical analysis, the values of "R^2" and the "adjusted R^2" are found above 0.99 for all the three forms of empirical equations obtained. Also, the AIC and BIC are obtained in negative real numbers for the quartic and cubic forms of equations. Those indices are close to zero for the quadratic equations also (Table XX). Hence, the quadratic

TABLE XXI
COMPARISONS ON ACTUAL DISTANCE OF NATURALLY OCCURRED EARTH FAULTS, DISTANCE OF FAULT INDICATED BY THE DPR, AND DISTANCE CALCULATED WITH NEW ALGORITHM

Date of Earth Fault	Actual Distance of fault, in km	Fault distance indicated by existing system, in km	Percentage variation from actual	Fault distance calculated using new algorithm, in km	Percentage variation from actual, when new algorithm is used
16.06.2017	16.300	19	16.56 %	16.500	1.22 %
24.01.2018	21.500	25	16.27 %	21.200	1.42 %
10.02.2018	27.200	30	10.29 %	27.400	0.73 %
22.02.2018	06.700	07	04.48 %	06.700	0.00 %

equation is considered feasible for making an empirical equation for the parasite capacitance of OHE inside the railway tunnel. Newly generated empirical quadratic equation for the parasite capacitance of high-voltage ac electric railway traction line inside a railway tunnel with the standard dimensions shall almost equal to

$$C_{\text{pt}} = 10^{-12} L_t (1.79 H_t^2 - 9.1 H_t + 41.75) \text{ Farads} \quad (9)$$

where "C_{pt}" is the parasite capacitance of conventional 25-kV ac electric traction wire within a railway tunnel of standard dimension in "farads," "L_t" is the length of the railway tunnel in meters, and "H_t" is the height of the bottom conductor (contact wire) of OHE from the rail level in meters.

From the experimentations, it is revealed that the parasite capacitance of high-voltage ac electric traction lines (OHE) drawn inside the railway tunnels is around 3× higher than that of the traction lines drawn at the plane surface area for its normal height. Also, it comes to light that the variation in the parasite capacitance of OHE is not decaying as the height increases, but it traces a parabolic path. There available an optimum point (height of OHE) at which the parasite capacitance is the minimum. However, the said minimum value itself is about 2× higher than the lowest parasite capacitance of OHE at the plane area. The minimum parasite capacitance of OHE inside the BG railway tunnel is obtained at around 2.5-m high from rail level. However, the said height of OHE is unacceptable in high-voltage ac electric traction system on safety and operational points of views. The minimum height of OHE is prescribed is 4.98 m from the year 2004 onward (which was 4.58 m prior to 2004). Hence, it is important to note that the traction line impedance will vary significantly inside the railway tunnels, which is turn will give erratic input to the distance protection relay for judging the distance of persisting earth fault on OHE at hilly areas.

IV. PROPOSED MODEL OF HIGH-VOLTAGE AC ELECTRIC RAILWAY TRACTION LINE

From the survey and the subsequent experiments conducted at various electrified railway sections, it is discovered that the variations in the parasite capacitance of OHE happen mainly due to the variations in its clearances from the earth or earthed structures. Since those variations in the clearance of OHE from earth/earthed structures are not regular, the entire length of OHE is proposed to subdivide into several blocks, and distinct line parameters are assigned for each block of OHE (Fig. 20).

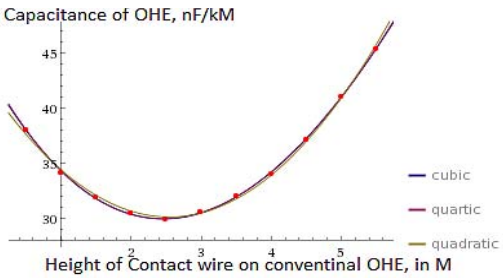

Fig. 19. Plot on the capacitance of conventional OHE inside the railway tunnel.

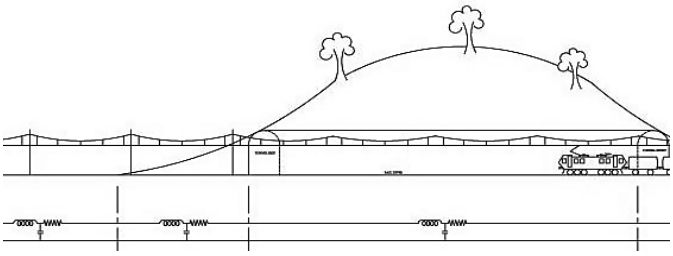

Fig. 20. Segregation of line parameters of OHE in tune with changes in topographical features.

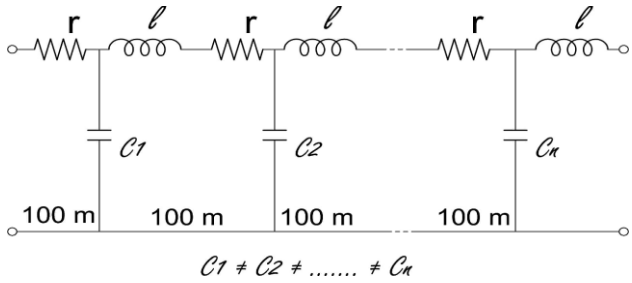

Fig. 21. Conceptual dynamic model of OHE with varying line capacitance.

Furthermore, for easy assessment of line parameters, the entire length of the OHE is subdivided into 100 long blocks for the theoretical calculations of line impedance per unit length (100 m), duly incorporating the average parasite capacitances of OHE for every 100 m length at various topographical features, such as plane area, earth cuttings, and tunnels. Resistance (R_o) and inductive reactance (L_o) per unit length are directly adopted from the prevailing theoretical values [5].

Capacitive reactance of every 100 m blocks, namely, c_1, c_2, $c_3 \ldots c_n$, are assessed separately by using the newly formed empirical formulae (3)–(9) for different topographical features and made a conceptual dynamic model for OHE (Fig. 21).

A. Application of Dynamic Model of OHE in Modifying Fault Locating Algorithm

A modified algorithm for calculating the fault distance on OHE for the accurate calculation of earth fault distance is suggested herewith, in the following steps (Fig. 22).

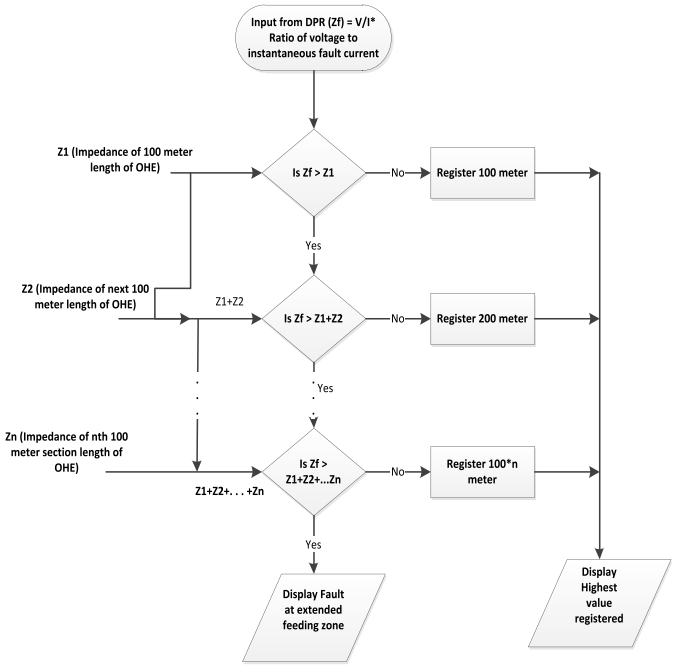

Fig. 22. Modified flowchart for earth fault pinpointing algorithm.

Step 1: Segregate the entire length of OHE into many blocks of 100 m long.

Step 2: Conduct detailed survey on every block to record the values of the physical variables, namely, the height of OHE (bottom contact wire) for the plane area and inside the tunnels, and height of OHE and measurements of profiles (base width, height, and slope) of earth cuttings.

Step 3: Calculate the parasite capacitances for each block using the newly discovered empirical equations [(4), Tables XIII, (6)–(9)] appropriately.

Step 4: Calculate the impedances for every 100 m blocks, namely, $z_1, z_2, z_3, \ldots, z_n$ using the values obtained in step 3 along with the standard values of resistance and inductive reactance [5] of 25-kV ac OHE.

Step 5: Incorporate the distinct impedances obtained in the preceding step in the software programming.

Step 6: Derive the impedance Z_f, up to the faulty point using the established equation, $Z = V/I$, where V is the real-time voltage and I is the instantaneous current.

Step 7: Compare the value of loop impedance, Z_f with the value z_1. If Z_f is lesser than z_1, declare, "fault location is within 100 m" of the electric supply point. Else, go to the next step (Fig. 22).

Step 8: Compare the value of Z_f with the combined value of z_1 and z_2 in the next step. If Z_f is lesser than $z_1 + z_2$, declare, "fault location is in between 100 and 200 m" from the electric supply point. Else, go to the next step.

Further steps are the iteration of the previous step by comparing the combined values of z_1, z_2, and z_3 and so on till it arrived "z_n," and declare, "fault locations within $(n-1)$*100 m to n*100 m " at the step when the Z_f is found lesser than the $\sum_{k=1}^{n} z_k$ but more than $\sum_{k=1}^{n-1} z_k$.

V. Validation of the Proposed Dynamic Model and Modified Algorithm

An algorithm to pinpoint the persisting earth fault distance on high-voltage ac traction lines duly incorporating the dynamic parameters of it is suggested in Section IV (Fig. 22). The said algorithm is found useful to calculate the fault distance even without the help of a software controlled module of DPR. It is practically implemented on trial basis, in parallel with the existing system of fault location of DPR, by making a chart for the impedances for every 100 m length of OHE for a feeding sector of 35 km length (Eraniel and Balaramapuram), in the traction power control room at Trivandrum Division of Indian Railway Organization for manually calculating the distance of earth fault occurred. (Table XXI).

The proposed algorithm designed theoretically to pinpoint the fault within 100 m from the actual fault location. However, the calculations made on the distance of naturally occurred earth faults from the supply feeding point with the help of newly developed algorithm (Fig. 22) are found varies from -200 to $+200$ m practically (Table XXI).

One of the reasons for this variation could be the effect of humidity in the surrounding air at such topographical areas, whose variation could not be formulated due to the tropical climatic condition of the experiment region (sample space), where humidity was found more or less constant in all seasons.

VI. Conclusion

From the study conducted at the survey regions, it is observed that the accuracy of the prevailing system for pinpointing the persisting faults on OHE is much deviates from the actual, due to various factors associated with the topography. Furthermore, intensive study conducted on 640-km stretch of railway system in India at many geographically different places revealed that the root cause of the variations in the parasite capacitances of high-voltage ac traction lines is the presence of earth/earth potential surface at the close proximity of uninsulated high-voltage ac traction lines, which is unique in power transmission/distribution system. Through a series of experimentations conducted on models of OHE, the variations in parasite capacitances between earth/earthed potential surfaces and the ac traction lines are quantified, and empirical equations to calculate the parasite capacitance of the ac traction lines for varying topographical features are proposed in this paper. Also, the developed algorithm has been applied for a feeding sector of 35 km length (Eraniel and Balaramapuram) at Trivandrum Division of Indian Railway Organization on trial basis and found extremely reliable over existing algorithm. The proposed methods have taken the effect of topographical features at the vicinity of electric traction line on modeling its line parameters but did not include the effect of humidity in the surrounding air. Hence, further research can be done on it duly considering the effect of humidity in surrounding air, so that the new methods can suggest a more realistic model of electric traction lines.

ACKNOWLEDGMENT

The authors would like to thank the Southern Railway administration in granting permission to conduct a research study on the security of the essential service network of railways. They would also like to thank Shri B. V. Chandrasekar, the Chief Electrical Distribution Engineer in encouraging the research study on actual high-voltage electric traction system to formulate the influencing factors of the reliability of traction network.

REFERENCES

[1] *List of Countries by Rail Transport Network Size*, Int. Union Railways, 2016.
[2] *Data Tables: Planning Commission*, Government India, India, 2015.
[3] J. Serrano, C. A. Platero, M. López-Toledo, and R. Granizo, "A novel ground fault identification method for 2×5 kV railway power supply systems," *Energies*, vol. 8, no. 7, pp. 7020–7039, 2015.
[4] J. Serrano, C. A. Platero, M. López-Toledo, and R. Granizo, "Influence of high-speed train power consumption on a novel ground fault identification method for 2×25 kV railway power supply systems," *Int. J. Transp. Develop. Integr.*, vol. 1, no. 3, pp. 471–480, 2017.
[5] A. Mariscotti and P. Pozzobon, "Synthesis of line impedance expressions for railway traction systems," *IEEE Trans. Veh. Technol.*, vol. 52, no. 2, pp. 420–430, Mar. 2003.
[6] K. K. Agarwal, "Automatic fault location and isolation system for the electric traction overhead lines," in *Proc. ASME/IEEE Joint Railroad Conf.*, Washington, DC, USA, Apr. 2002, pp. 117–122.
[7] Z. Han, Y. Zhang, S. Liu, and S. Gao, "Modeling and simulation for traction power supply system of high-speed railway," in *Proc. Asia–Pacific Power Energy Eng. Conf.*, Mar. 2011, pp. 1–4.
[8] U. J. Shenoy, K. G. Sheshadri, K. Parthasarathy, H. P. Khincha, and D. Thukaram, "MATLAB/PSB based modeling and simulation of 25 kV AC railway traction system—A particular reference to loading and fault conditions," in *Proc. IEEE Int. Conf. TENCON*, Nov. 2004, pp. 508–511.
[9] Z. Han, Z. Dong, S. Gao, and Z. Bo, "Protection scheme for out-of-phase short-circuit fault of traction feeding network," *J. China Railway Soc.*, vol. 22, no. 4, pp. 24–27, 2000.
[10] W. Cheng, G. Q. Xu, and L. H. Mu, "A novel fault location algorithm for traction network based on distributed parameter line model," in *Proc. CSU-EPSA*, 2005, pp. 63–66.
[11] M. Deshpande, *Electrical Power Systems Design*. New York, NY, USA: McGraw-Hill, 2001.
[12] T. Gonen, *Electrical Power Transmission System Engineering: Analysis and Design*. Boca Raton, FL, USA: CRC Press, 2015.
[13] M. G. Dwek, *Modern Power Station Practice: Ehv Transmission*. Oxford, U.K.: Pergamon Press, 1991, ch. 9.
[14] Y. H. Song, Ed. *Flexible AC Transmission Systems (FACTS)*, Inst. Eng., London, U.K., 1999.
[15] S. Avdakovic, A. Nuhanovic, M. Kusljugic, and M. Music, "Wavelet transform applications in power system dynamics," *Electr. Power Syst. Res.*, vol. 83, no. 1, pp. 237–245, 2012.
[16] A. Bernadić and Z. Leonowicz, "Fault location in power networks with mixed feeders using the complex space-phasor and Hilbert–Huang transform," *Int. J. Elect. Power Energy Syst.*, vol. 42, pp. 208–219, Nov. 2012.
[17] H. Jung, Y. Park, M. Han, C. Lee, H. Park, and M. Shin, "Novel technique for fault location estimation on parallel transmission lines using wavelet," *Int. J. Elect. Power Energy Syst.*, vol. 29, pp. 76–82, Jan. 2007.
[18] R. Mardiana, H. A. Motairy, and C. Q. Su, "Ground fault location on a transmission line using high-frequency transient voltages," *IEEE Trans. Power Del.*, vol. 26, no. 2, pp. 1298–1299, Apr. 2011.
[19] Y. Zhou, G. Xu, and Y. Chen, "Fault location in power electrical traction line system," *Energies*, vol. 51, no. 2, pp. 5002–5018, 2012.
[20] X. Lin, H. Weng, and B. Wang, "A generalized method to improve the location accuracy of the single-ended sampled data and lumped parameter model based fault locators," *Int. J. Elect. Power Energy Syst.*, vol. 31, no. 5, pp. 201–205, 2009.
[21] C. Wang and X. Yin, "Comprehensive revisions on fault-location algorithm suitable for dedicated passenger line of high-speed electrified railway," *IEEE Trans. Power Del.*, vol. 27, no. 4, pp. 2415–2417, Oct. 2012.
[22] G. Xu, Y. Zhou, and Y. Chen, "Model-based fault location with frequency domain for power traction system," *Energies*, vol. 6, no. 7, pp. 3097–3114, 2013.
[23] Z. Y. Xu, Z. P. Su, J. H. Zhang, A. Wen, and Q. X. Yang, "An interphase distance relaying algorithm for series-compensated transmission lines," *IEEE Trans. Power Del.*, vol. 29, no. 2, pp. 834–841, Apr. 2014.
[24] M. V. Mynam, M. Donolo, and A. Guzmán, "Improve transmission fault location and distance protection using accurate line parameters," in *Proc. GRIDTECH*, New Delhi, India, 2015, pp. 1–13.
[25] W. H. Kersting, *Distribution System Modeling and Analysis*. Boca Raton, FL, USA: CRC Press, 2006.
[26] H. Partab, *Modern Electric Traction*. India: Dhanpath Rai & Co., 1992, pp. 162–171.
[27] T. P. Control, "Log of events on earth faults," Traction Power Control, Trivandrum, India, 2015.
[28] S. N. Singh, *Transmission and Distribution Electric Power Generation*. New Delhi, India: PHI Learn., 2011, p. 135.
[29] Wolfram Alpha LLC. (2018). *Wolfram|Alpha: Computational Intelligence*. [Online]. Available: https://www.wolframalpha.com
[30] K. P. Burnham and D. R. Anderson, "Multimodel inference: Understanding AIC and BIC in model selection," *Sociol. Methods Res.*, vol. 33, no. 2, pp. 261–304, 2004.
[31] *Railway Developments*, Indian Railways, Bengaluru, India, 2014.
[32] *Indian Railways Manual of AC Traction Maintenance and Operation Volume-I. Indian Railways Manual of AC Traction Maintenance and Operation Volume-II*, Indian Railways, New Delhi, India, 1993.

Devender Kumar Saini (M'17) received the M.Tech. and Ph.D. degrees, with a focus on controller design for uncertain interval systems and their order reduction, from IIT Roorkee, Roorkee, India, in 2009 and 2013, respectively.

He is currently an Assistant Professor with the Department of Electrical Power and Energy, College of Engineering Studies, University of Petroleum and Energy Studies, Dehradun, India. His current research interests include protection for integrated renewable energy sources with distribution grid, fault detection and protection, modeling of uncertain interval systems, and robust control and challenges in integration of RE sources with DT grid.

Ravikumaran Nair received the B.Tech. degree from Calicut University, Malappuram, India, and the M.Tech degree from Kerala University, Thiruvananthapuram, India.

He is currently an Electrical Engineer with Indian Railways, Thiruvananthapuram, in senior executive cadre. Now he has 26 years of experience in high-voltage electrical traction installations.

Dr. Nair was a recipient of the Gold medalist in Officers' training at the National Academy of Indian Railways (erstwhile, Railway Staff College), Baroda, India, and 10 awards from various levels within 25 years of railway service, for designing and developing economic and energy efficient infrastructural electrical traction systems, for meritorious services.

Monika Yadav (M'17) received the master's degree in electrical engineering from the Indian School of Mines, Jharkhand, India, in 2015, where she is currently pursuing the Ph.D. degree in power system engineering.

She was with the University of Petroleum and Energy Studies, Dehradun, India, where she is currently an Assistant Professor with the Department of Electrical Power and Energy. Her current research interests include solar technology and micro grid and power system protection schemes.

Rajendra Prasad was born in Saharanpur, India, in 1953. He received the B.Sc. degree (Hons.) from Meerut University, Meerut, India, in 1973, and the B.E., M.E., and Ph.D. degrees in electrical engineering from the University of Roorkee, Roorkee, India, in 1977, 1979, and 1990, respectively.

From 1979 to 1983, he has served as an Assistant Engineer with Madhya Pradesh Electricity Board, Madhya Pradesh, India. From 1983 to 1996, he was a Lecturer with the Electrical Engineering Department, University of Roorkee. He was an Assistant Professor with the Department of Electrical Engineering, IIT Roorkee, Roorkee, India, from 1996 to 2001, where he was an Associate Professor from 2001 to 2009. He is currently a Professor with the Department of Electrical Engineering, IIT Roorkee. He has authored or co-authored around 200 papers in various journals/conferences and received 12 awards on his publications in various national/international journals/conferences proceeding papers. His current research interests include statistics, data analysis, control, optimization, system engineering and model order reduction of large-scale systems.

Ain Shams Engineering Journal 9 (2018) 1591–1600

Contents lists available at ScienceDirect

Ain Shams Engineering Journal

journal homepage: www.sciencedirect.com

Engineering Physics and Mathematics

Onset of triply diffusive convection in a Maxwell fluid saturated porous layer with internal heat source

Mukesh Kumar Awasthi [a], Vivek Kumar [b,*], Ravi Kumar Patel [a]

[a] Department of Mathematics, University of Petroleum and Energy Studies, Dehradun 248007, Uttarakhand, India
[b] Department of Mathematics, Shri Guru Ram Rai (P.G.) College, Dehradun 248001, Uttarakhand, India

ARTICLE INFO

Article history:
Received 19 January 2016
Revised 21 October 2016
Accepted 17 November 2016
Available online 16 December 2016

Keywords:
Triple-diffusive convection
Maxwell fluid
Internal heat source
Porous medium
Solute gradients

ABSTRACT

A linear stability analysis is performed for the onset of triple-diffusive convection in the presence of internal heat source in a Maxwell fluid saturated porous layer. The layer is considered to be heated and soluted from below. The porous medium is taken as isotropic and homogeneous. Within the framework of linear stability theory and normal made technique, a dispersion relation is obtained. Stationary Rayleigh number and Oscillatory Rayleigh numbers for the onset of instability is determined numerically and results are depicted graphically. The sufficient conditions for the non-existence of overstability are also derived. It has been found that Lewis numbers have destabilizing effect while the solute Rayleigh numbers play stabilizing role.

© 2016 Ain Shams University. Production and hosting by Elsevier B.V. This is an open access article under the CC BY-NC-ND license (http://creativecommons.org/licenses/by-nc-nd/4.0/).

1. Introduction

The onset of convective instability in a non-Newtonian fluid layer in porous media has attracted considerable attention, due to the large demands of such diverse fields as bio-rheology, geophysics, and petroleum industries. Some other examples are oil recovery, food processing, the spread of contaminants in the environment and in various processes in the chemical as well as materials industry. The problem on the thermal convection in a viscoelastic fluid was studied by many authors [1–4].

The double-diffusive convection is a convection in which the fluid contains two components with different molecular conductivities. Double diffusive convection is described by well mixed convecting layers and takes place if gradients of two competing stratifying agencies (heat and salt or any two solute concentrations) having different diffusivities are simultaneously exist. The most interesting impact of double-diffusive instabilities is that even stabilizing overall density gradient can destabilize the system when the density gradients caused by individual components are opposed. It is observed that when the two individual diffusing components are opposed, salt fingers occur when the component with the smaller diffusivity is destabilizing, while oscillatory convection occurs when the faster diffusing component is destabilizing [5].

The problem of double diffusive convection in porous media has attracted considerable interest over the last few decades due to its relevance and applications in many fields such as oceanography, geophysics, electrochemistry and migration of moisture. It is valuable to point out that the first viscoelastic rate type model, which is still used widely, is due to Maxwell. Wang and Tan [6] also considered the stability analysis of double diffusive convection in a Maxwell fluid saturated porous medium. The problem of double-diffusive convection in a viscoelastic saturated porous layer has been studies by several researchers in the literature ([7–10]).

Although, the subject of double diffusive convection is very important research field but there are many situations where more than two components are involved like the solidification of molten alloys, geothermally heated lakes, magmas and their laboratory models and sea water. Therefore, triple-diffusive convection is more realistic as compared to double-diffusive convection. The linear stability of triply diffusive convection in a binary Maxwell fluid saturated porous layer was investigated by Zhao et al. [11]. They found that increasing Lewis number decreases oscillatory critical Rayleigh number. Kumar et al. [12,13] considered the stability of triply diffusive convection in a viscoelastic porous layer in the presence of magnetic field.

A practical situation in which a porous medium has its individual source of heat can occur through radioactive decay or through,

* Corresponding author.
E-mail addresses: mukeshiitr.kumar@gmail.com (M.K. Awasthi), vivek.shrawat@gmail.com (V. Kumar), ravikumarpatel28@gmail.com (R.K. Patel).
Peer review under responsibility of Ain Shams University.

Production and hosting by Elsevier

http://dx.doi.org/10.1016/j.asej.2016.11.012
2090-4479/© 2016 Ain Shams University. Production and hosting by Elsevier B.V.
This is an open access article under the CC BY-NC-ND license (http://creativecommons.org/licenses/by-nc-nd/4.0/).

in the present perspective, a relatively weak exothermic reaction which can take place within the porous material. These situations occur very frequently in nuclear reactions, geophysics, reactor safety analysis, nuclear energy, metal waste form development, storage of radioactive materials and crystal growth.

A weak nonlinear analysis of the natural convection in a rotating anisotropic porous layer with internal heat generation was studied by Bhadauria et al. [14]. Bhadauria [15] solved the problem of double-diffusive natural convection in an anisotropic porous layer in the presence of an internal heat source. Subsequently, few more studies on internal heat generation on the onset of convection in porous medium have appeared [16–18]. Ellahi et al. [19] applied a hybrid method based on pseudo-spectral collocation in the sense of least-square method to examine the magnetohydrodynamic (MHD) flow of non-Newtonian fluid. They considered the incompressible electrically conducting fluid saturates the porous space between two boundaries. The effects of porosity on stress-jump and stress-continuity conditions are studied by Rashidi et al. [20]. They found that for high porosity, there is a large difference between two boundary conditions for the velocity profile along the horizontal and vertical directions in the porous layer. Kandelousi [21] studied the hydrothermal behavior of nanofluid fluid between two parallel plates and found that heat transfer enhancement has direct relationship with Reynolds number when power law index is equals to zero but opposite trend is observed for other values of power law index. Sheikholeslami and Ganji [22] considered two-dimensional laminar-forced convection nanofluids flow over a stretching surface in a porous medium and found that found that choosing Titanium oxide as the nanoparticle and Ethylene glycol as base fluid proved to have the highest cooling performance for this problem. Sheikholeslami et al. [23] studied the natural convection heat transfer of Cu-water nanofluid in a cold outer circular enclosure containing a hot inner sinusoidal circular cylinder in the presence of horizontal magnetic field.

To the best of our knowledge, the triple-diffusive problem which also introduces penetrative convection in a Maxwell fluid with internal heat source has not been investigated yet. Therefore, it is an attempt has been made to study the linear stability analysis of the triple-diffusive convection in a viscoelastic fluid saturated porous layer with internal heat source using the Darcy-Maxwell model. Our aim is to study the effect of viscoelastic as well as other parameters on the onset criteria for stationary and oscillatory triple-diffusive convection. Employing the linear stability analysis, the analytical Rayleigh number has been obtained using normal mode technique.

2. Formulation on the problem

We consider an infinite horizontal porous layer of an incompressible, thermally conducting Maxwell type viscoelastic fluid with internal heat source, confined between two planes situated at $z=0$ and $z=d$ (Fig. 1), acted upon by a gravity field $\mathbf{g}(0,0,-g)$. The temperature T and solute concentrations $C^{(1)}$ and $C^{(2)}$ at the bottom and top surfaces $z=0$, $z=d$ are T_0 and T_1; $C_0^{(1)}$, $C_1^{(1)}$ and $C_0^{(2)}$, $C_1^{(2)}$, respectively. We consider that temperature difference ΔT and concentration differences $\Delta C^{(1)}$ and $\Delta C^{(2)}$ are maintained between the lower and upper boundaries throughout the analysis. When fluid flows through a porous medium, the gross effect is represented by Darcy's law, the equations of continuity and motion for a Maxwell viscoelastic fluid with internal heat source through porous medium take the form

$$\nabla\cdot\mathbf{q}=0, \tag{1}$$

$$\frac{\rho_0}{\varepsilon}\left(1+\bar{\lambda}\frac{\partial}{\partial t}\right)\frac{\partial\mathbf{q}}{\partial t}=\left(1+\bar{\lambda}\frac{\partial}{\partial t}\right)(-\nabla p+\mathbf{g}\rho)-\frac{v}{k_1}\mathbf{q}, \tag{2}$$

where $\mathbf{q}$ is the Darcian (filter) velocity, ε denotes medium porosity, k_1 represents the medium permeability, p denotes the pressure, $\bar{\lambda}$ denotes relaxation time parameter, Q shows internal heat source and $v(=\mu/\rho)$ is kinematic viscosity. Taking an average of the fluid velocity over a volume V, we get the intrinsic average velocity $\mathbf{v}$, which is related to Darcian(filter) velocity $\mathbf{q}$ by the Dupuit-Forchheimer relationship $\mathbf{v}=\mathbf{q}/\varepsilon$. A porous medium of very low permeability allows us to use the Darcy's model. For a medium of very large stable particle suspension, the permeability tends to be small justifying the use of Darcy's model. This is because the viscous drag force is negligibly small in comparison with Darcy's resistance due to the large particle suspension.

The equation of heat conduction and solute concentrations can be written as

$$\sigma\frac{\partial T}{\partial t}+(\mathbf{q}\cdot\nabla)T=k_T\nabla^2T+Q(T-T_0) \tag{3}$$

$$\varepsilon\frac{\partial C^{(1)}}{\partial t}+(\mathbf{q}\cdot\nabla)C^{(1)}=k_{C_1}\nabla^2C^{(1)}, \tag{4}$$

$$\varepsilon\frac{\partial C^{(2)}}{\partial t}+(\mathbf{q}\cdot\nabla)C^{(2)}=k_{C_2}\nabla^2C^{(1)}. \tag{5}$$

Here, $t, v, k_T, k_{C_1}, k_{C_2}$ are the time, kinematic viscosity, effective thermal diffusivity and effective solute diffusivities of the medium, respectively. The heat capacities for fluid and solid matrix are represented by c_f and c_m, respectively. The constant $\sigma=(\rho c)_m/(\rho c)_f$ represents the ratio of heat capacities. Since density variations are mainly due to variations in temperature and solute concentrations, the equation of state, following Boussinesq approximation, for the fluid layer is given by [Zhao et al. (16)]

$$\rho=\rho_0\left[1-\alpha_T(T-T_0)+\alpha_{C_1}(C-C_0^{(1)})+\alpha_{C_2}(C-C_0^{(2)})\right]. \tag{6}$$

Here $\rho, \rho_0, \alpha, \alpha'$ and α'' denote the fluid density, reference density, thermal and solvent coefficients of expansion, respectively. The thermal and solute boundary conditions are given as

$$\begin{aligned} &T=T_0+\Delta T;\quad C^{(1)}=C_0^{(1)}+\Delta C^{(1)};\quad C^{(2)}=C_0^{(2)}+\Delta C^{(2)},\quad at\ z=0\\ &T=T_0;\quad C^{(1)}=C_0^{(1)};\quad C^{(2)}=C_0^{(2)},\quad at\ z=d. \end{aligned} \tag{7}$$

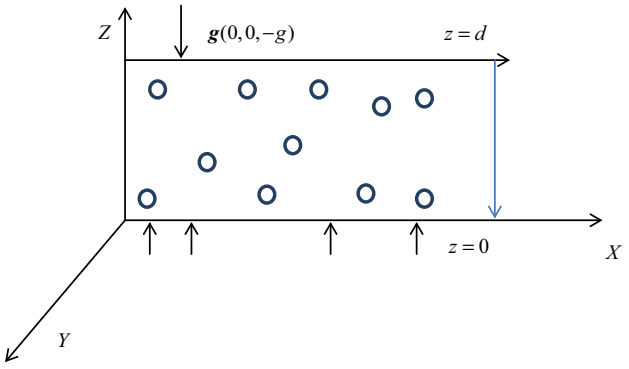

Figure 1. Geometry of the problem.

3. Basic state and perturbation equations

The basic state was assumed to be quiescent and is given by

$$\begin{aligned} &\mathbf{q}=(0,0,0),\quad T=T_b(z),\quad p=p_b(z),\quad C^{(1)}=C_b^{(1)}(z),\\ &C^{(2)}=C_b^{(2)}(z),\quad \rho=\rho_b(z), \end{aligned} \tag{8}$$

which satisfy the following conditions

$$\frac{dp_b}{dz} = -\rho_b g, \quad \frac{d^2C_b^{(1)}}{dz^2} = 0, \quad \frac{d^2C_b^{(2)}}{dz^2} = 0,$$
$$k_T\frac{d^2(T_b - T_0)}{dz^2} + Q(T_b - T_0) = 0. \tag{9}$$

Then the steady state solution is given by

$$T_b = T_0 + \Delta T\frac{\mathrm{Sin}\sqrt{R_i}(1-z/d)}{\mathrm{Sin}\sqrt{R_i}}, \quad C_b^{(1)} = C_0^{(1)} + \Delta C^{(1)}(1-z/d),$$
$$C_b^{(2)} = C_0^{(2)} + \Delta C^{(2)}(1-z/d)$$

and

$$p_b = p_0 + \rho_0 \mathbf{g} z\left(1 - \alpha_T\Delta T\frac{\mathrm{Sin}\sqrt{R_i}(1-z/d)}{\mathrm{Sin}\sqrt{R_i}} + \alpha_{C_1}\Delta C^{(1)}(1-z/d) + \alpha_{C_2}\Delta C^{(2)}(1-z/d)\right)$$

Here $R_i = Qd^2/k_T$ is the internal Rayleigh number. To use linearized stability theory and normal mode technique, we assume small perturbations on the basic state solution. Let us assume $\mathbf{q}(u,v,w) = 0 + \mathbf{q}(u',v',w')$, $\rho = \rho_b + \rho'$, $p = p_b + p'$, $T = T_b + T'$, $C^{(1)} = C_b^{(1)} + C^{(1)'}$ and $C^{(2)} = C_b^{(2)} + C^{(2)'}$ denote the perturbations in the fluid velocity, density, pressure and temperature and concentrations, respectively. The change in density ρ' caused mainly by the perturbations in temperature and concentrations is given by

$$\rho' = -\rho_0[\alpha_T T' - \alpha_{C_1}C^{(1)'} - \alpha_{C_2}C^{(2)''}]. \tag{11}$$

The linearized perturbation equations can be written as

$$\nabla\cdot\mathbf{q}' = 0, \tag{12}$$

$$\frac{\rho_0}{\varepsilon}\left(1+\bar{\lambda}\frac{\partial}{\partial t}\right)\frac{\partial\mathbf{q}'}{\partial t} = \left(1+\bar{\lambda}\frac{\partial}{\partial t}\right)\left[-\nabla p' - g\rho_0\left(\alpha_T T' - \alpha_{C_1}C^{(1)\prime} - \alpha_{C_2}C^{(2)\prime}\right)\right] + \frac{\nu}{k_1}\mathbf{q}', \tag{13}$$

$$\sigma\frac{\partial T'}{\partial t} + \frac{\partial T_b}{\partial z}w' = k_T\nabla^2 T' + QT', \tag{14}$$

$$\varepsilon\frac{\partial C^{(1)'}}{\partial t} - w'\frac{\Delta C^{(1)}}{d} = k_{C_1}\nabla^2 C^{(1)'}, \tag{15}$$

$$\varepsilon\frac{\partial C^{(2)'}}{\partial t} - w'\frac{\Delta C^{(2)}}{d} = k_{C_2}\nabla^2 C^{(2)'}. \tag{16}$$

Here primes indicate the perturbed quantities. Eliminating pressure term from the momentum equation and introducing the following non-dimensional quantities:

$$x = x^*d, \quad t = \frac{\sigma d^2}{k_T}t^*, \quad q' = \frac{k_T}{d}q'^*, \quad T' = (\Delta T)T'^*, \quad C^{(1)'} = (\Delta C^{(1)})C^{(1)'*},$$
$$C^{(2)'} = (\Delta C^{(2)})C^{(2)'*}. \tag{17}$$

Using the above non-dimensional variables in the Eqs. (13)–(16) and eliminating asterisks, we get the following equations

$$\left(1+\lambda\frac{\partial}{\partial t}\right)\left[\frac{\eta}{Va}\frac{\partial}{\partial t}\left(\nabla^2 w'\right) - Ra\nabla_1^2\left(T' - N_1C^{(1)'} - N_2C^{(2)'}\right)\right] + \nabla^2 w' = 0, \tag{18}$$

$$\left(\frac{\partial}{\partial t} - \nabla^2 - R_i\right)T' + w'f(z) = 0, \tag{19}$$

$$\left(\eta\frac{\partial}{\partial t} - \frac{1}{Le_1}\nabla^2\right)C^{(1)'} - w' = 0, \tag{20}$$

$$\left(\eta\frac{\partial}{\partial t} - \frac{1}{Le_2}\nabla^2\right)C^{(2)'} - w' = 0. \tag{21}$$

Here, $\lambda = \bar{\lambda}\kappa/d^2$ denotes the relaxation number (also known as Deborah number), $Da = k_1/d^2$ is the Darcy number, $Pr = \mu/\rho_0 k_T$ represents the Prandtl number, $\eta = \varepsilon/\sigma$ is the normalized porosity, $Va = \varepsilon Pr/Da$ represents the Vadasz number, $Ra = \rho_0 g\alpha_T k_1/\mu k_T$ is the thermal Rayleigh number, $N_1 = \alpha_{C_1}\Delta C^{(1)}/\alpha_T\Delta T$ denotes the buoyancy ratio, $N_2 = \alpha_{C_2}\Delta C^{(2)}/\alpha_T\Delta T$ denotes the analogous buoyancy ratio, $Le_1 = k_T/k_{C_1}$ represents the Lewis number, $Le_2 = k_T/k_{C_2}$ is the analogous Lewis number and $f(z) = \frac{\partial T_b}{\partial z}$, where T_b in non-dimensional form is

$$T_b = \frac{\mathrm{Sin}\sqrt{R_i}(1-z)}{\mathrm{Sin}\sqrt{R_i}}, \tag{22}$$

It is assumed that the boundary of the system is isothermal and isosolutal. Therefore, the boundary conditions for perturbation variable are given by

$$w' = 0, \quad T' = 0, \quad C^{(1)'} = 0, \quad C^{(2)'} = 0 \quad \text{at } z = 0, 1. \tag{23}$$

4. Normal mode technique

In this section, we discuss the linear stability analysis. According to the normal mode analysis, convective motion is assumed to exhibit horizontal periodicity. Then the perturbed quantities can be assumed to be periodic waves of the form:

$$\left[w, T', C^{(1)'}, C^{(2)'}\right] = [W(z), \Theta(z), \Gamma(z), \Psi(z)]\exp\{ik_x x + ik_y y + nt\}, \tag{24}$$

where k_x and k_y are the wave numbers in x and y directions respectively, $k = (k_x^2 + k_y^2)^{1/2}$ is the resultant wave number of propagation and n is the growth rate. Infinitesimal perturbations of the rest state may either damp or grow depending on the value of the parameter n. Substituting Eq. (24) in Eqs. (18)–(21), we obtain

$$(1+\lambda n)\left[\frac{\eta n}{Va}(D^2 - a^2)W + a^2Ra(\Theta - N_1\Gamma - N_2\Psi)\right] + (D^2 - a^2)W = 0, \tag{25}$$

$$\left(n - (D^2 - a^2) - R_1\right)\Theta + Wf(z) = 0, \tag{26}$$

$$\left(n\eta - \frac{1}{Le_1}(D^2 - a^2)\right)\Gamma - W = 0, \tag{27}$$

$$\left(n\eta - \frac{1}{Le_2}(D^2 - a^2)\right)\Psi - W = 0. \tag{28}$$

Now the boundary conditions becomes

$$W = 0, \quad \Theta = 0, \quad \Gamma = 0, \quad \Psi = 0 \quad \text{at } z = 0, 1. \tag{29}$$

To satisfy the boundary condition (29), we assume the solution of Eqs. (25)–(28) in the form

$$\begin{pmatrix} W(z) \\ \Theta(z) \\ \Gamma(z) \\ \Psi(z) \end{pmatrix} = \begin{pmatrix} W_0 \\ \Theta_0 \\ \Gamma_0 \\ \Psi_0 \end{pmatrix}\mathrm{Sin}\, m\pi z, \quad (m = 1, 2, 3\ldots). \tag{30}$$

It has been observed that the fundamental mode i.e. $m = 1$ is the most unstable mode. Therefore, we take $m = 1$ in Eq. (30). Substituting the above expression into Eqs. (25)–(28), we get

$$(1+\lambda n)\left[\frac{\eta n}{Va}\delta^2 W_0 - a^2Ra(\Theta_0 - N_1\Gamma_0 - N_2\Psi_0)\right] + \delta^2 W_0 = 0, \tag{31}$$

$$(n + \delta^2 - R_i)\Theta_0 + 2FW_0 = 0, \tag{32}$$

$$\left(n\eta + \frac{1}{Le_1}\delta^2\right)\Gamma_0 - W_0 = 0, \tag{33}$$

$$\left(n\eta + \frac{1}{Le_2}\delta^2\right)\Psi_0 - W_0 = 0. \tag{34}$$

Here $\delta^2 = \pi^2 + a^2$ and $F = \int_0^1 f(z)\mathrm{Sin}^2\pi z dz$. Above equations can be written as in matrix form as

$$\begin{pmatrix} \frac{n\eta}{Va}\delta^2 + \frac{\delta^2}{(1+\lambda n)} & a^2 Ra & N_1 a^2 Ra & N_2 a^2 Ra \\ 2F & (n+\delta^2 - R_i) & 0 & 0 \\ 1 & 0 & -\left(n\eta + \frac{\delta^2}{Le_1}\right) & 0 \\ 1 & 0 & 0 & -\left(n\eta + \frac{\delta^2}{Le_2}\right) \end{pmatrix} \begin{pmatrix} W_0 \\ \Theta_0 \\ \Gamma_0 \\ \Psi_0 \end{pmatrix} = 0. \quad (35)$$

For the non-trivial solution of the above system of homogeneous equations, we get

$$Ra_T = \frac{1}{2F}\left[\frac{Ras_1(R_i - n - \delta^2)}{(Le_1 n\eta + \delta^2)} + \frac{Ras_2(R_i - n - \delta^2)}{(Le_2 n\eta + \delta^2)} + \frac{(R_i - n - \delta^2)}{a^2}\left(\frac{n\eta\delta^2}{Va} + \frac{\delta^2}{1+\lambda n}\right)\right], \quad (36)$$

where $Ras_1 = RaN_1Le_1, Ras_2 = RaN_2Le_2$ are the solute Rayleigh numbers for different solutes. For neutral stability, we have $n = i\omega$ in Eq. (36), we get

$$Ra_T = \Delta_1 + i\omega\Delta_2, \quad (37)$$

where

$$\Delta_1 = \frac{1}{2F}\left[\begin{array}{c} \frac{Ras_1(\delta^2 R_i - \eta\omega^2 Le_1 - \delta^4)}{(Le_1^2\omega^2\eta^2 + \delta^4)} + \frac{Ras_2(\delta^2 R_i - \eta\omega^2 Le_2 - \delta^4)}{(Le_2^2\omega^2\eta^2 + \delta^4)} \\ +\delta^2\left(\frac{n\omega^2(1+\lambda^2\omega^2) + (R_i - \lambda\omega^2 - \delta^2)Va}{a^2 Va(1+\lambda^2\omega^2)}\right) \end{array}\right], \quad (38)$$

$$\Delta_2 = \frac{1}{2F}\left[\begin{array}{c} \frac{Ras_1(\eta Le_1(\delta^2 - R_i) - \delta^2)}{(Le_1^2\omega^2\eta^2 + \delta^4)} + \frac{Ras_2(\eta Le_2(\delta^2 - R_i) - \delta^2)}{(Le_2^2\omega^2\eta^2 + \delta^4)} \\ -\delta^2\left(\frac{\eta\delta^2(1+\lambda^2\omega^2) + (1-\lambda\delta^2)Va - R_i(\eta + \eta\lambda^2\omega^2 - \lambda Va)}{a^2 Va(1+\lambda^2\omega^2)}\right) \end{array}\right], \quad (39)$$

Since Ra_T is a physical quantity, it must be real. Hence, from Eq. (37), it follows that either $\omega = 0$(steady onset, principle of exchange of stabilities) or $\Delta_2 = 0$ ($\omega \neq 0$, oscillatory onset, overstability).

5. Stationary convection

For the validity of principle of exchange of stabilities (i.e. steady case), we have $\omega = 0$ at the margin of stability. Then Rayleigh number at which the marginally stable steady modes exist becomes

$$Ra_T^{st} = -\frac{1}{2F}\left[\frac{Ras_1(\delta^2 - R_i)}{\delta^2} + \frac{Ras_2(\delta^2 - R_i)}{\delta^2} + \frac{\delta^2(\delta^2 - R_i)}{a^2}\right], \quad (40)$$

In the absence of internal heat source i.e. $Q = 0$, we have $R_i = 0$ and $F(z) = -1/2$. So we obtain

$$Ra_T^{st} = \left[Ras_1 + Ras_2 + \frac{(\pi^2 + a^2)^2}{a^2}\right]. \quad (41)$$

This is the same expression as obtained by Zhao et al. [11]. Again if $Ras_1 = 0$ and $Ras_2 = 0$, the stationary Rayleigh number reduces to the classical result

$$Ra_T^{st} = \frac{(\pi^2 + a^2)^2}{a^2}, \quad (42)$$

Furthermore, Eq. (40) gives the critical value of Rayleigh number $Ra_{T,c}^{st} = 4\pi^2$ for $a_c^{st} = \pi$.

6. Oscillatory convection

For oscillatory case, $\Delta_2 = 0(\omega \neq 0)$, we obtain

$$a_1(\omega^2)^3 + a_2(\omega^2)^2 + a_3\omega^2 + a_4 = 0. \quad (43)$$

Here, $a_1 = Le_1^2 Le_2^2\lambda^2\eta^5\delta^2(\delta^2 - R_i)$,

$$a_2 = \left\{\begin{array}{l} \delta^6\eta^3\lambda^2(Le_1^2 + Le_2^2)(\delta^2 - R_i) + Le_1^2 Le_2^2\delta^2\eta^4\{\eta(\delta^2 - R_i) + V_A(1 - \delta^2\lambda) \\ +\lambda R_i V_A\} + a^2\delta^2\lambda^2\eta^2 Le_1^2 Ras_2 Va(1 - \eta Le_2) \\ +a^2\delta^2\lambda^2\eta^2 Le_2^2 Ras_1 Va(1 - \eta Le_1) a^2\lambda^2\eta^3 Le_1 Le_2 R_i Va(Le_1 Ras_2 + Le_2 Ras_1) \end{array}\right\},$$

$$a_3 = \left\{\begin{array}{l} (\delta^6\eta^3(Le_1^2 + Le_2^2) + \delta^{10}\eta\lambda^2)(\delta^2 - R_i) + a^2\delta^6 Ras_1 Va(1 - \eta Le_1)(\lambda^2 + \eta^2 Le_2^2) \\ +a^2\delta^2 Ras_2 Va(1 - \eta Le_2)(\delta^4\lambda^2 + \eta^2 Le_1^2) + \delta^6\eta^2 Va(1 - \delta^2\lambda)(Le_1^2 + Le_2^2) \\ +\delta^6\eta^2\lambda R_i Va(Le_1^2 + Le_2^2) + a^2\delta^4\eta\lambda^2 R_i Va(Le_1 Ras_1 + Le_2 Ras_2) \\ a^2\eta^3 Le_1 Le_2 R_i Va(Le_1 Ras_2 + Le_2 Ras_1) \end{array}\right\}$$

$$a_4 = \left\{\begin{array}{l} \delta^{10}\lambda R_i Va + +a^2\delta^4\eta R_i Va(Le_1 Ras_1 + Le_2 Ras_2) + \delta^{10}\eta(\delta^2 - R_i) \\ +\delta^{10} Va(1 - \delta^2\lambda) \\ +a^2\delta^6 Ras_2 Va(1 - \eta Le_2) + a^2\delta^6 Ras_1 Va(1 - \eta Le_1) \end{array}\right\}$$

Now Eq. (37) with $\Delta_2 = 0$, gives

$$Ra_T^{osc} = \frac{1}{2F}\left[\begin{array}{c} \frac{Ras_1(\delta^2 R_i - \eta\omega^2 Le_1 - \delta^4)}{(Le_1^2\omega^2\eta^2 + \delta^4)} + \frac{Ras_2(\delta^2 R_i - \eta\omega^2 Le_2 - \delta^4)}{(Le_2^2\omega^2\eta^2 + \delta^4)} \\ +\delta^2\left(\frac{n\omega^2(1+\lambda^2\omega^2) + (R_i - \lambda\omega^2 - \delta^2)Va}{a^2 Va(1+\lambda^2\omega^2)}\right) \end{array}\right], \quad (44)$$

We find the oscillatory neutral solution from Eq. (44). It proceeds as follows: First determine the number of positive solutions of Eq. (43). If there is none, then no oscillatory instability is possible. If there are three values then the minimum of Ra_T^{osc} from Eq. (44) with ω^2 given by Eq. (43) gives the oscillatory neutral Rayleigh number. Since Eq. (41) is a cubic equation in ω^2, it can give rise to more than one positive value ω^2 for fixed values of the other parameters.

7. Case of overstability

In the section, we examine the possibility for which instability may arise as oscillations of increasing amplitude. Since, we wish to find the Rayleigh number for the onset of instability via a state of pure oscillatory motion, we first assume that ω is real and we look for the conditions for which ω^2 is positive in Eq. (43). From Eq. (43), it is clear that if $\delta^2 > R_i$, $1 > \delta^2\lambda, 1 > \eta Le_1, 1 > \eta Le_2$ then all coefficients are positive. So Eq. (43) does not admit any positive value of ω^2.

Therefore, oscillatory convection is not possible if $\delta^2 > R_i$, $1 > \delta^2\lambda, 1 > \eta Le_1, 1 > \eta Le_2$ i.e. $\frac{d^2}{\lambda_1\kappa} > \pi^2 + a^2 > \frac{Qd^2}{k_T}, k_T < \min\left(\frac{\sigma}{\varepsilon}k_{C_1}, \frac{\sigma}{\varepsilon}k_{C_2}\right)$.

8. Results and discussion

In this section, the numerical computation has been carried out using the stability condition presented in previous section. Using the linear theory, which is based on usual normal mode technique, we have derived the onset criteria for stationary and oscillatory convection. The expressions of stationary Rayleigh number and oscillatory Rayleigh number are given by the Eqs. (40) and (44), respectively. The marginal stability curves in plane for stationary as well as oscillatory modes are displayed through various figures for fixed values of the parameters i.e. normalized porosity $\eta = 0.5$, relaxation number $\lambda = 0.01$, solute Rayleigh number $Ras_1 = 500$, analogous solute Rayleigh number $Ras_2 = 400$, internal Rayleigh number $R_i = 3$, Lewis number $Le_1 = 7$, analogous Lewis number $Le_2 = 5$ and Vadasz number $V_A = 12$.

Fig. 2 shows the comparison between marginal stability curves of Rayleigh number for stationary as well as oscillatory convection modes in case of double diffusive convection with those obtained for triple diffusive convection (present analysis). The marginal curves for stationary and oscillatory modes for double diffusive

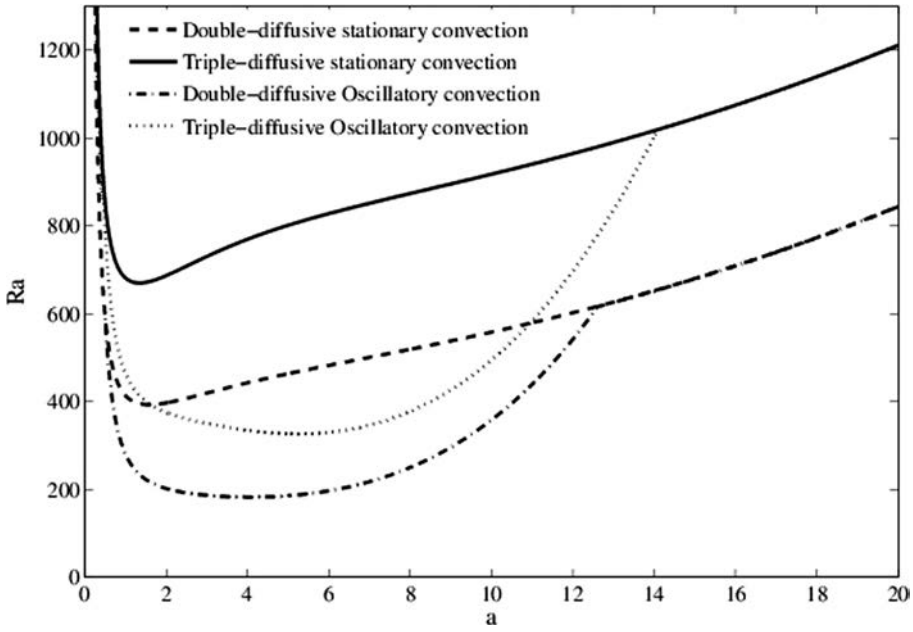

Figure 2. Comparison between double-diffusive convection and triple-diffusive convection.

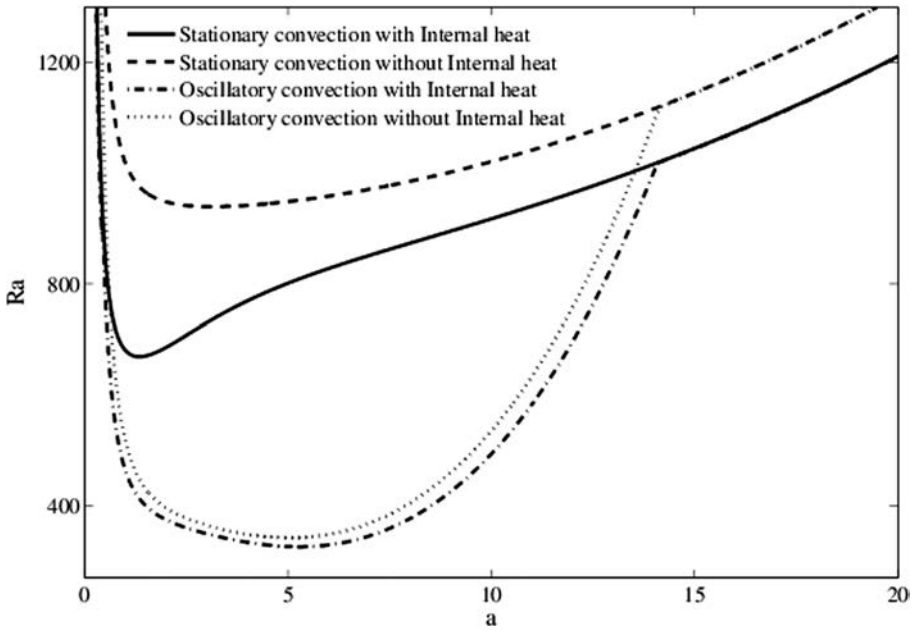

Figure 3. Effect of internal Rayleigh number on stationary convection and oscillatory convection.

convection are same as obtained by Zhao et al. [11]. It seems that addition of an extra salt increases the fluid layer concentration which absorbs heat from the system and system gets stabilize.

In some cases, it is found that the material offers its own source of heat, and this leads to a different way in which a convective flow can be set up through the local heat generation within a fluid layer. The comparison between neutral Rayleigh number curves has been compared in Fig. 3 with and without internal heat source. The presence of internal heat source increase the temperature of the fluid layer and causes the destabilizing effect.

The effect of normalized porosity parameter η on the marginal curves is shown in Fig. 4. It is observed that as the normalized porosity parameter increases, the minimum of the Rayleigh number decreases and this indicates that the effect of normalized porosity parameter is to advance the onset of triple-diffusive convection. As porosity of the medium is ratio of void space to the total space and therefore, we can say that the greater void space well make the system unstable. We also found that the effect of normalized porosity is significant for small η.

In Fig. 5, the effect of relaxation time parameters shown on the marginal curves for Rayleigh numbers. The value for Deborah number λ for dilute polymeric solution is most likely in the range [0.1,2]. At present, there are no experimental data available for comparison and, therefore, we have considered a wide range of values for the parameters. Basically, the Deborah number is used in rheology to describe how fluid and material is. The smaller the Deborah number, the more fluid the material appears. The parameter λ that relates to the relaxation time to the thermal

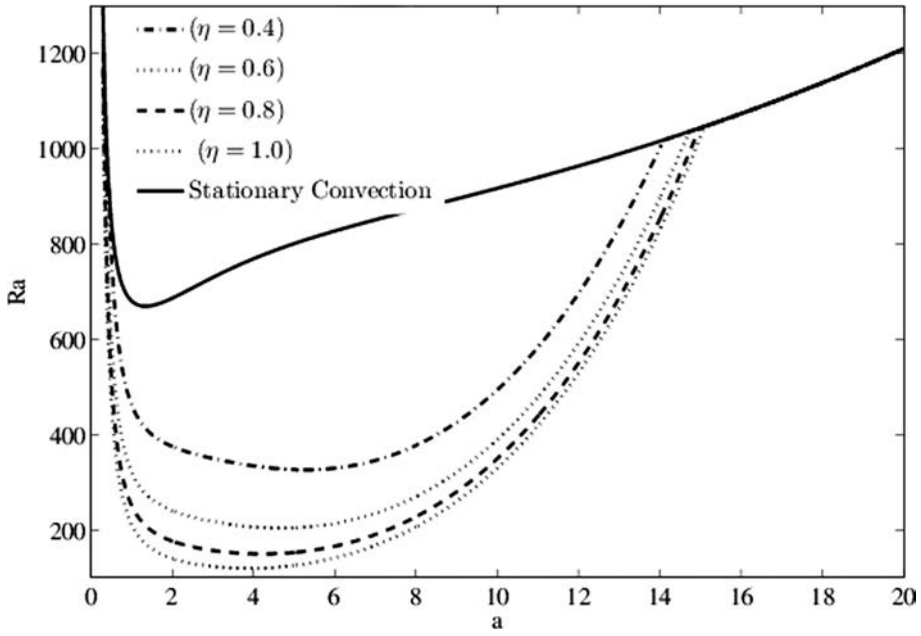

Figure 4. Effect of normalized porosity on oscillatory convection.

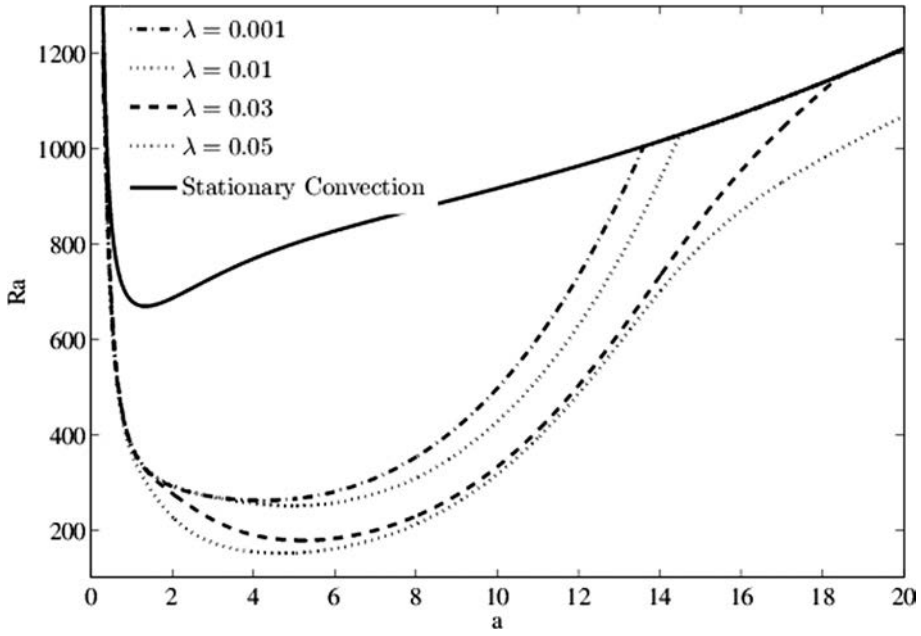

Figure 5. Effect of relaxation time parameter on oscillatory convection.

diffusion time is of order one for most viscoelastic fluids. From the figure, it is found that an increase in the value of relaxation time parameter is to advance the onset of triply diffusive convection and decrease the minimum of the Rayleigh number. If λ is large then the minimum of the Rayleigh number is small, which makes the onset of convection easier. Based on the theory of Maxwell fluid model, a fluid relaxation or characteristic time $\overline{\lambda}$ is defined to quantify the viscoelastic behavior [24]. Therefore, we can get a conclusion that the physical mechanism is the increasing relaxation time increases the elasticity of a viscoelastic fluid thus causing instability. As a result, the elasticity has a destabilizing effect on the Maxwell fluid layer in the porous media and the oscillatory convection is easy to occur for viscoelastic fluid.

Figs. 6 and 7 depict the effects of solute Rayleigh number Ras_1 and analogous solute Rayleigh number Ras_2 on the marginal stability curves for stationary modes as well as oscillatory modes. It is found that the effect of increasing Ras_1 and Ras_2 is to increase the value of the Rayleigh number for stationary mode as well oscillatory modes. It is shows that the effects of solute Rayleigh numbers have stabilizing effect to the system.

From Fig. 8, we observe that the an increase in internal Rayleigh number R_i decreases the stationary Rayleigh number which shows that internal Rayleigh number R_i postpone the stationary convection. Also, Oscillatory Rayleigh number decreases with an increase in internal Rayleigh number which means that internal Rayleigh number advances the onset of triple diffusive convection.

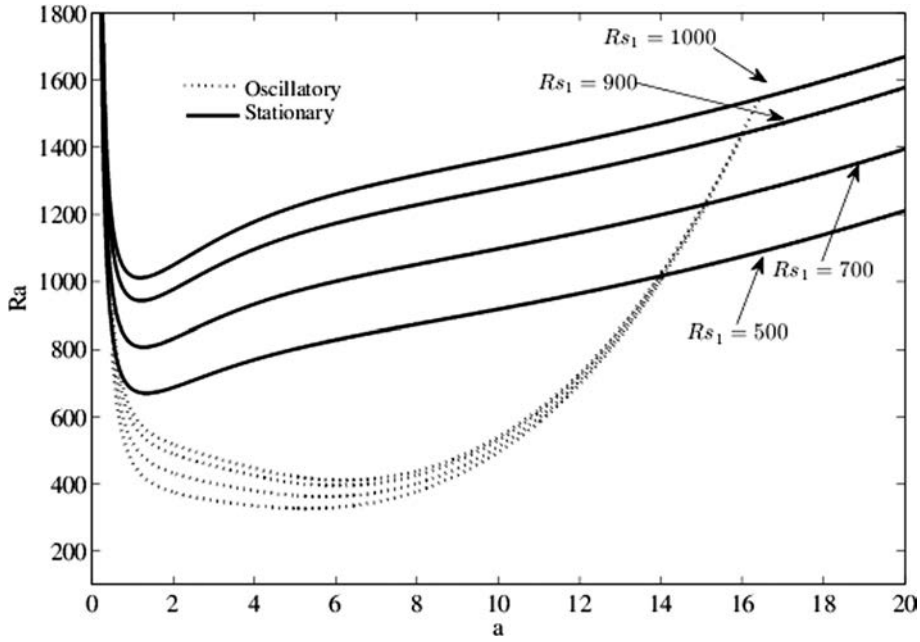

Figure 6. Effect of solute Rayleigh number on oscillatory convection.

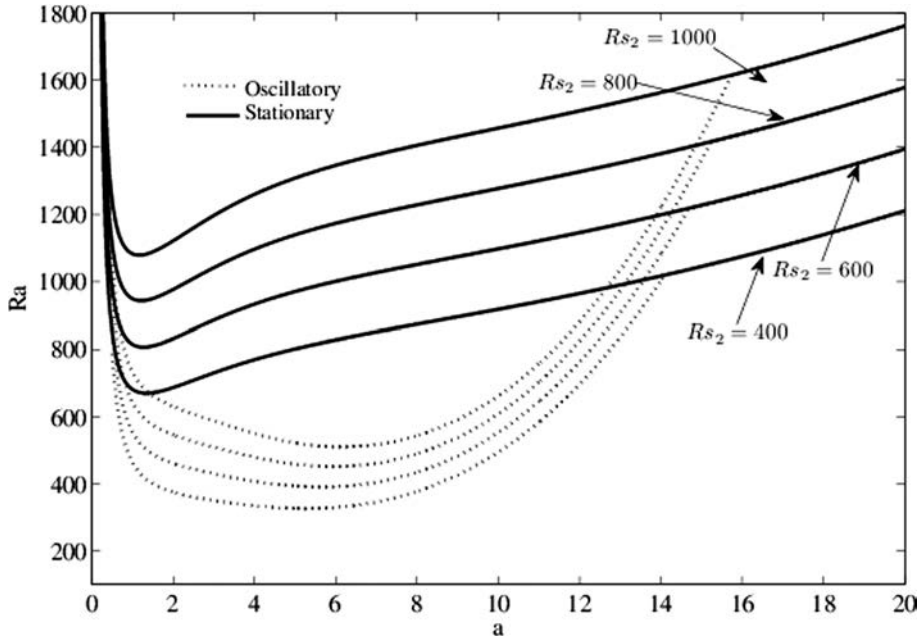

Figure 7. Effect of analogous solute Rayleigh number on oscillatory convection.

In Fig. 9, the variation of oscillatory Rayleigh number with respect to Lewis number of first concentration Le_1 is shown. The value of oscillatory Rayleigh number decreases when the value of Lewis number increases which shows that Lewis number of first concentration destabilizes the system. The Lewis number Le_1 is directly proportional to the thermal diffusivity and inversely proportional to the solute diffusivity of first concentration. As the thermal diffusivity increases the amplitude of disturbance waves also increases and system gets destabilize. If solute diffusivity of first concentration increases, Lewis number decreases therefore, solute diffusivity plays a stabilizing role.

The variation of oscillatory Rayleigh number with respect to Lewis number of second concentration Le_2 is shown in Fig. 10. With an increase in Lewis number, oscillatory Rayleigh number decreases which shows that Lewis number of second concentration destabilizes the system. For the same fluid, if we add second salts of high solute diffusivity, system stabilizes easily.

Fig. 11 depicts the effect of Vadasz number V_A on the neutral curves of oscillatory Rayleigh number. We observe that an increase in the value of the Vadasz number decreases the oscillatory Rayleigh number, indicating that the Vadasz number advances the onset of triple-diffusive convection. At constant porosity, Vadasz number is directly proportional to the Prandtl number and inversely propor-

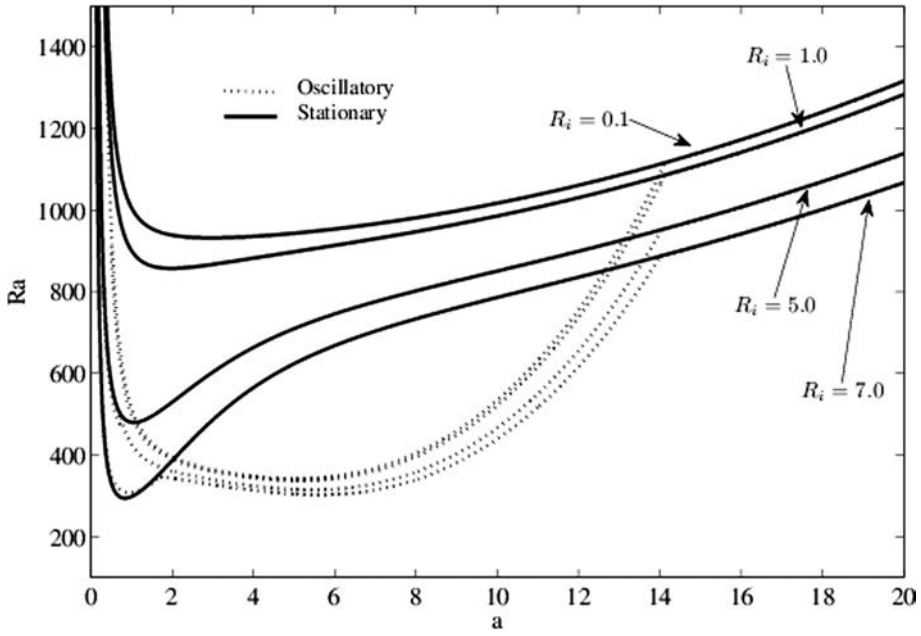

Figure 8. Variation of internal Rayleigh number on stationary convection and oscillatory convection.

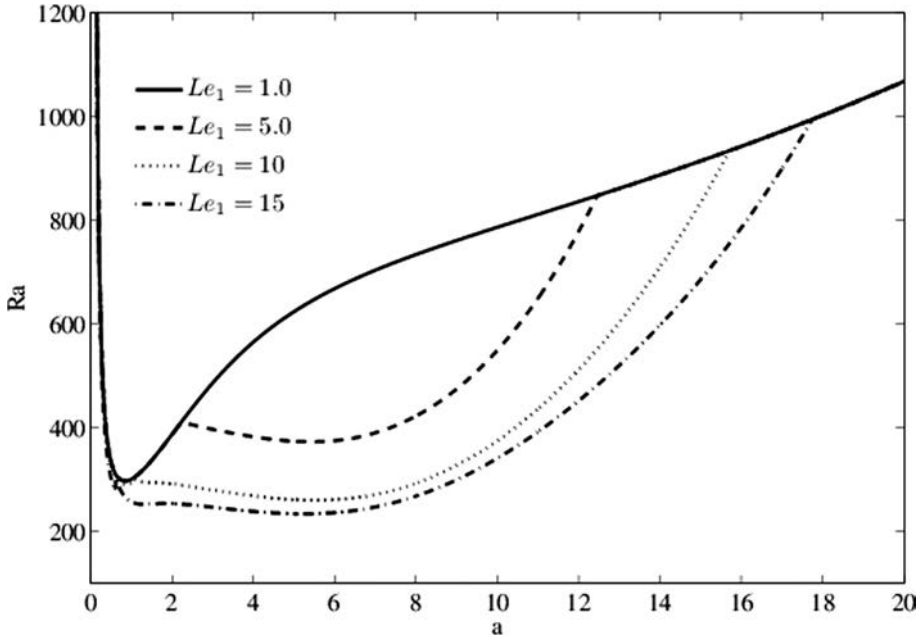

Figure 9. Effect of Lewis number on oscillatory convection.

tional to Darcy number. The increase in value of Darcy number *Da* is related to increase in medium permeability k_1 which has the tendency to retard the fluid flow and hence higher heating is required for the onset of convection. Therefore, *Da* delays the onset of convection in Maxwell saturated porous medium while Prandtl number advances the onset of convection. We also found that the Vadasz number has no effect on stationary convection.

9. Conclusions

The onset of triple-diffusive convection in a Maxwell viscoelastic fluid saturated isotropic and homogeneous porous layer in the presence of internal heat source is studied using linear stability analysis. An expression for Rayleigh number, for stationary convection and oscillatory convection is obtained. The main conclusions are:

I. The internal heat source has destabilizing effect in the stationary modes.
II. The viscoelastic parameter, Lewis number, porosity, Vadasz number have no effect on stationary convection while solute Rayleigh numbers enhance the stability in stationary mode.
III. Triple-diffusive convection stabilizes the stationary as well as oscillatory modes.
IV. The presence of internal heat source increases the onset of oscillatory convection.
V. The effect of normalized porosity and relaxation time parameter is to advance the onset of oscillatory convection.

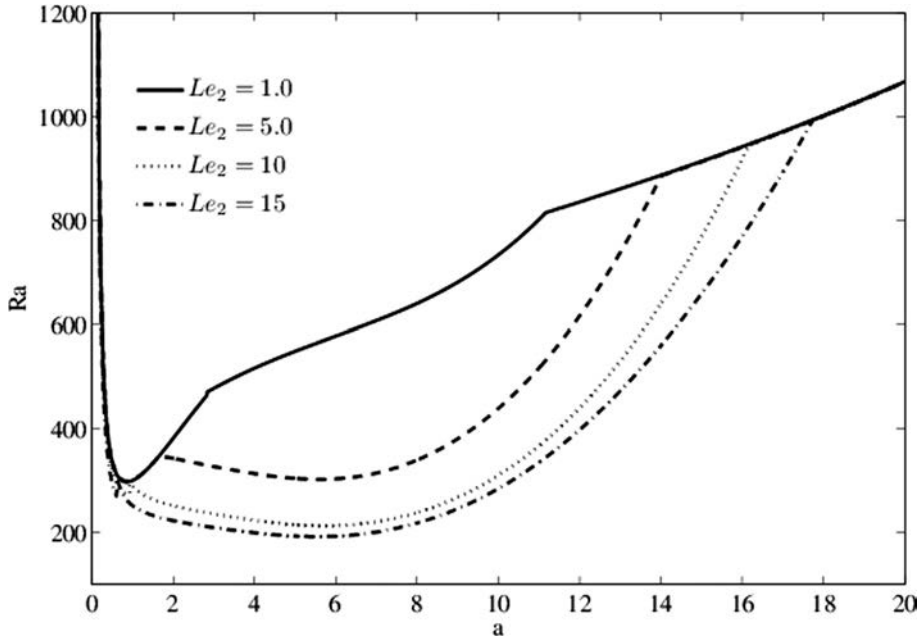

Figure 10. Effect of analogous Lewis number on stationary convection and oscillatory convection.

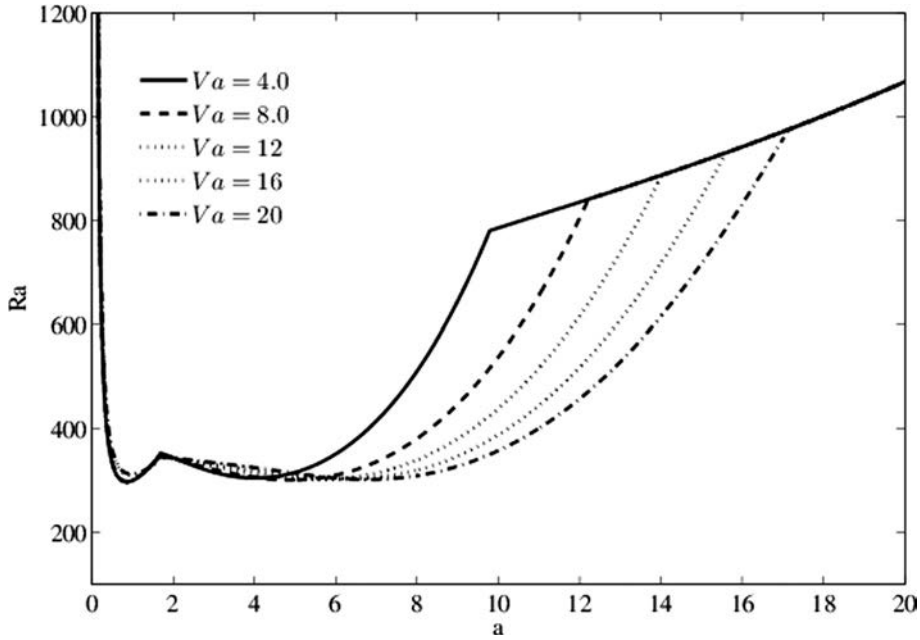

Figure 11. Effect of Vadasz number on oscillatory convection.

VI. The solute Rayleigh numbers are stabilizing the system while Lewis numbers have destabilizing effect.
VII. Vadasz number destabilizes the system in oscillatory mode.
VIII. The sufficient condition for the non-existent for overstability are

$$\frac{d^2}{\lambda_1 \kappa} > \pi^2 + a^2 > \frac{Qd^2}{k_T}, \quad k_T < \min\left(\frac{\sigma}{\varepsilon}k_{C_1}, \frac{\sigma}{\varepsilon}k_{C_2}\right).$$

References

[1] Takashima M. The effect of magnetic field on thermal instability in layer of Maxwell fluid. Phys Lett A 1970;33:371–2.
[2] Bhatia PK, Steiner JM. Thermal instability in a viscoelastic fluid layer in hydromagnetics. J Math Anal Appl 1973;41:271–83.
[3] Buchaskii LM, Stolin AM, Khudyaev SI. Theory of thermal instability of the flow of a viscoelastic fluid. J Appl Mech Tech Phys 1979;20:350–5.
[4] Kim MC, Lee SB, Kim S, Chung BJ. Thermal instability of viscoelastic fluids in porous media. Int J Heat Mass Transfer 2003;46:5065.
[5] Shivakumara IS, Naveen Kumar SB. Linear and weakly nonlinear triple diffusive convection in a couple stress fluid layer. Int J Heat Mass Transfer 2014;68:542–53.
[6] Wang S, Tan W. Stability analysis of soret-driven double-diffusive convection of Maxwell fluid in a porous medium. Int J Heat Fluid Flow 2011;32:88–94.
[7] Gaikwad SN, Malashetty MS, Rama Prasad K. Linear and nonlinear double diffusive convection in a fluid saturated anisotropic porous layer with cross diffusion effects. Transp Porous Media 2009;80:537.
[8] Malashetty MS, Biradar Bharati S. The onset of double diffusive reaction-convection in an anisotropic porous layer. Phys Fluids 2011;23:064102.

[9] Malashetty MS, Biradar Bharati S. The onset of double diffusive convection in a binary Maxwell fluid saturated porous layer with cross-diffusion effects. Phys Fluids 2011;23:064109.
[10] Kumar V, Kumar P. Thermosolutal convection in a viscoelastic dusty fluid with hall currents in porous medium. Egypt J Basic Appl Sci 2015;2:221–8.
[11] Zhao M, Wang S, Zhang Q. Onset of triply diffusive convection in a Maxwell fluid saturated porous layer. Appl Math Model 2014;38:2345–52.
[12] Sharma PK, Malik H, Kumar V, Kumar P. Triply-diffusive magneto convection in viscoelastic fluid through porous medium. Int Trans Appl Sci 2014;6 (4):495–510.
[13] Kumar V, Kumar P, Awasthi MK. Hydrodynamic and hydromagnetic triply diffusive convection in a viscoelastic fluid through porous medium. Special Top Rev Porous Media 2015;6(3):297–311.
[14] Bhadauria BS, Kumar A, Kumar J, Sacheti NC, Chandran P. Natural convection in a rotating anisotropic porous layer with internal heat generation. Transp Porous Media 2011;90:687–705.
[15] Bhadauria BS. Double-diffusive convection in a saturated anisotropic porous layer with internal heat source. Transp Porous Media 2012;92:299–320.
[16] Yuji T, Yasushi T. Effects of heat source distribution on natural convection induced by internal heating. Int J Heat Mass Transfer 2005;48:1164–74.
[17] Capone F, Gentile M, Hill AA. Double-diffusive penetrative convection simulated via internal heating in an anisotropic porous layer with through-flow. Int J Heat Mass Transfer 2011;54:1622–6.
[18] Bhadauria BS, Hashim I, Siddheshwar PG. Effects of time-periodic thermal boundary conditions and internal heating on heat transport in a porous medium. Transp Porous Media 2013;97:185–200.
[19] Ellahi R, Shivanian E, Abbasbandy S, Hayat Tasawar. Analysis of some magnetohydrodynamic flows of third order fluid saturating porous space. J Porous Media 2015;18(2):89–98.
[20] Rashidi S, Nouri-Borujerdi A, Valipour MS, Ellahi R, Pop I. Stress jump and continuity interface conditions for a cylinder embedded in a porous medium. Transp Porous Media 2015;107(1):171–86.
[21] Kandelousi Mohsen Sheikholeslami. KKL correlation for simulation of nanofluid flow and heat transfer in a permeable channel. Phys Lett A 2014;378(45):3331–9.
[22] Sheikholeslami M, Ganji DD. Heated permeable stretching surface in a porous medium using nanofluids. J Appl Fluid Mech 2014;7(3):535–42.
[23] Sheikholeslami M, Gorji-Bandpy M, Ganji DD, Soleimani Soheil, Seyyedi SM. Natural convection of nanofluids in an enclosure between a circular and a sinusoidal cylinder in the presence of magnetic field. Int Commun Heat Mass Transfer 2012;39:1435–43.
[24] Chhabra RP, Richardson JF. Non-Newtonian flow in the process industries. London: Butterworth-Heinemann; 1999.

Vivek Kumar received his M.Sc. (Mathematics) and M. Phil (Mathematics) degree from the Ch. Charan Singh University, Meerut (UP), India. He has obtained his Ph.D degree in Mathematics from same university in 2012. His research interests are Fluid Mechanics, Hydrodynamic stability and viscous potential flow. Currently he is working as Assistant Professor in the Department of Mathematics, Shri Guru Ram Rai (P.G.) College, Dehradun (Uttarakhand), India.

Mukesh Kumar Awasthi has done his post-graduation in Mathematics from the University of Lucknow in the year 2007. He has obtained his Ph.D degree in Mathematics from Indian Institute of Technology Roorkee in 2012. His research interests are Fluid Mechanics, Hydrodynamic stability, viscous potential flow, Numerical solution of PDE, Mathematical modeling and Computational Physics. Currently he is working as Assistant Professor in the Department of Mathematics, University of Petroleum and Energy Studies, Dehradun (Uttarakhand), India.

Enzyme and Microbial Technology 118 (2018) 92–101

Contents lists available at ScienceDirect

Enzyme and Microbial Technology

journal homepage: www.elsevier.com/locate/enzmictec

Sustainable power generation from sewage and energy recovery from wastewater with variable resistance using microbial fuel cell

Debajyoti Bose[a,*], Himanshi Dhawan[b], Vaibhaw Kandpal[b], Parthasarthy Vijay[b], Margavelu Gopinath[c]

[a] Department of Electrical, Power & Energy, University of Petroleum & Energy Studies, Energy Acres, Bidholi, Dehradun 248007, UK, India
[b] Department of Chemical Engineering, University of Petroleum & Energy Studies, Energy Acres, Bidholi, Dehradun 248007, UK, India
[c] Department of Biotechnology, Selvam College of Technology, Salem Road (NH-7), Pappinaickenpatti (Post), Namakkal, 637003, Tamil Nadu, India

ARTICLE INFO

Keywords:
Wastewater
MFC
Bacteria
Nanowires
Bioelectricity

ABSTRACT

Wastewater from sewage sources contribute significantly to water pollution from domestic waste; one way to recover energy from these sources while at the same time, treating the water is possible using Microbial Fuel Cell. In this work, a two chambered microbial fuel cell was designed and fabricated with carbon cloth electrodes and Nafion-117 membrane, having Platinum as the catalyst. Wastewater from an organic load of 820 ± 30 mg/l reduced to around 170 mg/l, with the change in pH from 7.65 ± 0.6 to 7. 31 ± 0.5; over the time of operation the biochemical oxygen demand from an initial 290 ± 30 mg/l reduced to 175 ± 10 mg/l. Open circuit voltage was achieved mostly between 750–850 mV, with inoculated sludge produced a peak open circuit voltage of 1.45 V between fed-batch cycles. For characterization of power generated, polarization curves are evaluated with varying resistance to examine system stability with varying resistance. The current density and power density are reported to peak at 0.54 mA/m^2 and 810 ± 10 mW/m^2 respectively. The development of stable biofilms on the anode contributes to the power generation and was evaluated using microscopic analysis, this shows bacteria present in wastewater are electroactive microbial species which can donate electron to an electrode using conductive appendages or nanowires, while consuming the organic matter present in the wastewater. Such systems employ microbial metabolism for water treatment and generate electricity.

1. Introduction

Economic growth of nations has always depended on fossil fuels, over the past century, however with their depleting reserves and continuing damaging impact to the environment means they cannot sustain the global economy indefinitely. The Paris accord (COP 21) famously spoke about bringing down net CO_2 emissions significantly with a global commitment. [1] One projection of population growth coupled with current economic growth shows a requirement of global demand of 41 TW by 2050, at current energy consumption rate [2]. As the population grows exponentially, energy requirements do too. Thus, using conventional sources to power these requirements, will release additional CO_2 emissions over and above what is released now, thereby accelerating environmental damage and climate change. [3] An efficient method of energy production to meet this global demand on carbon neutral basis has to be emphasized.

Microbial Fuel Cells or MFCs represent an efficient route to convert the energy in wastewater to electricity, while at the same time treating the wastewater. [4] The trend in the energy economy to move towards clean form of energy and its recovery from waste are key drivers for this technology [5]. Further, such systems can support the Water infrastructure, with the advantage being non-combustion based processes that represent a direct conversion of organic matter to energy using bacteria present in it. One projection showed about 2.4 billion people globally lack adequate sanitation and the means to afford it [3], one major constituent in this regard is the wastewater generated from Sewage. For instance, in India an estimated 28, 354 million Litres per day. (MLD) of sewage is generated by the major cities, and the sewage treatment capacity is around 11, 786 MLD and reuse of this treated water is restricted to agricultural and industrial purpose. [6] While these numbers change every year, the important thing is to interpret them, as in the context of MFCs these represent an opportunity for energy recovery and wastewater treatment.

Any wastewater treatment plant has 4–10% amount of energy in that water than we use to treat that wastewater, so if this energy can be extracted, even a small fraction of it, we can make wastewater self-

* Corresponding author.
E-mail address: dbose@ddn.upes.ac.in (D. Bose).

https://doi.org/10.1016/j.enzmictec.2018.07.007
Received 10 June 2018; Received in revised form 14 July 2018; Accepted 30 July 2018
Available online 03 August 2018
0141-0229/ © 2018 Elsevier Inc. All rights reserved.

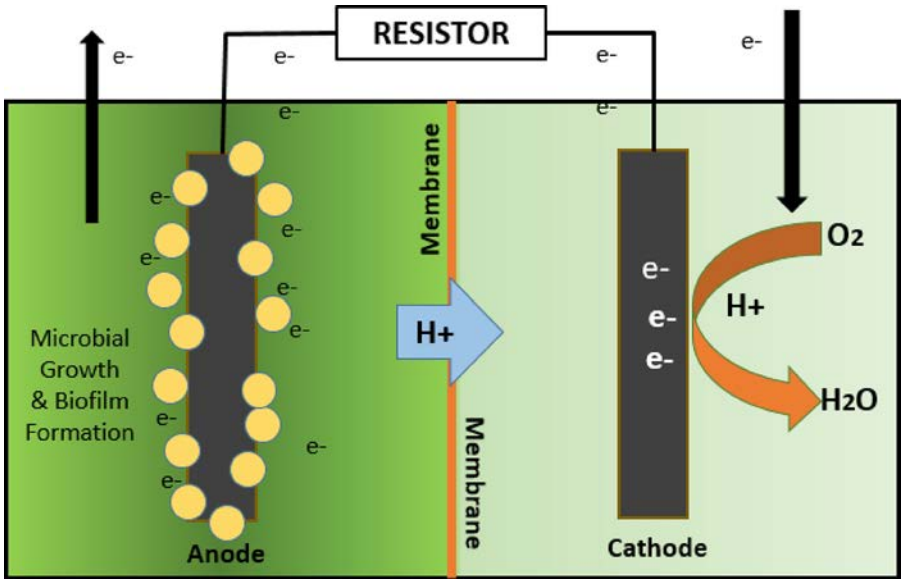

Fig. 1. In MFCs, the wastewater is charged in the anode, where microbes can utilize the organic loading in the water, to release electrons to a conductive carbon electrode, which then transfers the electron to the cathode, via the load circuit to complete the reaction, the voltage drop measured across the resistance is utilized to compute the power generated by the system. The anode and the cathode are separated by a membrane, the electrical power generated is direct current (DC).

sufficient. As shown in Fig. 1, MFCs are electrochemical systems, where the wastewater goes in the anode and a conductive solution for ion transfer and oxygen reduction is at the cathode. The microbial growth takes place on the anode, in the form of biofilms, which are capable of electron transfer by breaking down organic matter present in the wastewater, these electrons then travel the length of the circuit through load (shown here as resistor) to the cathode, and the process is completed. The membrane separates the anode from the cathode and drives the ion transfer owing to different potentials of the electrodes. [7] This aspect of bacteria decomposing organic matter is based on relatively recent discoveries, which showed that microbes can donate electrons to an electrode [8]. The mechanism for electron transfer by the bacteria is via conductive appendages called nanowires, or directly through point of contact on the anode [9].

Present work has utilized a two chambered MFC, with carbon electrodes and Platinum catalyst, having Nafion-117 as the membrane. Wastewater from a sewage treatment plant was utilized for energy recovery and wastewater treatment. Data was recorded on 24 h' basis, in a fed-batch cycle for an initial open circuit analysis. The same was followed by bioelectricity generation by measuring voltage across external resistors on 24-hour basis and its effect on COD of the wastewater. Both Current and Power density were calculated by normalizing them to the anode surface area. A relation was established between volume of working liquid with the COD removal efficiency and bioelectricity production in the form of Coulombic efficiency. Change in absorbance property of wastewater was evaluated using UV–vis spectrophotometry. AFM imaging is done for the anode surface morphology, and SEM for evaluating development of stable biofilms on the anode.

2. Materials and methods

2.1. System fabrication and assembly

For the MFC, plexiglass reactor was fabricated as shown in Fig. 2A, a circular housing holding the anode, membrane and the cathode (Fig. 2B), connected to cylindrical chambers (for the anode liquid and cathode liquid respectively). There is an inset for the anode and cathode wires from which it is connected to the respective electrodes. Gaskets are used to ensure proper system fitting (Fig. 2C). The end plates press the gaskets towards the electrode holdings and the entire system is bolted together. Data was recorded using a fully calibrated multi-meter (KELVIN 50LE, United States).

2.2. Wastewater

The University Sewage treatment plant (STP) was the source of the wastewater; untreated water was collected from the inlet channel. As explained in the later section, for one study, the sludge from sewage was inoculated with sucrose solution [10] to see the effect of substrate concentration on voltage.

2.3. Electrodes

Plain Carbon cloth (Type CC4P, E-TEK, USA) without wet proofing electrode is used as the anode and Carbon cloth with platinum (as catalyst) coating is used as the cathode (Fig. 2D). For the cathode, commercially available Platinum (10 wt.% Pt/C, E-TEK) was mixed with 5% Nafion™ (acting as a chemical binder) liquid solution to form a paste (8-µl-binder per mg-Pt/C catalyst) and was applied to one side of the electrode and dried at room temperature for 48 h. The side with the catalyst loading faces the membrane. [11] The use of carbon based electrodes is common in MFCs as they have higher conductivity and are well suited for microbial growth. [12,][13] In the anode chamber, wastewater (from sewage) is the liquid used and for the cathode chamber, phosphate buffer is used. Phosphate buffer is prepared by dissolving potassium phosphate dibasic (Mol. Wt. 268 g/mol, molarity 0.0754 M) and potassium phosphate monobasic (Mol. Wt. 138 g/mol, molarity 0.0246 M) in demineralized water. The function of the phosphate buffer is to maintain the solution conductivity at the cathode, and to ensure ease of ion transfer from the biofilm development [14].

2.4. Membrane

Nafion-117 (Dupont, USA) was used as the membrane owing to its high permeability, with reducing unwanted substrate flux from anode to cathode (i.e. fuel crossover) and improving Coulombic efficiency. [15] Pre-treatment and activation of Nafion-117 membrane allowed removal of any impurities that were present in the film [16]. This was done by keeping it for 1 to 1.5 h in 3% H2O2, followed by washing with deionized water, 0.5 M H2SO4 followed by again washing with deionized water. This method for pre-treatment of Nafion-117 has been modified from one study to activate and remove impurities from the membrane surface. After this, the system was bolted together, the anode and cathode chambers were filled with deionized water when the MFC was not being used to maintain the PEM's good conductivity [9].

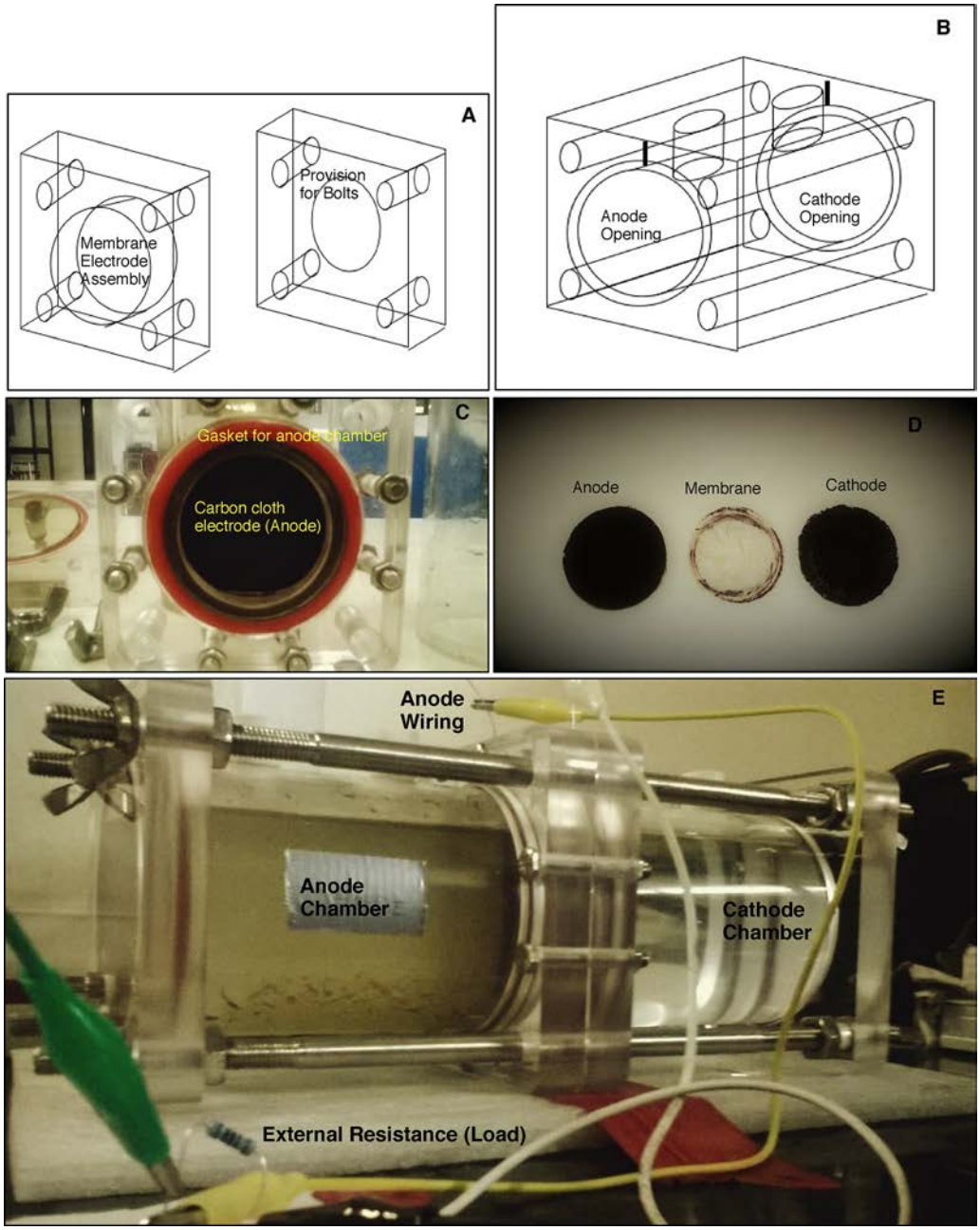

Fig. 2. (A) CAD of the Membrane-Electrode assembly cube with provision for bolts at the corners (B) The cube is shown bolted together, with the anode and cathode on both sides, and the membrane in between them (C) Actual setup with plexiglass showing the anode with the gasket provision for attaching the anode chamber (D) The electrodes and the membrane (E) Assembled MFC setup with wastewater in the anode, and phosphate buffer in the cathode, connected to an external load.

2.5. Operation

Wastewater analysis was performed in batch mode with working liquid volume of 250 ml for both the anode and cathode liquid; under ambient temperature of 25 ± 3 °C. Fig. 2E shows the MFC wired to the data acquisition system.

2.6. Measurements

Voltage drop was recorded across the arms of the resistor using a fully calibrated multi-meter (KELVIN 50LE, USA). For chemical characterization of the wastewater COD, BOD and UV–vis Spectrophotometry was done before and after it was fed to the system, to see the change in organic load in it. Open Circuit voltage was computed directly by connecting the anode and cathode wires to the data acquisition system. For electrical power generation, external resistors were connected to the anode and cathode wires and voltage drop was measured across the arms of resistor to obtain polarization curves. [17] Using ohm's law (V = I.R), current was calculated, using P = V. I, power generation was calculated [12]. Further, this current and power generation was normalized to the anode surface area to calculate current density (mA/m^2) and power density (mW/m^2) [18]. Coulombic efficiency was calculated using the same external resistor based on changes in COD concentration [19]. Atomic Force Microscopy (AFM) imaging was done for evaluating the surface morphology of the anode and Scanning Electron Microscopy (SEM) was done to evaluate the development of nanowires on the anode as a mode of electron transfer.

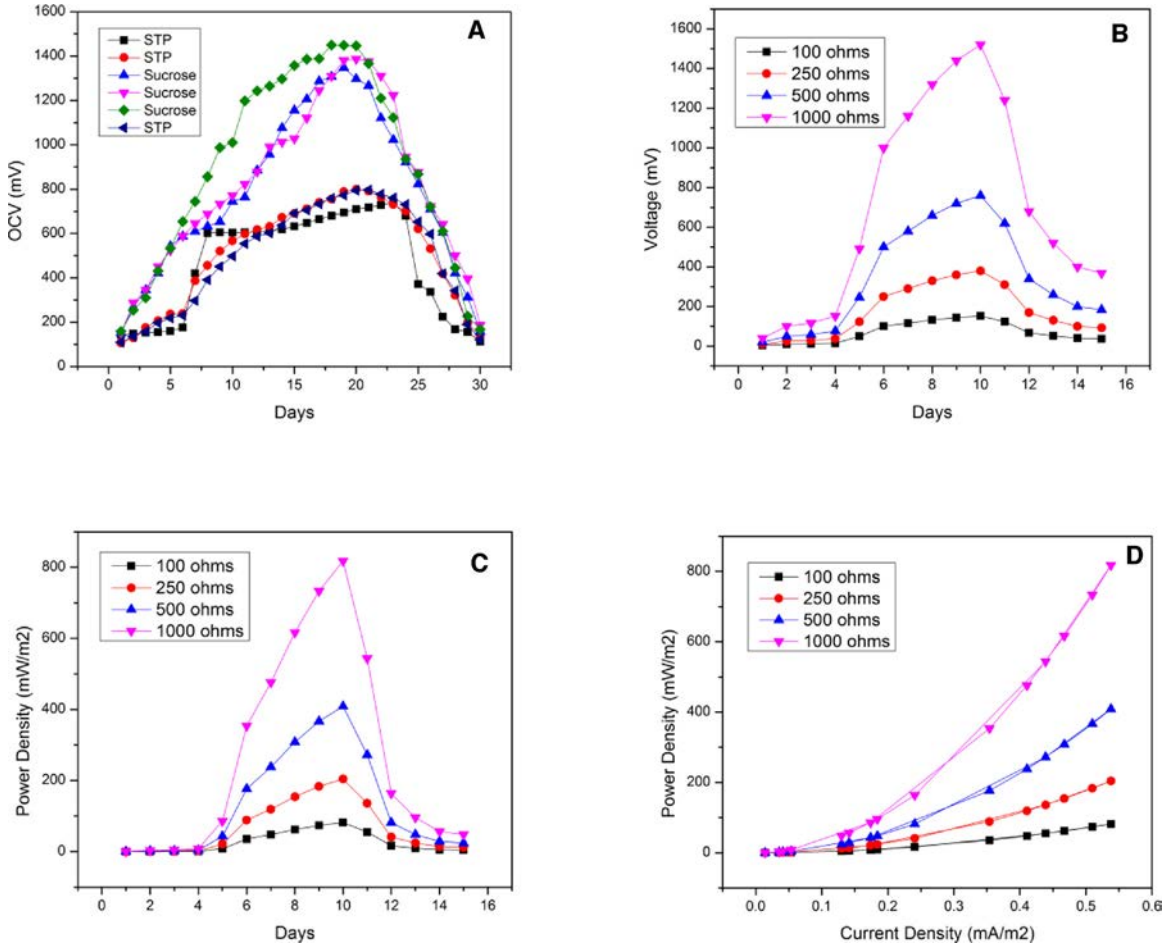

Fig. 3. (A) The wastewater from the Sewage Treatment Plant (STP) generated voltages between 750–850 mV, with an inoculated sludge the value further stablized at 1.30–1.45 V between cycles (B) Polarization curves obtained by varying resistances with peak voltage at 1500 ± 20 mV (C) Power density over days peaked at mW/m^2 (D) Power density shown as a function of current density over the total days of operation.

3. Results and discussions

3.1. Open circuit analysis

The wastewater charged in the system produced a peak voltage of around 800 ± 30 mV after two weeks of operation, and with other cycles of similar nature, the generated voltage would reach a peak value between 750–850 mV, this voltage generation is measured by directly connecting the cathode and anode wire to the data acquisition system. As shown in Fig. 3A, further some amount of sludge from the STP was inoculated with sucrose solution (10% by weight), to see the effect of substrate addition on MFC performance. This achieved a peak voltage of 1.45 V. This shows in mixed cultures, such as wastewater streams, different bacteria can grow setting different potentials. [20] Following peak voltage generation, a decline was observed due to depletion of organic matter. Open circuit analysis implies infinite resistance and zero current, and sets the potential for the voltage that can be achieved with wastewater streams theoretically [12]. An important thing to remember here is that effective COD removal is only possible when system generates current i.e., using a resistor to connect the anode and the cathode [11], further this reduces the time of operation as well, thereby achieving high COD removal rates.

3.2. Power generation

As resistances are decreased from open circuit potential, the voltage decreases. [21] And power generation pattern from these systems can be observed. As shown in Fig. 3B, the polarization curves give a measure of how the MFC system performs over varying resistance. The resistors used for the polarization studies are 100 Ω, 250 Ω, 500 Ω and 1000 Ω. Further the current density and powerdensity were calculated by normalizing the anode surface area to the current and power generated by the system.

$$I_{Density} \frac{V_{MFC}}{R \times A_{anode}} \quad (1)$$

$$P_{Density} \frac{V_{MFC}^2}{R \times A_{anode}} \quad (2)$$

As shown in Eq. (1), $I_{Density}$ is the current density (computed in mA/m^2), V_{MFC} is the voltage drop recorded across the external resistor (R), and A_{anode} is the surface area of the anode (28.26 cm^2), where the microbial growth takes place which is responsible for the electron transfer through it. [8] Similarly, in Eq. (2) $P_{Density}$ is the power density (computed in mW/m^2). The Power density was recorded with a peak value of around 817 mW/m^2 with the 1000 Ω resistor (Fig. 3C) and the Current density was found to be around 0.55 mA/m^2 (Fig. 3D).

The voltage generated in a MFC is far more intricate to predict or understand as compared to a chemical fuel cell [22]. In the MFC, the bacteria take time to colonize the electrode and produce enzymes or structures that are needed for electron transfer from outside its cell. In mixed cultures these electroactive microorganisms can grow [23], setting different potentials further even in pure culture. These potentials cannot be easily predicted. However, there are limits to maximum voltage generated by these systems based on thermodynamic

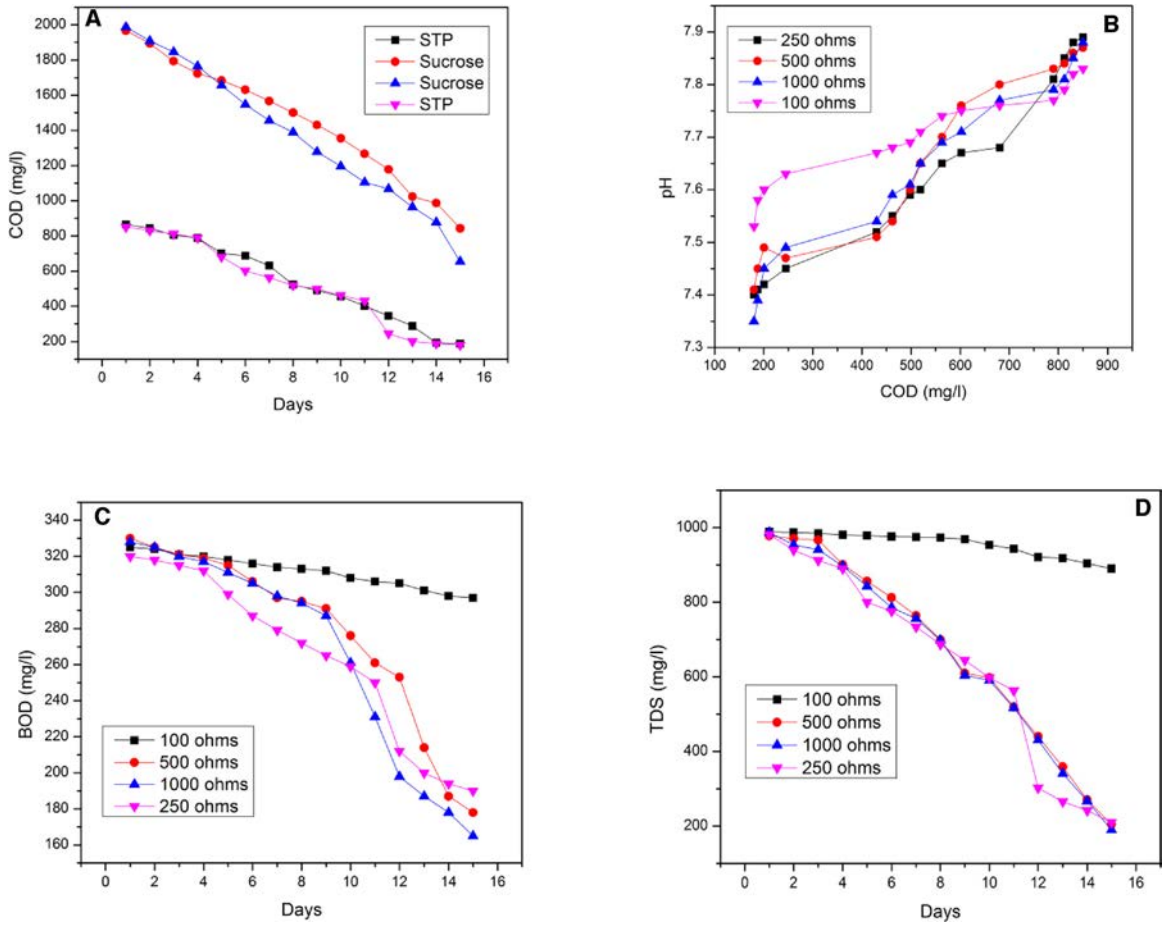

Fig. 4. (A) COD removal rate over days of operation with wastewater from the STP and with sucrose as substrate (B)) With the decrease in COD concentration pH from an initial range of 7.89 ± 0.2 came to close to clean water pH of 7.3 ± 0.15 (C) BOD content of the wastewater saw a constant decrease up to 175 ± 15 mg-BOD/l, this indicates that MFCs have higher organic load removal rates with external load attached, instead of when in open circuit condition (D) TDS removal efficiency with varying resistance. gone [32]. However, it is seen that when the COD level reaches around 180-170 mg-COD/l and the electricity generation almost stops.

relationship between the electron donors (i.e., the substrates) and acceptors (oxidizers).

Coulombic efficiency (CE) for the existing system was evaluated to be 32%, which as studies have suggested is higher for Nafion membrane based MFCs compared to those obtained from membrane-less MFCs [18,20,24]. At present most literature has reported CE ranging from 5% to 59% for wastewater having complex substrates [25–27]. Improvements for accessibility of further insoluble substrates thereby leading to better organic matter degradation and more stable anodic biofilms will be the key for achieving higher CEs.

3.3. Chemical characterizations

The COD removal efficiency for all cycles was around 78%, mostly declining from an initial 820 ± 30 mg/l to around 180 ± 30 mg/l over two weeks of operation as shown in Fig. 4A, the pH during the same period of operation stabilized at around 7.3 ± 0.15 (basic range) from an initial 7.89 ± 0.2 as shown in Fig. 4B. The current produced by the system helps in faster COD consumption rates, which reduce the loss to background processes as well, further this means the COD can be removed from the aerobic microbes to make electricity at faster rates [28]. For COD analysis, an evaluation of microbial metabolism for contaminant removal was also evaluated using sucrose solution [29] as substrate, which increased the COD to around 1960 ± 20 mg/l. The same however observed a similar trend in COD consumption by the microbes, the study was continued till it reached the STP concentration rates (of around 820 ± 30 mg/l). This shows increase in sludge material can accelerate removal rates with higher resistance, further this opens up the scope of MFC systems to be effectively integrated with wastewater treatment plants, where significant amount of sludge can be added to the wastewater itself [30], and in the process, treat the waste and the sludge, while generating electricity.

The current density and COD removal plummets after about week of operation. When the current density plummets, this shows the system is not generating enough electrical power. [31] For practical purposes the electricity should be generated till the COD is completely

As shown in Fig. 4C, the effect of varying resistance on BOD concentration, most efficient removal is achieved with the highest resistance (1000 Ω), the BOD content of the wastewater from an initial 300 ± 20 mg-BOD/l decreased over the next two weeks of operation and part of the BOD removal is directly attributed to power generation, as the comparative analysis with current density shows. Similar to the COD removal curve, the same drop in current density is observed for the BOD removal rate as well which stabilizes around 175 ± 15 mg-BOD/l. This drop in current density is attributed to the active electric field inside the system [3], which is triggered by the ion transfer owing to the different electrode potentials. For instance, the wastewater and the negatively charged materials are forming the anode potential, and the positively charged species are attributing to the cathode, and this accelerates the flux of organics to the anode.

Further, as shown in Fig. 4D, the dissolved solids content measured as the total dissolved solutes (TDS) dropped down from an initial

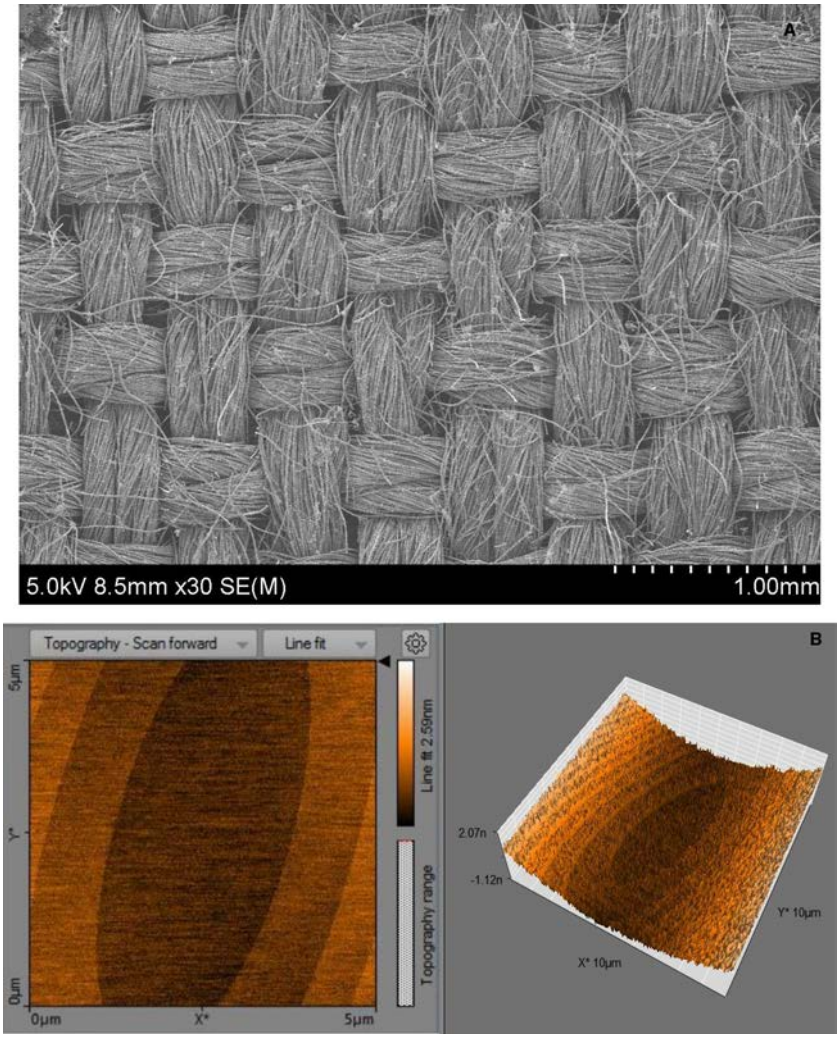

Fig. 5. (A) SEM image of carbon cloth anode (B) 5-micron scan of the anode surface (Carbon cloth) by AFM imaging and 3D view of the 5 µm scan of the anode surface.

960 ± 20 mg/l of soluble organic load to 200 ± 12 mg/l in the wastewater with varying resistance, giving an overall removal efficiency of 78%, thus it is expected that production of solid matter from the MFC will be reduced to around 40% of that generated from an aerobic process. This gives MFC based systems the advantage of systematic cost reduction for solids handling at a treatment facility, and thus reflects a savings in capital expenditures [33].

A Solid Contact unit would require energy input for reactor mixing and then the treatment, such can be avoided with MFC based water treatment processes; another advantage of this would be reducing the biogas formation, which can adversely affect power production as methane [34]. One study showed that a 40% solids reduction from wastewater sources can yield an electrical equivalent of 151 kW [35]. The effect of removal of dissolved solids can also improve the settling characteristics of MFC biofilms.

3.4. Polarization curves

It is seen that with most studies with the wastewater, the low resistance usually attributes to low power and related organic load removal efficiency. [36] The potentials of the anode and the cathode set the limits for the maximum voltage achievable for power generation, using the potentials, substrates such as sucrose can be used to accelerate the biochemical basis for power generation.

A critical thing to remember here is the energy recovery from the wastewater is essential. And this can be accelerated with external resistance and by increasing the organic loading. The drop in COD level is attributed to the chemical flux (J) in the biofilm, as the anode and the cathode are at different potentials, this accelerates the flux of organics to the anode; mathematical simplification for the Chemical flux using Nernst-Planck equation shows a direct influence on diffusion coefficient in these electrical fields [3], so when the microbes run out of food (the mg-COD/l of the organics) the electrical field starts to collapse, as the electrical field starts to collapse, a flux is experienced by the biofilm due to shortened supply of organics and everything comes to a halt.

The chemical flux into the biofilm (J) is consistent with first order kinetics, where k_1 represents first order rate constant as a function of microbial kinetics. The flux of ions under the influence of ionic concentration gradient ($\nabla . c$) and an electric field (E) is given by the Nernst-Planck equation [31] as:

$$\frac{\partial c}{\partial t} = -\nabla . J \tag{3}$$

Where $\frac{\partial c}{\partial t}$ is the change in concentration of substrate over time, and J is the chemical flux into the biofilm [37], which can be further written as:

$$J = -\left[D\nabla c + \frac{Dze}{k_B T} c\left(\nabla \varnothing + \frac{\partial A}{\partial T}\right)\right] \tag{4}$$

Where D is the diffusivity of the chemical specie, c is the change in

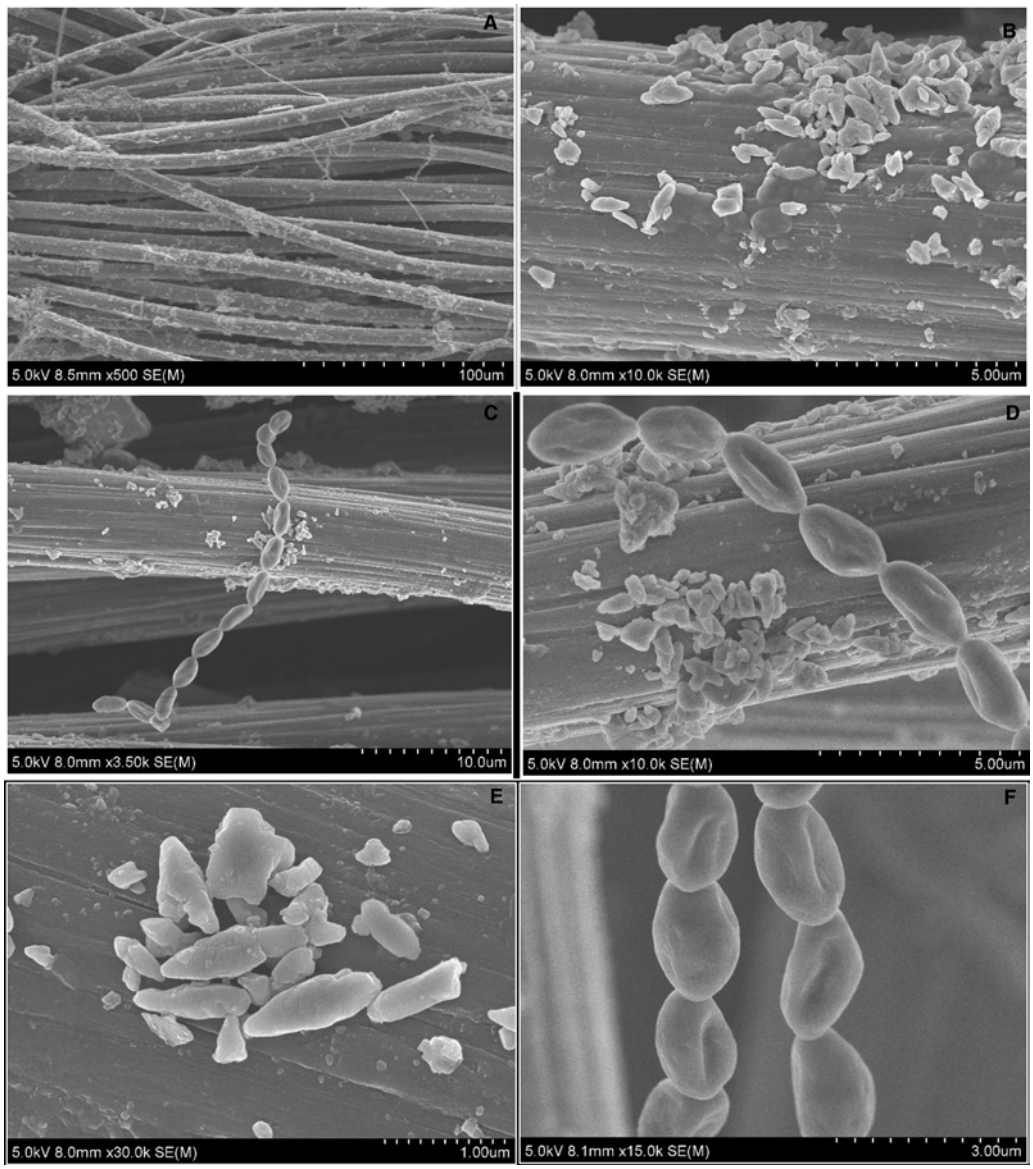

Fig. 6. (A) 100 μm imaging of carbon cloth after MFC operation, with visible bacteria growth and nanowires formation (B) 5 μm imaging of the anode with bacteria colony on it (C) Conductive appendages formed by bacteria for electron transfer to the anode (D) 5 μm view of bacteria chains formed (E) Colonies formed on the anode (F) 3 μm imaging of the conductive appendages.

concentration, z is the valence of ionic specie, e is the element charge, k_B is the Boltzmann constant, $\varnothing$ is the electric potential, and A is the magnetic vector potential.

Now substituting the value for chemical flux (J) into Eq. (3) to simplify the Nernst-Planck equation for the diffusion coefficient (D) as a function of the electric field [38] (given by$\overline{\nabla}\varphi$) the same can be written as:

$$J = [uc_i - Dc_i] - \frac{ziDF\nabla\varnothing}{RTc \downarrow i} \tag{5}$$

Setting time derivative to zero, and the fluid velocity to zero (with only ion specie movement):

$$J = [0 - Dc_i] - \frac{ziDF\Delta E}{RT\Delta x\, c \downarrow i} \tag{6}$$

The above can be further simplified and written as:

$$J = -\left(\frac{1 + F\Delta E}{RT}\right)D \Big\downarrow c\, 10 - \frac{\Delta c \downarrow i}{\Delta x} \tag{7}$$

Eq. (5) shows the chemical flux into the biofilm *(J)* can have a factor of ten impact on the effect of diffusion coefficient *(D)* in these electrical fields [39,40], so when the microbes starts running out of the substrate, the electrical field starts to fall, no organic load is regenerated in batch operation to the electrodes and this brings down both the COD and the BOD content of the wastewater, thus decreasing the current density.

3.5. Microscopic Analysis

Scanning Electron Microscopy or SEM is a powerful tool for analysing structures as shown in Fig. 5A, for the carbon cloth anode. Atomic Force Microscopy (AFM) is used to evaluate surface topographies, as shown in Fig. 5B, the topographical images were obtained at the resolution of 5 μm in contact mode operation. The steps between terraces comprise a staircase [22] of increasing brightness (height) from the centre of the anode toward the circumference.

As shown in the images of Fig. 6, bacteria capable of exo-electrogenic activity forms the background of MFC technologies. [3] Mixed cultures present in wastewater streams which forms electroactive

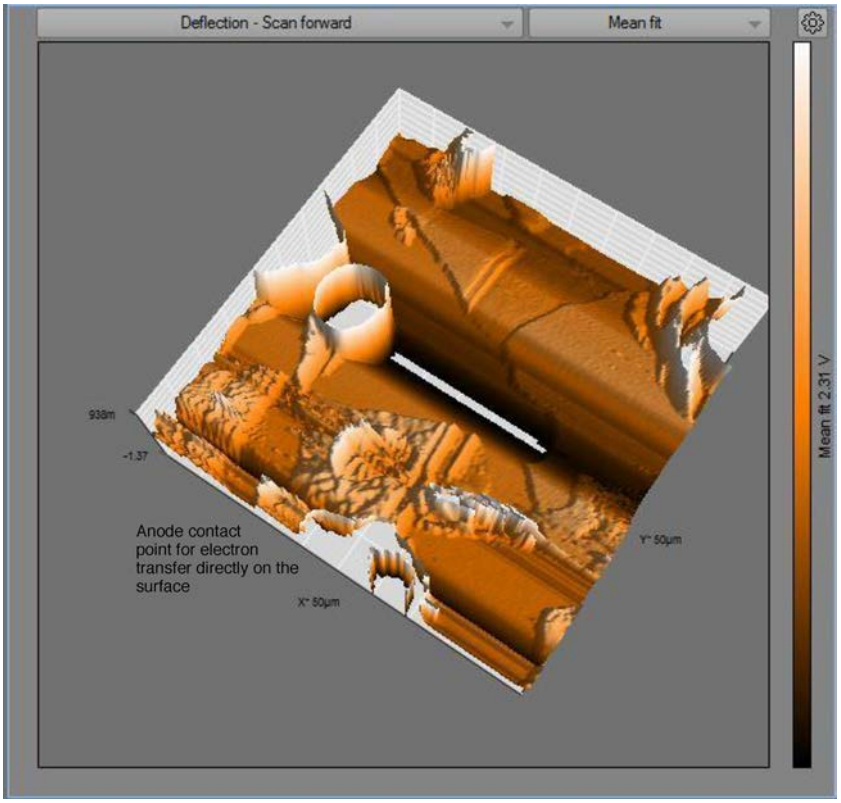

Fig. 7. Surface of the anode (AFM scan at 50 µm) showing protrusions or surface blebs, enabling cell-surface electron transfer by the bacteria.

biofilms in MFCs suggest the sheer diversity of microbial communities, which so far are known to transfer electrons to anode surface via two mechanisms, namely electron shuttling through self-produced mediators and nanowires [21]. Several studies have shown similar bacteria metabolism using.

Pseudomonas aeruginosa, *Geobacter* and *Shewanella* species. [3,33] In addition to these electrons transfer routes, studies have shown *Shewanella* have been effective for ferric iron reduction through membrane-bound electron carriers. [41]

It is interesting to note that apart from conductive nanowires, electron transfer by the bacteria is also possible from surface of the cell to the anode. [22] Close examination of the anode using AFM imaging (Fig. 7) reveal protrusion on the surface that are not nanowires, and certainly could be conductive points of contact. This shows mixed bacteria present in sewage have more adhesive linking with the anode under anaerobic conditions, thus allowing closer contact required for electron transfer from the cell surface even without the use of conductive appendages.

Although, it must be said that such information on electron transfer mechanisms are critical to describe how bacteria colonize and maintain viable cells on the surface of the electrode [42], the future scope in this can be the exploration of competition among bacteria for the surface to maintain anodic potentials.

3.6. Spectrophotometry analysis

UV-Vis spectrophotometer is an effective tool along with COD determination, to evaluate mass concentration of ions in a liquid sample. Here, the wastewater was evaluated using the spectrophotometer before it is fed and after the end of one complete cycle, to evaluate the difference in absorption property. As shown in Fig. 8, deionized water is used as a reference (ideal absorption property), and a comparison has been made with wastewater, before and after putting into the system.The effect of pH, operating temperature, substrate concentration, and electrode material are model parameters to understand system performance and anomalies associated with such systems. Understanding the biofilm formation is interesting, as an accurate modelling of biofilms is a demanding task, given the interactions of living, self-organizing organisms i.e. the bacteria. However, taking these interactions into consideration and the experimental justification of systematic MFC performance, one can speculate to explain the evolution of biofilm, like attachment, growth and decay. For instance, we know that biofilm stability is not consistent with wastewater having acidic pH, and system performance is usually stable at pH over seven, studies with domestic wastewater and acetate has confirmed the same [18,31,37,43].

4. Conclusion

Wastewater from sewage contributes to significant water pollution globally, this work found these sources to be an effective fuel in MFCs for energy recovery and removing the contaminants in the process. Such sources using the present system produced OCV in the range of 750–850 mV, further with increase in substrate concentration, value increased to around 1.3–1.45 V. Polarization curves showed an overall current density of 0.54 mA/m^2 and power density of 810 ± 10 mW/m [2]. COD removal efficiency of around 78% was achieved with reducing the overall COD to around 170 mg/l, along with effective BOD removal from 290 ± 30 mg/l to 175 ± 10 mg/l and TDS removal from 960 ± 20 mg/l to 200 ± 12 mg/l, further a significant relation is established between the organic load and the potentials set at the anode and cathode which makes this system efficient. Carbon cloth is used as electrodes due to its conductive nature, and Nafion-117 is used as membrane owing to its good thermal stability and high porosity. Microscopic analysis revealed how bacteria is able to form stable biofilms on the anode for generating this bioelectricity.

An interesting aspect of biofilm formation in the MFC on the anode is that the anode doesn't appear to foul over time. This means bacteria

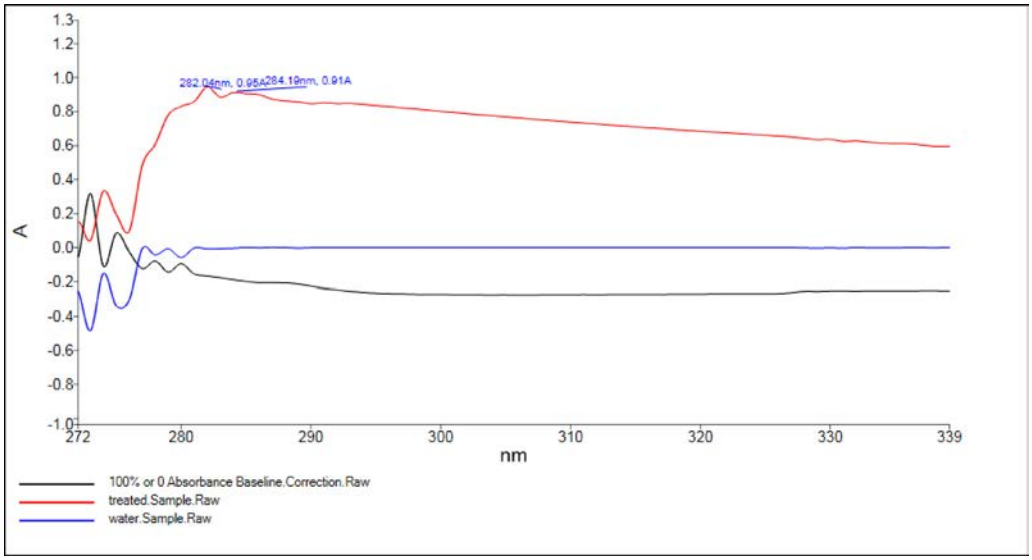

Fig. 8. UV Spectrophotometry for wastewater, the red line represents the treated sample, and the blue line represents the untreated wastewater, as a function of baseline absorbance (DI water), the absorption property of treated water has improved significantly after a batch MFC operation (For interpretation of the references to colour in this figure legend, the reader is referred to the web version of this article).

on the surface remains viable and able to continuously use the surface for electron transfer. Hence, it is reasonable to hypothesize that there are mechanisms through which bacteria can colonize on surfaces without any ecological damage, and use these colonization strategies to occupy a unique niches leading to MFC technology being a non-combustion based energy recovery process that can be an integral part of new frontiers of energy exploration, wherein a wastewater treatment plant can be converted to a power plant.

Acknowledgments

This work was supported by SEED division of R&D at University of Petroleum & Energy Studies, Dehradun, India. The authors are thankful to Dr. Jitendra K. Pandey and his research team for their continuous support and guidance. The authors are grateful to Dr. Shailey Singhal and Dr. Kamal Bansal for supporting this project during its infancy through various research initiatives.

References

[1] A. Bows-Larkin, All adrift: aviation, shipping, and climate change policy, Clim. Policy 15 (2015) 681–702.
[2] S. Banerjee, M.N. Musa, A.B. Jaafar, Economic assessment and prospect of hydrogen generated by OTEC as future fuel, Int. J. Hydrogen Energy 42 (2017) 26–37.
[3] B.E. Logan, Microbial Fuel Cells, John Wiley & Sons, 2008.
[4] D. Bose, M. Gopinath, P. Vijay, Sustainable power generation from wastewater sources using microbial fuel cell, Biofuels, Bioprod. Bioref. (2018).
[5] K. Caneon, S.A. Kumar, N. Joris, Modelling of regeneration and filtration mechanism in diesel particulate filter for development of composite regeneration emission control system, Arch. Mech. Eng. 65 (2018).
[6] D. Cardoen, P. Joshi, L. Diels, P.M. Sarma, D. Pant, Agriculture biomass in India: part 2. Post-harvest losses, cost and environmental impacts, Resour. Conserv. Recycl. 101 (2015) 143–153.
[7] G. Hernández-Flores, et al., Batch operation of a microbial fuel cell equipped with alternative proton exchange membrane, Int. J. Hydrogen Energy 40 (2015) 17323–17331.
[8] J.R. Kim, S. Cheng, S.-E. Oh, B.E. Logan, Power generation using different cation, anion, and ultrafiltration membranes in microbial fuel cells, Environ. Sci. Technol. 41 (2007) 1004–1009.
[9] S. Cheng, H. Liu, B.E. Logan, Power densities using different cathode catalysts (Pt and CoTMPP) and polymer binders (Nafion and PTFE) in single chamber microbial fuel cells, Environ. Sci. Technol. 40 (2006) 364–369.
[10] S. Nasirahmadi, aa. Safekordi, Whey as a substrate for generation of bioelectricity in microbial fuel cell using E.cOli, Int. J. Environ. Sci. Technol. (Tehran) 8 (2011) 823–830.
[11] S.S. Kumar, S. Basu, N.R. Bishnoi, Effect of cathode environment on bioelectricity generation using a novel consortium in anode side of a microbial fuel cell, Biochem. Eng. J. 121 (2017) 17–24.
[12] H.C. Boghani, R.M. Dinsdale, A.J. Guwy, G.C. Premier, Sampled-time control of a microbial fuel cell stack, J. Power Sources 356 (2017) 338–347.
[13] R. Saravanan, et al., Membraneless dairy wastewater-sediment interface for bioelectricity generation employing sediment microbial fuel cell (SMFC), African J. Microbiol. Res. 4 (2010) 2640–2646.
[14] S. Venkata Mohan, G. Mohanakrishna, B.P. Reddy, R. Saravanan, P.N. Sarma, Bioelectricity generation from chemical wastewater treatment in mediatorless (anode) microbial fuel cell (MFC) using selectively enriched hydrogen producing mixed culture under acidophilic microenvironment, Biochem. Eng. J. 39 (2008) 121–130.
[15] M. Rahimnejad, T. Jafary, F. Haghparast, G.D. Najafpour, A.A. Ghoreyshi, Nafion as a nanoproton conductor in microbial fuel cells, Turkish J. Eng. Environ. Sci. 34 (2010) 289–291.
[16] S. Venkata Mohan, S. Veer Raghavulu, P.N. Sarma, Influence of anodic biofilm growth on bioelectricity production in single chambered mediatorless microbial fuel cell using mixed anaerobic consortia, Biosens. Bioelectron. 24 (2008) 41–47.
[17] R.K. Goud, P.S. Babu, S.V. Mohan, Canteen based composite food waste as potential anodic fuel for bioelectricity generation in single chambered microbial fuel cell (MFC): bio-electrochemical evaluation under increasing substrate loading condition, Int. J. Hydrogen Energy 36 (2011) 6210–6218.
[18] K.-Y. Kim, W. Yang, P.J. Evans, B.E. Logan, Continuous treatment of high strength wastewaters using air-cathode microbial fuel cells, Bioresour. Technol. 221 (2016) 96–101.
[19] C. Lee, J. Chen, Y. Cai, Bioelectricity generation and organic removal in microbial fuel cells used for treatment of wastewater from fish-market, J. Environ. Eng. Manag. 20 (2010) 173–180.
[20] D. Bose, V. Kandpal, H. Dhawan, P. Vijay, M. Gopinath, Energy recovery with microbial fuel cells: bioremediation and bioelectricity, Waste Bioremediation, Springer, 2018, pp. 7–33.
[21] E.D. Penteado, C.M. Fernandez-Marchante, M. Zaiat, E.R. Gonzalez, M.A. Rodrigo, On the effects of Ferricyanide as cathodic mediator on the performance of microbial fuel cells, Electrocatalysis 8 (2017) 59–66.
[22] F. Qian, M. Baum, Q. Gu, D.E. Morse, A 1.5 μL microbial fuel cell for on-chip bioelectricity generation, Lab Chip 9 (2009) 3076.
[23] D. Call, B.E. Logan, Hydrogen production in a single chamber microbial electrolysis cell lacking a membrane, Environ. Sci. Technol. 42 (2008) 3401–3406.
[24] R. Uma Maheswari, C. Mohanapriya, P. Vijay, K.S. Rajmohan, M. Gopinath, Bioelectricity production and desalination of Halomonas sp.–the preliminary integrity approach, Biofuels (2016) 1–9.
[25] G.U. Semblante, et al., Fate of trace organic contaminants in oxic-settling-anoxic (OSA) process applied for biosolids reduction during wastewater treatment, Bioresour. Technol. (2017).
[26] G. Schneider, T. Kovács, G. Rákhely, M. Czeller, Biosensoric potential of microbial fuel cells, Appl. Microbiol. Biotechnol. 100 (2016) 7001–7009.
[27] C. Lopez, C. Santoro, P. Atanassov, M.D. Yates, L.M. Tender, Microbial fuel cell anode materials: supporting biofilms of geobacter sulfurreducens, Meeting Abstracts, The Electrochemical Society, 2016, p. 1852.
[28] J. Huang, et al., Performance evaluation and bacteria analysis of AFB-MFC enriched with high-strength synthetic wastewater, Water Sci. Technol. 69 (2014) 9–14.
[29] N.M. Daud, S. Rozaimah, S. Abdullah, H.A. Hasan, Z. Yaakob, Production of biodiesel and its wastewater treatment technologies : a review, Process Saf. Environ. Prot. 94 (2014) 487–508.
[30] E. Herrero-Hernández, T.J. Smith, R. Akid, Electricity generation from wastewaters with starch as carbon source using a mediatorless microbial fuel cell, Biosens. Bioelectron. 39 (2013) 194–198.
[31] B.E. Logan, et al., Microbial fuel cells: methodology and technology, Environ. Sci. Technol. 40 (2006) 5181–5192.
[32] H. Liu, R. Ramnarayanan, B.E. Logan, Production of electricity during wastewater treatment using a single chamber microbial fuel cell, Environ. Sci. Technol. 38 (2004) 2281–2285.

[33] V.R. Nimje, et al., Comparative Bioelectricity Production from Various Wastewaters in Microbial Fuel Cells Using Mixed Cultures and a Pure Strain of Shewanella Oneidensis. Bioresource Technology vol. 104, Elsevier Ltd, 2012.
[34] P.V. Pannirselvam, M.M. Cansian, M. Cardoso, a.H.F. Costa, R.S. Kempegowda, Optimization Of Integrated Clean Production Of Pyrogas, Biogas, Methanol, Bioelectricity, Fertilizer And Feed From Agro Wastes With Reduced Emission, (2011).
[35] V.B. Oliveira, M. Simões, L.F. Melo, A. Pinto, Overview on the developments of microbial fuel cells, Biochem. Eng. J. 73 (2013) 53–64.
[36] D. Bose, A. Bose, S. Mitra, H. Jain, P. Parashar, Analysis of sediment-microbial fuel cell power production in series and parallel configurations, Nat. Environ. Pollut. Technol. 17 (2018).
[37] B.E. Logan, K. Rabaey, Conversion of wastes into bioelectricity and chemicals by using microbial electrochemical technologies, Science (80-.) 337 (2012) 686–690.
[38] Y. Kim, R.D. Cusick, B. Logan, Reverse Electrodialysis Supported Microbial Fuel Cells and Microbial Electrolysis Cells, (2015).
[39] S. Hays, F. Zhang, B.E. Logan, Performance of two different types of anodes in membrane electrode assembly microbial fuel cells for power generation from domestic wastewater, J. Power Sources 196 (2011) 8293–8300.
[40] X. Zhang, et al., COD removal characteristics in air-cathode microbial fuel cells, Bioresour. Technol. 176 (2015) 23–31.
[41] Y. Qiao, X.-S. Wu, C.M. Li, Interfacial electron transfer of Shewanella putrefaciens enhanced by nanoflaky nickel oxide array in microbial fuel cells, J. Power Sources 266 (2014) 226–231.
[42] E. Fernando, T. Keshavarz, G. Kyazze, Enhanced bio-decolourisation of acid orange 7 by Shewanella oneidensis through co-metabolism in a microbial fuel cell, Int. Biodeterior. Biodegradation 72 (2012) 1–9.
[43] D. Bose, A. Bose, Electrical power generation with himalayan mud soil using microbial fuel cell, Nat. Environ. Pollut. Technol. 16 (2017) 433–439.

The current issue and full text archive of this journal is available on Emerald Insight at:
www.emeraldinsight.com/1463-5771.htm

Received 4 May 2017
Revised 14 September 2017
23 March 2018
Accepted 13 April 2018

The influence of social media marketing activities on customer loyalty

A study of e-commerce industry

Mayank Yadav
Department of Marketing, School of Business, University of Petroleum and Energy Studies, Dehradun, India, and
Zillur Rahman
Indian Institute of Technology, Roorkee, India

Abstract

Purpose – The purpose of this paper is to examine the impact of perceived social media marketing activities (SMMAs) on customer loyalty via customer equity drivers (CEDs) in an e-commerce context.
Design/methodology/approach – The study surveyed 371 students from a large university in India. The data were analyzed via confirmatory factor analysis and the research hypotheses were examined using SEM.
Findings – The study revealed three key findings. First, perceived SMMAs of e-commerce comprise five dimensions, namely, interactivity, informativeness, word-of-mouth, personalization and trendiness. Second, perceived SMMAs of e-commerce have significantly and positively influenced all the drivers of customer equity (CEDs). Third, the CEDs of e-commerce exhibit a significant and positive influence on customer loyalty toward the e-commerce sites.
Practical implications – This study will help e-commerce managers to boost customer loyalty toward the e-commerce sites through perceived SMMA.
Originality/value – The study is the first to identify five dimensions of e-commerce perceived SMMA. The current study also introduces the stimulus–organism–response model as a theoretical support to connect perceived SMMAs of e-commerce to customers' loyalty via CEDs. This is supposed to be the first study to examine the impact of perceived SMMA on customer loyalty toward the e-commerce sites via CEDs in the e-commerce industry.

Keywords Social media marketing, Social media, Customer loyalty, E-commerce, Customer equity drivers, E-commerce sites

Paper type Research paper

1. Introduction

Social media marketing (SMM) is a prominent research stream over the past decade, which delineates the varying aspects of customer relationships. Its prominence among users could be endorsed by 2.27bn and 1.49bn monthly and daily active users, respectively, on Facebook as of September 2018 (Facebook, 2018). These statistics prove that more than 50 percent of the internet users (4.15bn as per Internet World Stats, 2018) are active users of Facebook. This huge customer base makes social media quite popular not only among users but also among the companies, which utilize social media as a marketing communication medium (Hood and Day, 2014; Yadav and Rahman, 2016). The majority of the companies have integrated links to social media sites in order to communicate and build better customer relationships (Choi *et al.*, 2016; Yadav *et al.*, 2016). As per Honigman (2012), more than a million of marketing websites have integrated Facebook. In addition, the pervasive acceptance of social media is evident from the fact that 93 percent of users of these platforms believe that all firms should ensure their presence in social media (Pham and Gammoh, 2015; Yadav and Rahman, 2017b). It also provides companies various prospects to connect with customers in distinctive ways. Whether it is about addressing customers' complaint, encouraging an exclusive instantaneous chat with the celebs of a TV event or

Benchmarking: An International Journal
Vol. 25 No. 9, 2018
pp. 3882-3905
© Emerald Publishing Limited
1463-5771
DOI 10.1108/BIJ-05-2017-0092

merely sending out promotional coupons, social media is a doorway to initiate prompt and often, instant value and enhance equity. Hence, social media offers marketers an opportunity to connect directly with customers, strengthen their communication and pitch supreme value proposition to their top customers irrespective of their locations.

Also, about 39 percent of the users use social media to gain information about various products and services (Casey, 2017). As e-shopping is the new and popular shopping trend (Yan *et al.*, 2016) and social media always remains trendy due to its interactivity and relationship building potential, it is important to study SMM in e-commerce context (Kwahk and Ge, 2012). This enhanced acceptance of social media as an effective means of socialization and information dissemination has cemented the way for the advent of a new e-commerce, which is now referred to as social commerce (Liang *et al.*, 2011; Zhang, Lu, Gupta and Zhao, 2014). SMM is considered to be an eminent component of social commerce activities (Liang and Turban, 2014), which includes various tools like user ratings, reviews, recommendations, referrals, internet forums, online communities and social shopping/group buying (Hajli, 2015). As the prime objective of any marketing program is to boost stakeholders' value and to develop and sustain strong relationships with customers (Kotler and Keller, 2016), and the foundation of social media is also relationships, this study examines the impact of perceived social media marketing activities (SMMAs) on relationship variable customer loyalty. Also, in the extant literature, there is a paucity of investigations on the impact of SMM on customer loyalty, and this gap has been well endorsed in the extant literature (Nambisan and Watt, 2011; Senders *et al.*, 2013; Yadav and Rahman, 2017a). Various studies in an e-commerce context have also acknowledged the importance of SMM (Lee and Phang, 2015; Wang *et al.*, 2015; Yan *et al.*, 2016; Zhang, Lu, Gupta and Zhao, 2014; Zhang and Benyoucef, 2016), but there are limited studies like Zhang *et al.* (2016) which link SMM with customer loyalty in the e-commerce industry. In addition, there is also an absence of studies in the Indian context which investigates the impact of SMM on customer loyalty (Yadav and Rahman, 2017a).

This paper contributes substantially to the extant marketing literature in social media by bridging the above-mentioned research gaps in the following ways. First, the present research is the first to decisively examine the impact of perceived SMMAs on customer loyalty via customer equity drivers (CEDs) in the e-commerce industry, where loyalty in this study is the loyalty of customers toward the e-commerce sites. Second, the current study introduces the stimulus–organism–response (S–O–R) model (Section 2.1) to connect perceived SMMA of e-commerce to customers' loyalty via CED. The S–O–R model asserts that certain characteristics of an environment or stimuli (here SMMA) arouse the cognitive and emotional state (here CED) of consumers, which yields some behavioral responses (here customer loyalty) as a consequence (Donovan and Rossiter, 1982). Although the existing research has enriched the cognizance of the effect of the human–computer interface on consumer behavior (Jiang *et al.*, 2011; Parboteeah *et al.*, 2009), SMM is not exhaustively examined. Third, based on the prior literature on SMM in an e-commerce context, we identified and validated five dimensions of perceived SMMA, namely, interactivity, informativeness, personalization, trendiness and word-of-mouth (WOM). These five activities capture key attributes of SMM and thus further irradiate this phenomenon. We are of the opinion that the current framework of perceived SMMA would be beneficial for evaluating SMM programs and customer behavior in an e-commerce context.

2. Theoretical background

2.1 The S–O–R model

The S–O–R model (Mehrabian and Russell, 1974) which was reformed by Jacoby (2002) is applied as a theoretical underpinning to justify an integrative model presented in this study. The S–O–R model endorses that certain characteristics of an environment or stimuli

(here perceived SMMA) arouse the cognitive and emotional state (here CED) of consumers, which yields some behavioral responses (here customer loyalty) as a consequence (Donovan and Rossiter, 1982). The S–O–R model was adapted by Baker *et al.* (1994) in retailing, wherein environmental cues, specifically, ambient conditions, design factors were conceptualized as stimuli. Studies that have incorporated S–O–R model in retail context have endorsed that retail/e-retail environment stimuli have an influence on customers' inner states, which consequently incite their behavior to e-retail/retail platform. In the case of e-retail/e-commerce, the stimuli relate to the activities/characteristics of the e-commerce environment in which the customers interact (Eroglu *et al.*, 2003). The inner states are the emotional and cognitive states, which the customers possess, encompassing their experiences, insights and assessments (Jiang *et al.*, 2011). The responses in the model symbolize consumer behavior, for example, purchase behavior, customer loyalty, online communication in e-commerce (Sautter *et al.*, 2004). The application of S–O–R model as a comprehensive theory is apposite for the current study due to various justifications. Primarily, the S–O–R model has been employed extensively in prior studies on consumer behavior in e-commerce (Islam and Rahman, 2017; Koo and Ju, 2010; Mollen and Wilson, 2010; Parboteeah *et al.*, 2009; Zhang, Lu, Gupta and Zhao, 2014; Zhang and Benyoucef, 2016). For example, applying S–O–R model, Koo and Ju (2010) investigated the influence of atmospheric cues on customers' emotional states and subsequent online shopping intention. Zhang, Lu, Gupta and Zhao (2014) also employed S–O–R model to inspect the influence of technical features of social commerce on consumers' online experience and subsequent social commerce intention. The findings of the above studies have endorsed the significance and pertinence of the model to elucidate individuals' internal states and behavioral responses to online environmental stimuli. Furthermore, given the crucial role of perceived SMMA and CED in influencing consumers' behavior (customer loyalty) in e-commerce, the S–O–R framework offers a structured approach to evaluate the impact of perceived SMMA as environmental stimuli on CED (cognitive and affective aspects) and subsequently their effect on customers' loyalty (customer behavior) for e-commerce SMM. E-commerce social media refer to the social media activities of an e-commerce site (reviews, ratings, etc.) which is either present on its official site or on the other social media sites like Facebook, Twitter, etc.

2.2 Perceived SMMA as environmental stimuli (S)

As per Kaplan and Haenlein (2010), "Social Media is a group of Internet-based applications that build on the ideological and technological foundations of Web 2.0, and that allow the creation and exchange of User Generated Content" (p. 61). Social media platforms can be a social networking site, blog, wikis, virtual social worlds, and it can also be integrated with various sites in the form of their web-links, user reviews and ratings, recommendations and referrals, user wishlists and finally various forums and communities (Hajli, 2015). These all platforms are extensively employed for SMM. Owing to the prominence of SMM, it is crucial to define SMM. As per Tuten and Solomon (2016), SMM "is the utilization of social media technologies, channels, and software to create, communicate, deliver, and exchange offerings that have value for an organization's stakeholders." In an e-commerce context SMM could be defined as, "a process by which companies create, communicate, and deliver online marketing offerings via social media platforms to build and maintain stakeholder relationships that enhance stakeholders' value by facilitating interaction, information sharing, offering personalized purchase recommendations, and WOM creation among stakeholders about existing and trending products and services" (Yadav and Rahman, 2017b, p. 3). Perceived SMMAs facilitate in creating value, enhancing brand equity (BE) and in fostering customer relationships (Ismail, 2017; Kim and Ko, 2012). SMMA is a subcategory of online marketing/digital marketing that supports traditional promotion approaches.

SMMA transforms customers into marketers and brand advocates, who generate, modify and share pertinent online information regarding various brands and their respective products and services (Akar and Topcu, 2011; Ismail, 2017). Perceived SMMA could be defined "as consumers' perception of various SMMAs carried out by e-commerce sites" (Yadav and Rahman, 2017b, p. 3).

In the case of e-retail, the stimuli relate to the activities/characteristics of the e-commerce (hereby referred to as SMMA of e-commerce) social media environment in which the customers interact (Eroglu *et al.*, 2003). The current study accentuates the eminence of perceived SMMA as marketing stimuli to enhance customer experience and their subsequent behavior. Prior studies like Zhang and Benyoucef (2016), have also endorsed SMMA to be an environmental stimulus in the S–O–R model. Based on prior studies on SMM in e-commerce, we have considered five dimensions of perceived SMMAs, namely, interactivity, informativeness, personalization, trendiness and WOM. These five activities encapsulate various characteristics consumer perception of SMMA in an e-commerce context.

2.2.1 Perceived interactivity. This study defines perceived interactivity as customers' perception about the "extent to which e-commerce's social media facilitates customers to share content and views with the company and other customers." It is primarily a dynamic communication amongst companies and customers (Gallaugher and Ransbotham, 2010). Social interaction is a significant motivator for the development of customer-generated content (Daugherty *et al.*, 2008). Also, social media delivers customers not only space but also assistance for useful conversations and sharing of crucial ideas (Godey *et al.*, 2016). Social interaction clarifies that customers contribute toward companies' social media so that they could meet other like-minded customers, and discuss with them regarding various products on e-commerce sites (Muntinga *et al.*, 2011).

2.2.2 Perceived personalization. This study defines perceived personalization as customers' perception about the degree to which e-commerce site's social media offer tailored services to fulfill the preferences of a customer. The prime concern in e-commerce SMMAs is to offer tailored content as per customers' preferences. Personalizing e-commerce's social media, companies can deliver more individualistic experience, enhance brand affinity and loyalty toward e-commerce sites (Martin and Todorov, 2010). In SMM of e-commerce sites, information overload is largely witnessed, hence, perceived personalization will facilitate customers to shrink information screening cost and will consequently augment customers' decision quality and superior e-shopping experience (Tam and Ho, 2006).

2.2.3 Perceived informativeness. This study defines perceived informativeness as the customers' perception about the degree to which e-commerce social media offers accurate, useful and comprehensive information. Online customers generally select a product on the basis of sufficient and accurate information available on e-commerce sites or social media in the form of product features, reviews, ratings, etc. Therefore, consumers are eager to capture rich and valuable information with respect to a specific product on e-commerce social media (Kim *et al.*, 2010). Specifically, the perceived informativeness of SMMA of e-commerce may simplify the buying decision process of a customer and can facilitate them to take accurate decisions, which eventually enriches favorable attitude toward e-commerce site (Elliot and Speck, 2005). Also, high levels of informativeness provide suitable information on various products at B2C e-commerce sites and offer easy access to crucial information through search filters (Ranganathan and Ganapathy, 2002). This feature of SMMA of e-commerce sites helps customers in the evaluation of alternatives and finally makes their perfect choice (Aladwani and Palvia, 2002).

2.2.4 Perceived trendiness. This study defines perceived trendiness as the customers' perception about the extent to which e-commerce's social media offers trendy content. Social media offers cutting edge or latest information and hot news (Naaman *et al.*, 2011) and they

are also primary search platforms. As per Muntinga *et al.* (2011, p. 27), "trendy information on social media covers four sub-motivations: surveillance, knowledge, pre-purchase information, and inspiration." Surveillance symbolizes beholding and keeping informed about, individual's social surroundings. Knowledge symbolizes company relevant facts that customers acquire to benefit from other customers' awareness and proficiency in order to gain more pertinent facts about a company's product. Pre-purchase information signifies product reviews/ratings, recommendations/referrals and posts on brand communities to facilitate customers in taking a well-thought purchase decision. Finally, inspiration relates to customers following company relevant information and attaining innovative ideas – the company relevant information hence serves as a source of motivation or inspiration. For example, customers view images of other customers' shoes, mobiles, apparels, etc., to gain insights on their choice and trend.

2.2.5 Perceived word-of-mouth (WOM). This study defines perceived WOM as customers' perception about the degree to which e-commerce's customers recommend and share experience about e-commerce on social media. It has been recognized for several years as a foremost influence on customers' knowledge, feelings and behavior (Buttle, 1998). It has also been pronounced as an informal communication focused at other customers regarding the ownership, use or features of a specific product or its seller (Berger, 2014). E-WOM is customers' perception about a product available online. WOM has a direct effect on customers' faith and buying behavior (Duan *et al.*, 2008a, b). Online WOM minimizes the drawbacks of traditional WOM, hence, it is widely considered in e-commerce and marketing. Moreover, Web 2.0 has facilitated the growth of social media and making it the most prevalent online WOM (e-WOM) sharing medium. The online reviews/ratings are a significant source of WOM offered by e-commerce sites and have extensively influenced and assisted customers in making appropriate decisions (Cheung and Thadani, 2012; Duan *et al.*, 2008a, b). An industry survey demonstrated that 91 percent of the respondents consider online reviews, ratings, etc., before buying any product from e-commerce sites, nearly 46 percent of them endorsed the fact that these reviews affect their purchase decision (Cheung and Thadani, 2012). These reviews not only reduce perceived risk (Park and Kim, 2008) but also enhance customers' satisfaction (Liang *et al.*, 2006). The volume of these reviews has substantial relation with e-commerce sales (Yan *et al.*, 2016).

2.3 Customer equity drivers (CEDs) as customers' internal states (O)

The inner states are the emotional and cognitive states which the customers possess, encompassing their experiences, insights and assessments (Jiang *et al.*, 2011). Cognitive state signifies buyers' mental processes and encompasses of "everything that goes in the consumers' minds concerning the acquisition, processing, retention, and retrieval of information" (Eroglu *et al.*, 2001, p. 181). Affective state denotes the sentiments like "pleasure, arousal, and dominance (PAD)" exhibited by consumers ensuing the environmental stimuli (Mehrabian and Russell, 1974). In an e-commerce context, however, we postulate that "Dominance" could be a pertinent emotional response. It is likely that shoppers prefer online to traditional retail outlets due to enhanced autonomy over shopping process (Eroglu *et al.*, 2001). In this study, CEDs are considered as an organism state as they reflect various features of cognition and affection of customers in SMMA of e-commerce (Zhang and Benyoucef, 2016). Also in the prior literature (Zhang and Benyoucef, 2016), CED has been endorsed as an inner states of the consumers. There are primarily three CEDs, namely, value, brand and relationship equity (RE) as per Lemon *et al.* (2001).

2.3.1 Value equity (VE). As per Lemon *et al.* (2001, p. 22), "Value equity is defined as the customer's objective assessment of the utility of a brand, based on perceptions of what is given up for what is received." The three crucial influencers of VE are, namely, quality, price

and convenience (Vogel *et al.*, 2008). Perceived VE affects customer decisions. Although these perceptions are individualistic, they are recognizable. In an e-commerce industry, the extent of VE is an exhaustive evaluation of service quality of an e-commerce platform. The key dimensions for measuring VE in e-commerce industry are a price-quality ratio, ease of purchase and utility of the product and timing (Ou *et al.*, 2014).

2.3.2 Brand equity (BE). BE differs from VE in terms of customers' objective and subjective assessment of the utility of the product. BE is centered on subjective valuation whereas VE is more objective in nature. BE is defined as, "the customer's subjective and intangible assessment of the brand, above and beyond its objectively perceived value" (Lemon *et al.*, 2001, p. 22). Any brand has three strategic tasks. First, it facilitates in acquiring prospective customers. Second, it reminds existing customers about companies' offerings. Finally, it acts as an emotional bond between the company and its respective customers (Lemon *et al.*, 2001; Ou *et al.*, 2014; Vogel *et al.*, 2008). The brand also assists customers in developing a unique image of a specific product/service that extricates it from competitors (Keller *et al.*, 2015).

2.3.3 Relationship equity (RE). Extant literature has recognized the significance of relational aspect of modern marketing, which is quite significant from both theoretical and practical perspective (Morgan and Hunt, 1994). It is widely being acknowledged that customers differ in their perception about a specific brand as well as how they associate or connect to brands in general (Aggarwal, 2004). Lemon *et al.* (2001, p. 22) defined RE "as the tendency of the customer to stick with the brand, above and beyond the customer's objective and subjective assessments of the brand." A company can enjoy a strong brand and a valuable product, which may attract prospects. It can also retain the extant customers by fulfilling their expectations. However, with the paradigm shift from transactions centered marketing to relationship centered marketing, possessing a strong BE and generating VE is not adequate to retain the customers. The present necessity creates a strong foundation of customer–company relationships and this foundation is RE. Consumer–company relationships can be nurtured via various relationship building endeavors like loyalty programs, community development programs, reward programs, etc. (Rust *et al.*, 2004). Cultivating customer–company relationships can upsurge market share of the brand (Palmatier *et al.*, 2006), which enhances due to the higher retention rate of the existing customers (Gustafsson *et al.*, 2005) and also enhances customer loyalty (Morgan and Hunt, 1994; Vogel *et al.*, 2008).

2.4 Customer loyalty as customers' response (R)

The response component of the S–O–R model is the consequence in the form of consumers' outlook or avoidance actions (Donovan and Rossiter, 1982). Outlook behaviors comprise the positive actions that are demonstrated by the customers on particular situations by purchasing products and positive WOM, etc., while avoidance activities reveal the contrary responses, for instance, negative WOM, and no intentions to buy, etc. (Eroglu *et al.*, 2001; Islam and Rahman, 2017). As response could be both attitudinal and behavioral, the current study investigates customer loyalty as a response to perceived SMMA of e-commerce sites. As customer sovereignty is the prime constituent of marketing philosophy, hence, consumer-dedicated marketing theory and applications have emerged over the past 50 years (Rust *et al.*, 2004). The prime emphasis of marketing is to "deliver value to customers" and "recapture value from customers" in the form of customer loyalty and sales (Kotler and Keller, 2016). According to Oliver (1999, p. 34), loyalty can be defined as, "a deeply held commitment to rebuy or re-patronize a preferred product/service consistently in the future, thereby causing repetitive same brand or same brand-set purchasing, despite situational influences and marketing efforts having the potential to cause switching behavior."

Customer loyalty is essential to nurture relationships between customer and brand. Moreover, loyalty reduces marketing cost and enriches sales (Khan *et al.*, 2016; Kotler and Keller, 2016; Oliver, 1999; Vogel *et al.*, 2008). Hence, marketers should ascertain the highly rewarded consumers, fine-tune their marketing plan, retain valued consumers and boost customer loyalty (Yadav and Rahman, 2017a). Zeithaml *et al.* (1996) emphasized the significance of equity-based marketing strategy to enhance customer loyalty. Equity-based strategies have proved their significance in past studies (Dwivedi *et al.*, 2012; Ou *et al.*, 2014; Vogel *et al.*, 2008) in augmenting customer loyalty. Overall, enriching equity-centered marketing strategies will lead to enhanced customer loyalty (Ou *et al.*, 2014; Ravald and Gronroos, 1996; Vogel *et al.*, 2008; Zeithaml *et al.*, 1996).

3. Conceptual framework and hypotheses (Figure 1)

3.1 The impact of perceived SMMA on CED

The prime focus of marketing is to "create, communicate, and deliver value" (Kotler and Keller, 2016). Hence, any marketing activity will strive to enhance VE. In addition, not all customers are certain that possessing products will make them happy and will determine their social status. Prudent customers are value conscious they utilize resources cautiously (Lichtenstein *et al.*, 1990; De Young, 1986). Such customers are concerned about both quality and price (Sharma, 2011). They regularly visit social media sites and social commerce platforms to find out products that deliver optimum value; i.e. acquiring a product at the lowest available price without compromising on its quality and desired features. Also, customers believe that information retrieved from social media sites is more authentic as compared to company sites (Kaplan and Haenlein, 2010). For instance, price comparison site priceline.com has 715,500+ followers and 693,900+ likes on its Facebook page as of March 2018. The above statistics reveal that customers are interested in such services. The positive link between SMMA and VE has been endorsed by various empirical studies (Kim and Ko, 2012; Ismail, 2017). Thus, we hypothesize:

H1. Perceived SMMAs exhibit a direct positive influence on VE.

Primarily, the objective of any marketing is to establish a communication, which facilitates an organization to apprise customers of its offerings and eventually generate interest in

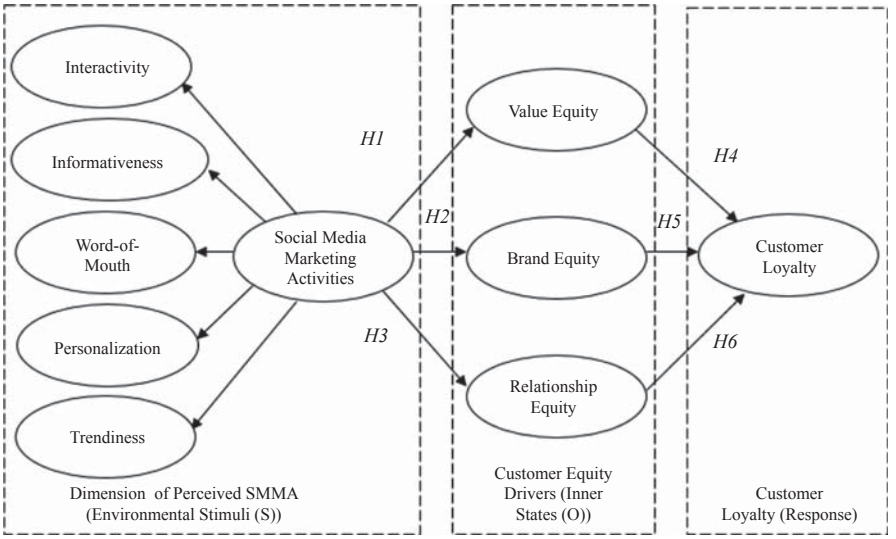

Figure 1.
The S–O–R theory based research model

those offerings (Kim and Ko, 2012). Schema theory supports the association between companies' communication and BE (Eysenck, 1984). It elucidates that customers associate communication stimuli with their previous acquaintance of similar communication events. The extent of fit influences the processing of the stimuli and customers' attitude formation (Goodstein, 1993). Thus, the communication stimuli elicit a positive effect on customers (Bruhn *et al.*, 2012), so that customers' perception of the stimuli positively influences overall BE. The positive link between perceived SMMA and BE has been endorsed by various empirical studies (Bruhn *et al.*, 2012; Kim and Ko, 2012; Godey *et al.*, 2016; Ismail, 2017). Thus, we hypothesize:

H2. Perceived SMMAs exhibit a direct positive influence on BE.

Social media is all about the relationship among users (Kaplan and Haenlein, 2010). The basic idea behind the Facebook's launch was connectedness with "FRIENDS" and establishing strong relationships. Each and everything on Facebook is built on the foundation of "FRIENDS," i.e. relationships. Hence, SMM is relationship-centric (Tuten and Solomon, 2016). Relationship marketing also accentuates the significance of developing, sustaining and augmenting strong relationships with customers (Kotler and Keller, 2016). The true value of marketing comes from strong customer relationships (Yadav, 2017). Certainly, the target of relationship marketing is to enhance customer share, not market share (Peppers and Roggers, 1995). Hence, it can be expected that SMMA will enhance RE. The positive link between SMMA and RE has been endorsed by various empirical studies (Al-alak, 2014; Kim and Ko, 2010, 2012). Thus, we hypothesize:

H3. Perceived SMMAs exhibit a direct positive influence on RE.

3.2 The influence of CEDs on customer loyalty

VE, the very first driver of customer loyalty, is the apparent proportion of what is taken (e.g. a product) to what is given (e.g. the price paid to obtain a product). Therefore, an optimum price to quality ratio symbolizes strong VE. If a product's "price-quality ratio" complements customer's "price-quality ratio" then the customer experiences inner fairness (Oliver and DeSarbo, 1988). Equity theory asserts that perceived equity generates affective states, which in turn generates positive attitudes, namely, satisfaction and loyalty (Homans, 1961). The above theory is well endorsed in empirical studies (Lam *et al.*, 2004; Vogel *et al.*, 2008; Yang and Peterson, 2004). Once a company offers superior benefits (with regard to perceived costs) to the customers competitively as compared to competitive offerings, it leads to enhanced customers' contentment which eventually leads to re-purchase intention thus potentially inducing customers' loyalty (Dwivedi *et al.*, 2012). Moreover, VE also affects customers' "switching propensity," a concept alike customer loyalty (Rust *et al.*, 2004). The positive link between VE and customer loyalty has been endorsed by various empirical studies (Dwivedi, *et al.*, 2012; Ou *et al.*, 2014; Vogel *et al.*, 2008; Zhang, Doorn and Leeflang, 2014). Thus, we hypothesize:

H4. VE exhibits a direct positive effect on customer loyalty.

BE is the subjective evaluation of a consumer's brand preference. It can also be described as the value addition to a product as a consequence of previous investment in the marketing mix of the firm (Keller, 1993). If customers evaluate a specific brand as robust, unique and appropriate, they exhibit high BE toward that brand (Verhoef *et al.*, 2007). As a brand features added value to a product, it augments the value as compared to a generic product. If customers consider a specific brand complements their image, then they develop a favorable image of the brand, which eventually enhances the likelihood of its brand preference over competitors. Similarly, Bolton *et al.* (2004) advocate that a positive opinion of

a brand can positively influence customers' affective commitment. As BE upsurges, customers' re-purchase willingness and price premium pertinent to the brand also increase (Aaker, 1991). Rust *et al.* (2004) assert that BE is expected to have an impact on customers' readiness to pay, repurchase intention and the probability of brand's recommendation. The positive link between BE and customer loyalty has been endorsed by various empirical studies (Dwivedi, *et al.*, 2012; Ou *et al.*, 2014; Vogel *et al.*, 2008; Zhang, Doorn and Leeflang, 2014). Thus, we hypothesize:

H5. BE exhibits a direct positive effect on customer loyalty.

RE comprises the components that establish a bond between customers and brands (Lemon *et al.*, 2001). High RE cultivates a "sense of belongingness" in the customers which creates a belief in customers that they are well treated by the company (Vogel *et al.*, 2008). Hence, the customers feel accustomed with the company, or the e-commerce site. They also develop trust on product quality and its delivery. A positive experience among the customers about the company indicates high RE of the brand (Hennig-Thurau *et al.*, 2002). The association between RE and customer loyalty can be elucidated by "social-exchange theory," which delineates how customers endeavor to establish and preserve relationships with companies (Morgan and Hunt, 1994). Prevailing high RE empowers customers to foresee future expedient relations with a company (Crosby *et al.*, 1990), and later create psychological interests (Dwyer *et al.*, 1987). These psychological interests encourage customers to maintain and fortify current relationship (Crosby *et al.*, 1990). Thus, favorable "RE" is expected to enhance consumer loyalty (Gustafsson *et al.*, 2005). The positive link between RE and customer loyalty has been endorsed by various empirical studies (Dwivedi *et al.*, 2012; Hennig-Thurau *et al.*, 2002; Ou *et al.*, 2014; Ravald and Gronroos, 1996; Reynolds and Betty, 1999; Vogel *et al.*, 2008; Zhang, Doorn and Leeflang, 2014). Thus, we hypothesize:

H6. RE exhibits a direct positive effect on customer loyalty.

4. Methodology

4.1 Sample and data collection

The respondents of the present study were the Indian students from a large university in India. To ensure that all survey participants are active participants of e-commerce SMM, we applied the following criteria:

- each participant uses social media daily (Facebook, Twitter, etc.), i.e. should be an active user of social media;
- each participant should have an account (at least two years old) with e-commerce sites (e.g. Amazon, Flipkart, etc.) and purchases goods from these websites or from the product links of these websites available on Facebook, Twitter, etc., at least once in every three months;
- provides rating, reviews and recommendations about the product after purchase from e-commerce sites, and/or refers to them before making any new purchase (either on e-commerce website or social media sites like Facebook, Twitter, YouTube, etc.); and
- likes Facebook brand pages of e-commerce sites.

The aforementioned criteria were stringently followed to guarantee only valid and pertinent participation. The respondents of the survey were invited to deliver their views about e-commerce site of their choice, and answer the survey questions with respect to their mentioned preferred e-commerce site (Islam *et al.*, 2017). However, due to the absence of any

list of e-commerce site members and its social media in India, we employed convenience sampling to collect data (Martin and Herrero, 2012, Ismail, 2017). Students were the target respondents in this study as they are tech-savvy (Islam and Rahman, 2017; Nadeem *et al.*, 2015), they possess a wide exposure of the internet (Bolton *et al.*, 2013), students are highest users of social media (Greenwood *et al.*, 2016, Kim and Ko, 2012) and they are exceptionally active contributors in social media and e-commerce (Ismail, 2017; Islam and Rahman, 2016). The data were collected for eight weeks and 401 responses were captured, 30 were eliminated due to incomplete data or data quality issues. Finally, 371 valid surveys forms (which included 65 percent males and 35 percent females, with age extending from 21 to 34 years) were retained. Of the 371 respondents, 185 (49.86 percent) were undergraduate students, 115 (30.99 percent) were postgraduate students and 71 (19.13 percent) were PhD scholars. The study is not limited to any specific e-commerce brand or product category and it is a study of e-commerce sites in general. The essence of such a generalized study lies in the fact that the results could be of help to practitioners in providing a holistic view while developing and maintaining e-commerce sites irrespective of the brand or product category they belong to.

4.2 Measures

The survey encompasses three sections: first the screening questions to meet criteria mentioned in Section 4.1. Second, 26 items related to the constructs (Table AI) and finally, questions on the demographic profile. A total of 15 items (Table AI) to measure perceived SMMAs were developed from previous studies on SMM, e-commerce and social commerce and also based on current scale development studies in online social media literature (e.g. Baldus *et al.*, 2015; DeVellis, 2016;) and previous scale development studies (Churchill, 1979; Gerbing and Anderson, 1988). We assessed CED by adapting eight items from Ou *et al.* (2014) and Verhoef *et al.* (2007). Customer loyalty was assessed by three items adapted from Wang *et al.* (2015). The responses were gathered on a seven-point Likert scale where 1 = "strongly disagree," and 7 = "strongly agree."

5. Analysis and results

To analyze the data and examine the hypotheses of the present study, we employed SPSS 21.0 and AMOS 22.0. SPSS was utilized for descriptive inquiry and "exploratory factor analysis" (EFA). Amos 22.0 was utilized for "confirmatory factor analysis" (CFA) and test the consistency and validity of the model. Finally, SEM was applied to examine the hypotheses of the study.

5.1 Perceived SMMA

Prior to investigating the effect of perceived SMMA on CED, the dimensions of SMMAs perceived by customers were revealed. As the dimensions of perceived SMMAs were not explicitly distinct, EFA and CFA were employed. Cronbach's α of each dimension was assessed to ascertain internal consistency of every dimension. EFA (Table I) delivered a five-factor solution with 15 items representing 5 dimensions of SMMA of e-commerce (three items each measuring "interactivity," "informativeness," "WOM," "personalization" and "trendiness"). The "Kaiser–Meyer–Olkin (KMO)" value came out to be 0.873 and "Bartlett's test of sphericity" reflected the merit of the correlation matrix. These five factors accounted for a total variance of 86.61 percent (Table I). Cronbach's α values ranged from 0.88 to 0.97, all above the suggested onset of 0.7 (Nunnally and Bernstein, 1994). CFA resulted in good model fit with 5 dimension and 15 items of SMMA: $\chi^2/df = 2.122$, GFI = 0.93, AGFI, 0.91, NFI, 0.97, CFI = 0.96, RMSEA = 0.051.

Construct	Items	Factor loadings 1	2	3	4	5
Informativeness	INF3	0.922				
	INF2	0.889				
	INF1	0.861				
Interactivity	INT3		0.902			
	INT1		0.858			
	INT2		0.814			
Trendiness	TREND1			0.890		
	TREND2			0.885		
	TREND3			0.799		
Personalization	PERS3				0.870	
	PERS2				0.830	
	PERS1				0.762	
WOM	WOM2					0.854
	WOM1					0.816
	WOM3					0.754
Cronbach α		0.972	0.975	0.960	0.919	0.884

Notes: Variance explained = 86.61 percent; KMO = 0.873; extraction method: principal component analysis with varimax rotation

Table I. Exploratory factor analysis for perceived SMMA

5.2 Measurement model

CFA (Figure 2) was applied on all the constructs in the model by taking SMMA as second-order construct (Godey *et al.*, 2016; Ismail, 2017, Kim and Ko, 2012; Yadav and Rahman, 2017b). The CFA model comprised of perceived SMMA along with CED, and customer loyalty. The test statistics revealed the satisfactory fit with the data. The model fit indices were χ^2/df = 2.07, GFI = 0.92, AGFI, 0.90, NFI, 0.95, CFI = 0.97, TLI = 0.96, RMSEA = 0.05 (Table II). To ascertain the construct reliability and validity following statistics were applied. The reliability of each construct was determined by Cronbach's α and composite reliability whose all values ranged from 0.84 to 0.97, all above the recommended range of 0.7 (Malhotra and Dash, 2016; Nunnally and Bernstein, 1994) and provided in Table III. To ascertain the construct validity, convergent and discriminant validities were assessed. Convergent validity was established by assessing the "average variance extracted" (AVE) and the loadings of the indicators. As all the values of AVE are above the recommended range of 0.5 and all the indicator loadings are 0.7 and above (Fornell and Larcker, 1981), the model is free from convergent validity issues (Hair *et al.*, 2014) which is evident from Table III. The discriminant validity is established when the square root of the AVE of every construct is higher than its respective inter-construct correlations (Hair *et al.*, 2014). It is explicit from Table IV that the above-mentioned criteria have been met and the model is free from discriminant validity issues.

5.2.1 Common method bias. We also applied common method bias (CMB) test, as CMB has been the foremost concern for the survey-based research and that too particularly where the self-reported instrument has been used (Podsakoff *et al.*, 2003). Following Podsakoff *et al.* (2003), the present study adopted the procedures suggested by Podsakoff *et al.* (2003), wherein use of statistical and study design technique is helpful in regulating CMB. Biasness could enter in the existing study through transient mood state where transient mood denotes the influences of the recent events in the manner in which respondent view themselves and the world present around them (Podsakoff *et al.*, 2003). Thus, for receiving honest responses, a positive assurance is given to the respondents that their responses would be kept anonymous. Harman's single-factor test was executed where all the items are subjected to unrotated principle component EFA with single-factor extraction. The result of

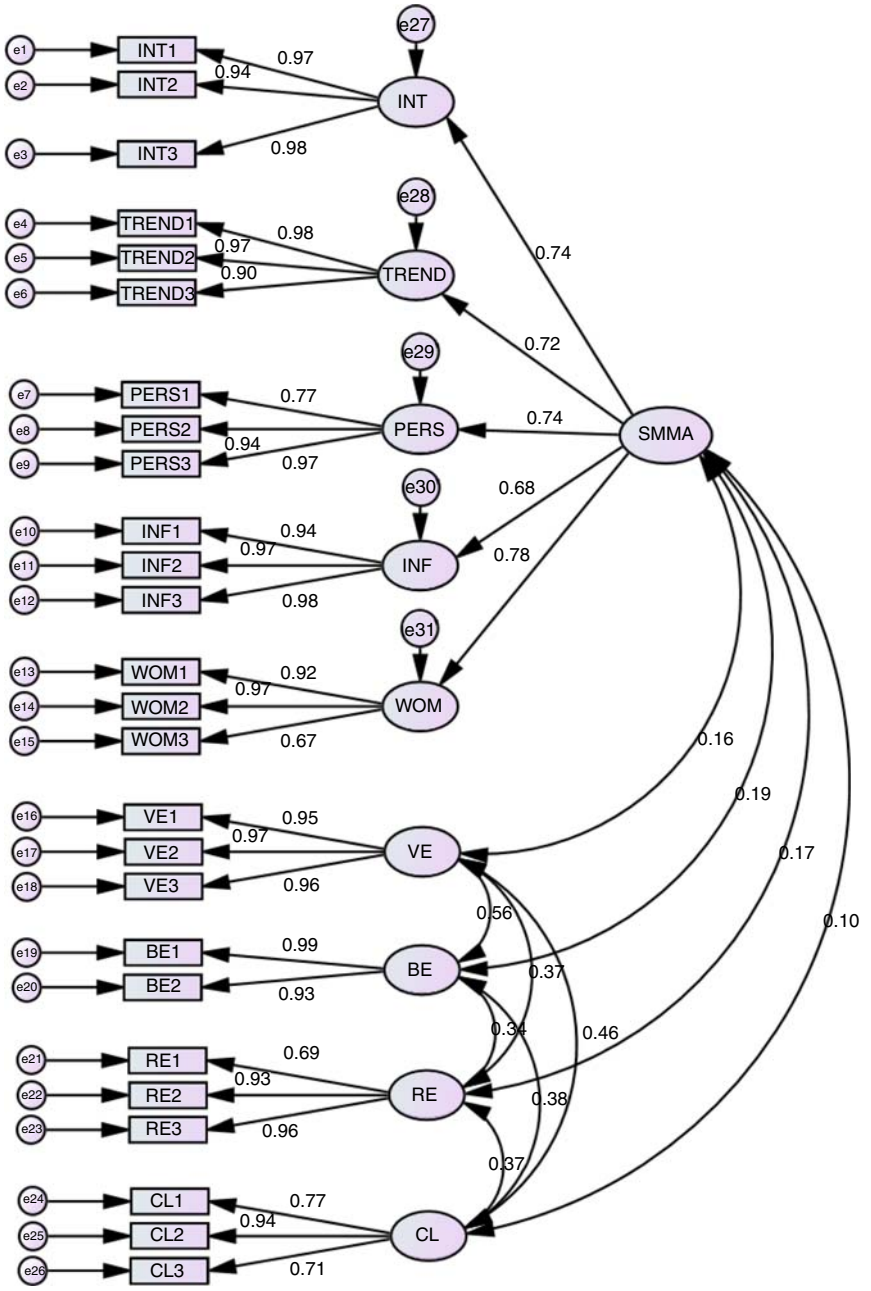

Figure 2.
Measurement model perceived SMMA–CEDs–customer loyalty

EFA shows that unrotated single factor explains only 29 percent of the variation, which is below 50 percent as suggested by Hair *et al.* (2014). This confirms the absence of CMB.

5.2.2 Non-response bias. Non-response bias has been examined by the researcher using one-way ANOVA test (Armstrong and Overton, 1977). For the bias examination "early" and

"late" responses of the 50 participants were compared. ANOVA means were compared of all the 26 observed variables. The results ruled out the presence of any non-response bias with respect to response time period.

5.3 Structural model

SEM was applied to the conceptual model as per Anderson and Gerbing (1988). All the actual and suggested measures of model fit are listed in Table II. The overall fit indices (χ^2/df = 2.64, GFI = 0.93, AGFI, 0.91, NFI, 0.94, CFI = 0.96, TLI = 0.95, RMSEA = 0.06) were good with the data and as per the suggested ranges by Hair *et al.* (2014). On achieving the recommended model fit, *H1–H6* were tested via SEM (Figure 3). All the paths between SMMA and CED were significant at $p < 0.001$. It is explicit from Table V that perceived SMMAs of e-commerce demonstrate significant and positive influence on its BE ($\beta = 0.23$; $t = 3.74$, $p < 0.001$), VE ($\beta = 0.20$; $t = 3.38$, $p < 0.001$) and RE ($\beta = 0.19$; $t = 3.25$, $p < 0.001$). This endorses the fact that SMMAs boost the CED of e-commerce sites. The results from Table V also reveal that CEDs, namely, VE ($\beta = 0.33$; $t = 5.10$, $p < 0.001$),

Table II. Measures of model fit

Fit index	χ^2/df	RMSEA	GFI	AGFI	NFI	CFI	TLI
Suggested range	< 3.00	⩽0.08	⩾0.90	⩾0.90	⩾0.90	⩾0.90	⩾0.90
Measurement model	2.07	0.05	0.92	0.90	0.95	0.97	0.96
Structural model	2.64	0.06	0.93	0.91	0.94	0.96	0.95

Table III. Construct reliability and convergent validity

Construct	Indicator	Standard loadings	AVE	CR	Cronbach's α
SMMA	Interactivity	0.74	0.53	0.85	0.86
	Informativeness	0.68			
	Word-of-mouth	0.78			
	Personalization	0.74			
	Trendiness	0.72			
Value equity	VE1	0.95	0.92	0.97	0.97
	VE2	0.97			
	VE3	0.96			
Brand equity	BE1	0.99	0.92	0.96	0.96
	BE2	0.93			
Relationship equity	RE1	0.69	0.76	0.90	0.89
	RE2	0.93			
	RE3	0.96			
Customer loyalty	CL1	0.77	0.66	0.85	0.84
	CL2	0.94			
	CL3	0.71			

Table IV. Descriptive statistics and discriminant validity

	RE	VE	SMMA	BE	CL	Mean	SD
RE	*0.871*					5.00	1.60
VE	0.373	*0.959*				4.95	1.83
SMMA	0.167	0.163	*0.728*			3.94	1.61
BE	0.339	0.557	0.185	*0.960*		5.12	1.58
CL	0.373	0.463	0.096	0.380	*0.812*	5.60	1.24

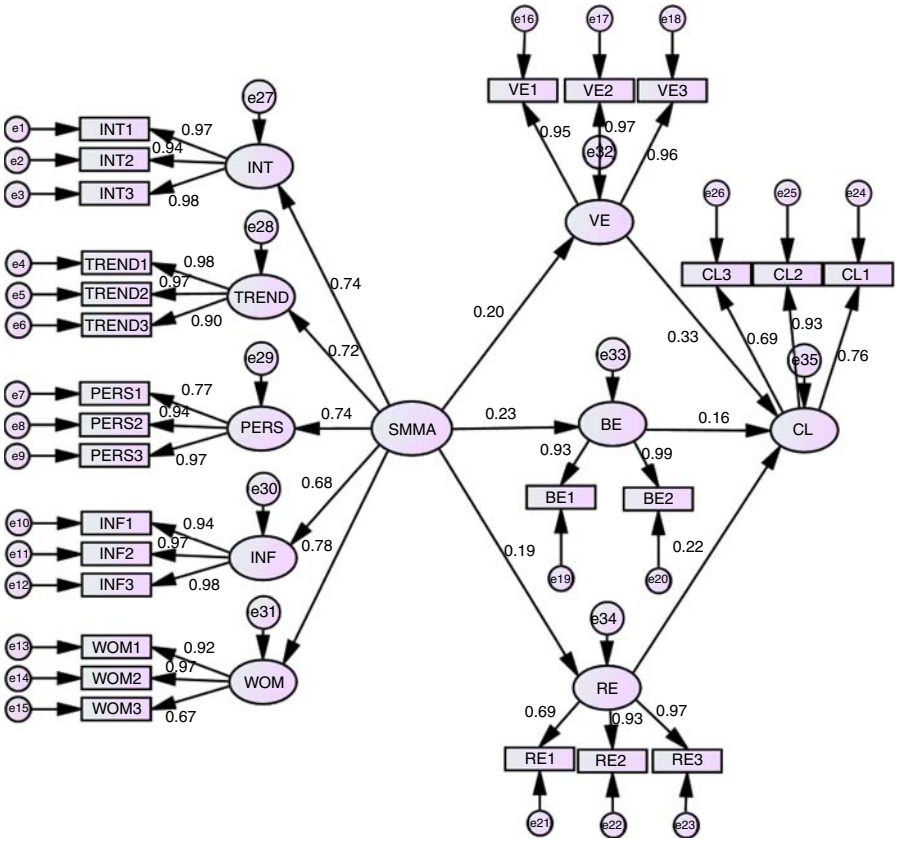

Figure 3.
Structural model perceived SMMA–CEDs–customer loyalty

Hypotheses	β	*t*-values	Test results
H1: SMMA–value equity	0.20***	3.38	Supported
H2: SMMA–brand equity	0.23***	3.74	Supported
H3: SMMA–relationship equity	0.19***	3.25	Supported
H4: Value equity–customer loyalty	0.33***	5.10	Supported
H5: Brand equity–customer loyalty	0.16***	2.65	Supported
H6: Relationship equity–customer loyalty	0.22***	3.84	Supported

Note: ***$p < 0.001$

Table V.
Hypotheses assessment results

BE ($\beta = 0.16$; $t = 2.65$, $p < 0.001$) and RE ($\beta = 0.22$; $t = 3.84$, $p < 0.001$) demonstrate significant positive impact on customer loyalty. The above results sustain the hypotheses of the study. Therefore, perceived SMMAs of e-commerce sites influence customer loyalty.

6. Discussion and implications

The findings from the analysis supported the various conclusions. First, SMMAs of e-commerce comprise five dimensions, namely, interactivity, informativeness, WOM, personalization and trendiness. Second, perceived SMMAs of e-commerce have significantly and positively influenced all the drivers of customer equity. These findings are in

conformance with previous studies (Kim and Ko, 2012; Srivastava *et al.*, 1998) that support that marketing activities enhance CED. Hence, SMMAs of e-commerce are an integrated marketing communication tool that delivers superior value to consumers in terms of authentic information from actual buyers, recommendations, reviews, etc., as compared to traditional media, which in turn enhances VE. Social media delivers customers a social space to exchange authentic and trendy information, interact with the company and/or other customers, also it offers customers a "voice" as WOM, regarding the products and services in e-commerce. The above phenomenon eventually enhances all the CED. Since the objective of any marketing program is to augment CED and customer relationships, SMMAs are an effective marketing communication medium. As e-commerce endeavors to deliver enhanced customer value, employing social media for marketing is a pertinent medium to build and preserve customers for e-commerce.

Third, all the CEDs of e-commerce exhibit a significant and positive influence on customer loyalty. The above finding is in conformance with extant studies (Dwivedi *et al.*, 2012; Ou *et al.*, 2014; Vogel *et al.*, 2008) in the literature. Also, VE and RE are prominent drivers of customer loyalty. This finding is in conformance with previous studies (Dwivedi *et al.*, 2012; Lemon *et al.*, 2001) which assert that value is the foundation of customer–company relationships. If the offerings of e-commerce do not meet consumers' expectations, then establishing BE will be futile (Vogel *et al.*, 2008). The positive association of RE with customer loyalty indicates that e-commerce companies should develop and preserve strong relationships with the customers. Hence, SMMA positively influences customer loyalty.

6.1 Theoretical implications

As the prime objective of any marketing program is to boost stakeholders' value and to develop and sustain strong relationships with customers (Kotler and Keller, 2016), and the foundation of social media is also relationships, this study assessed the impact of perceived SMMA on relationship variable customer loyalty. Also in the extant literature, there is a paucity of studies investigating the impact of SMM on customer loyalty (Nambisan and Watt, 2011; Senders *et al.*, 2013; Yadav and Rahman, 2017a). Various studies in e-commerce context have also acknowledged the importance of SMM (Lee and Phang, 2015; Wang *et al.*, 2015; Yan *et al.*, 2016; Zhang, Lu, Gupta and Zhao, 2014; Zhang and Benyoucef, 2016). In addition, there are limited studies like which links SMM with customer loyalty in the e-commerce industry. Also, there is also an absence of studies in an Indian context which investigates the impact of SMM on customer loyalty (Yadav and Rahman, 2017a).

This paper contributes substantially to the extant marketing literature in social media by bridging the above-mentioned research gaps the following ways. First, the present research is the first to decisively investigate the impact of perceived SMMA on CED and subsequently the most desired outcome customer loyalty. Second, the current study is the first to introduce the S–O–R model to connect perceived SMMA of e-commerce sites to customers' loyalty via CED, which provides this study strong theoretical foundation. Although the existing research has enriched the cognizance of the effect of the human–computer interface on consumer behavior (Jiang *et al.*, 2011; Parboteeah *et al.*, 2009) but SMM has not been examined in depth, the present research addresses this research lacuna. Third, based on the prior literature on SMM in an e-commerce context, we identified and validated five dimensions of perceived SMMA, namely, interactivity, informativeness, personalization, trendiness and WOM. These five activities capture key attributes of SMM and thus further irradiate this phenomenon. We are of the opinion that the current framework of perceived SMMA would be beneficial for evaluating SMM's effectiveness for enhancing customer loyalty.

6.2 Managerial implications

This study delivers various implications for practitioners as well. SMMA of e-commerce have significantly and positively influenced all the drivers of customer equity. This means managers should emphasize the significance of perceived SMMA to enhance CED. Since the objective of any marketing communication is to augment CED and customer relationships, SMMA is an effective marketing communication medium. As e-commerce endeavors to deliver enhanced customer value, employing social media for marketing is a pertinent medium to build and preserve customers for e-commerce. Managers should focus on all the five dimensions of SMM to enhance CED. Social media should be considered as a significant and efficient marketing tool (Yadav, 2017) which could compete with the other marketing channels like TV, newspaper, etc. This indicates that marketers should develop more interactive digital campaigns. There is never too late to establish your presence in social media as the concept of first-mover advantage does not exist in social media (Godey *et al.*, 2016) due to its high evolving nature. Perceived SMMA positively influenced customer loyalty through CED. This indicates that managers could use social media to enhance the loyalty of customers, but should employ traditional methods like, excellent e-commerce customer service, quality, the variety of products, etc., as well to convince consumers to pay a price premium and return back for future purchase. As e-commerce sites seek to enhance customers' loyalty in order to retain the existing ones and attract the prospects. The findings of this research will help to attain this objective and customer loyalty e-commerce site could be enhanced by focusing on effective SMMA comprising of all the five major dimensions. Based on the positive effect of all the CED on customer loyalty in this study, particularly, RE and VE, it can be inferred that e-commerce mangers should develop strong and cordial relationships with customers encashing the power of SMMA and also providing superior customer value. At last e-commerce managers should use social media prudently keeping the darker side of social media also into consideration.

7. Limitations and future research

As no research is impeccable, the present research also possesses some limitations that recommend research opportunities. First, the findings of the existing study cannot be generalized as it is limited to e-commerce industry, future research should validate its finding in various other industrial context. Also, as e-commerce is internet-centered industry, further replications could assess the appropriateness of SMMA across offline or non-internet industries employing longitudinal data.

Second, this study comprised only Indian customers. The outcomes plausibly extend to customers in other collectivist countries; however, this generalization demands confirmation. Particularly, studies in more individualistic nations and in nations that reveal higher (e.g. Philippines, Mexico, Malaysia) or lower (e.g. Germany, Japan, France) usage of social media (Statista, 2015). Third, the current study examined the impact of SMMA on customer loyalty, the future studies should examine the effect of SMMA on customer loyalty via relationship quality. Fourth, the study comprised university students who are active social media users, future studies should include both student and non-student samples to overcome bias generated by interview method and enhance the generalizability of the study. Fifth, the demographic variables might also influence the conceptual model, future studies should incorporate such variables in the analysis for a more exhaustive comprehension of SMM. Sixth, future studies may incorporate other models, which are the alternative to S–O–R to further develop SMM as a research domain. Finally, it is not always the case that social media disseminates positives. Acknowledging the perceived SMMA impacts on cognitive and affective states of consumers, what happens to loyalty in negative situations (negative reviews, negative WOM, etc.) could be another important avenue for future research.

References

Aaker, D.A. (1991), *Managing Brand Equity*, The Free Press, New York, NY.

Aggarwal, P. (2004), "The effects of brand relationship norms on consumer attitudes and behaviour", *Journal of Consumer Research*, Vol. 31 No. 1, pp. 87-101.

Akar, E. and Topcu, B. (2011), "An examination of the factors influencing consumers' attitudes toward social media marketing", *Journal of Internet Commerce*, Vol. 10 No. 1, pp. 35-67.

Aladwani, A.M. and Palvia, P.C. (2002), "Developing and validating an instrument for measuring user-perceived web quality", *Information & Management*, Vol. 39 No. 6, pp. 467-476.

Al-alak, B.A. (2014), "Impact of marketing activities on relationship quality in the Malaysian banking sector", *Journal of Retailing and Consumer Services*, Vol. 21 No. 3, pp. 347-356.

Anderson, J.C. and Gerbing, D.W. (1988), "Structural equation modeling in practice: a review and recommended two-step approach", *Psychological Bulletin*, Vol. 103 No. 3, pp. 411-423.

Armstrong, J.S. and Overton, T.S. (1977), "Estimating non response bias in mail surveys", *Journal of Marketing Research*, Vol. 14 No. 3, pp. 396-402.

Baker, J., Grewal, D. and Parasuraman, A. (1994), "The influence of store environment on quality inferences and store image", *Journal of the Academy Marketing Science*, Vol. 22 No. 4, pp. 328-339.

Baldus, B.J., Voorhees, C. and Calantone, R. (2015), "Online brand community engagement: scale development and validation", *Journal of Business Research*, Vol. 68 No. 5, pp. 978-985, doi: 10.1016/j.jbusres.2014.09.035.

Berger, J. (2014), "Word of mouth and interpersonal communication: a review and directions for future research", *Journal of Consumer Psychology*, Vol. 24 No. 4, pp. 586-607.

Bolton, R.N., Lemon, K.N. and Verhoef, P.C. (2004), "The theoretical underpinnings of customer asset management: a framework and propositions for future research", *Journal of the Academy of Marketing Science*, Vol. 32 No. 3, pp. 271-292.

Bolton, R.N., Parasuraman, A., Hoefnagels, A., Migchels, N., Kabadayi, S., Gruber, T., Loureiro, Y.K. and Solnet, D. (2013), "Understanding generation Y and their use of social media: a review and research agenda", *Journal of Service Management*, Vol. 24 No. 3, pp. 245-267.

Bruhn, M., Schoenmueller, V. and Schäfer, D.B. (2012), "Are social media replacing traditional media in terms of brand equity creation?", *Management Research Review*, Vol. 35 No. 9, pp. 770-790.

Buttle, F. (1998), "Word of mouth: understanding and managing referral marketing", *Journal of Strategic Marketing*, Vol. 6 No. 3, pp. 241-254.

Casey, S. (2017), "2016 Nielsen social media report," available at: www.nielsen.com/content/dam/corporate/us/en/reports-downloads/2017-reports/2016-nielsen-social-media-report.pdf (accessed March 7, 2017).

Cheung, C.M. and Thadani, D.R. (2012), "The impact of electronic word-of-mouth communication: a literature analysis and integrative model", *Decision Support Systems*, Vol. 54 No. 1, pp. 461-470.

Choi, E.K., Fowler, D., Goh, B. and Yuan, J. (2016), "Social media marketing: applying the uses and gratifications theory in the hotel industry", *Journal of Hospitality Marketing & Management*, Vol. 25 No. 7, pp. 771-796, doi: 10.1080/19368623.2016.1100102.

Churchill, G.A. (1979), "A paradigm for developing better measures of marketing constructs", *Journal of Marketing Research*, Vol. 16 No. 1, pp. 64-73, doi: 10.2307/3150876.

Crosby, L.A., Evans, K.R. and Cowles, D. (1990), "Relationship quality in services selling: an interpersonal influence perspective", *Journal of Marketing*, Vol. 54 No. 3, pp. 68-81.

Daugherty, T., Eastin, M.S. and Bright, L. (2008), "Exploring consumer motivations for creating user-generated content", *Journal of Interactive Advertising*, Vol. 8 No. 2, pp. 16-25.

De Young, R. (1986), "Some psychological aspects of recycling the structure of conservation satisfactions", *Environment and Behavior*, Vol. 18 No. 4, pp. 435-449.

DeVellis, R.F. (2016), *Scale Development: Theory and Applications*, 4th ed., Sage, London.

Donovan, R.J. and Rossiter, J.R. (1982), "Store atmosphere: an environmental psychology approach", *Journal of Retailing*, Vol. 58 No. 1, pp. 34-57.

Duan, W., Gu, B. and Whinston, A.B. (2008a), "Do online reviews matter? An empirical investigation of panel data", *Decision Support Systems*, Vol. 45 No. 4, pp. 1007-1016.

Duan, W., Gu, B. and Whinston, A.B. (2008b), "The dynamics of online word-of-mouth and product sales – an empirical investigation of the movie industry", *Journal of Retailing*, Vol. 84 No. 2, pp. 233-242.

Dwivedi, A., Merrilees, B., Miller, D. and Herington, C. (2012), "Brand, value and relationship equities and loyalty-intentions in Australian supermarket industry", *Journal of Retailing and Consumer Services*, Vol. 19 No. 5, pp. 526-536.

Dwyer, F.R., Schurr, P.H. and Oh, S. (1987), "Developing buyer–seller relationships", *Journal of Marketing*, Vol. 51 No. 2, pp. 11-27.

Elliot, M.T. and Speck, P.S. (2005), "Factors that affect attitude toward a retail web site", *Journal of Marketing Theory and Practice*, Vol. 13 No. 1, pp. 40-51.

Eroglu, S.A., Machleit, K.A. and Davis, L.M. (2001), "Atmospheric qualities of online retailing: a conceptual model and implications", *Journal of Business Research*, Vol. 54 No. 2, pp. 177-184.

Eroglu, S.A., Machleit, K.A. and Davis, L.M. (2003), "Empirical testing of a model of online store atmospherics and shopper responses", *Psychology & Marketing*, Vol. 20 No. 2, pp. 139-150.

Eysenck, M.W. (1984), *A Handbook of Cognitive Psychology*, Lawrence Erlbaum, London.

Facebook (2018), "Facebook Newsroom Stats", available at: https://newsroom.fb.com/company-info/ (accessed November 7, 2018).

Fornell, C. and Larcker, D.F. (1981), "Evaluating structural equation models with unobservable variables and measurement error", *Journal of Marketing Research*, Vol. 18 No. 1, pp. 39-50, doi: 10.2307/3151312.

Gallaugher, J. and Ransbotham, S. (2010), "Social media and customer dialogue management at Starbucks", *MIS Quarterly Executive*, Vol. 9 No. 4, pp. 197-212.

Gerbing, D.W. and Anderson, J.C. (1988), "An updated paradigm for scale development incorporating unidimensionality and its assessment", *Journal of Marketing Research*, Vol. 25 No. 2, pp. 186-192, doi: 10.2307/3172650.

Godey, B., Manthiou, A., Pederzoli, D., Rokka, J., Aiello, G., Donvito, R. and Singh, R. (2016), "Social media marketing efforts of luxury brands: influence on brand equity and consumer behavior", *Journal of Business Research*, Vol. 69 No. 12, pp. 5833-5841, doi: 10.1016/j.jbusres.2016.04.181.

Goodstein, R.C. (1993), "Category-based applications and extensions in advertising: motivating more extensive ad processing", *Journal of Consumer Research*, Vol. 20 No. 1, pp. 87-99.

Greenwood, S., Perrin, A. and Duggan, M. (2016), *Social Media Update-2016*, Pew Research Center, Washington, DC.

Gustafsson, A., Johnson, M.D. and Roos, I. (2005), "The effects of customer satisfaction, relationship commitment dimensions, and triggers on customer retention", *Journal of Marketing*, Vol. 69 No. 4, pp. 210-218.

Hair, J., Black, W., Babin, B. and Anderson, R. (2014), *Multivariate Data Analysis*, 7th ed., Pearson, Edinburgh.

Hajli, N. (2015), "Social commerce constructs and consumer's intention to buy", *International Journal of Information Management*, Vol. 35 No. 2, pp. 183-191, doi: 10.1016/j.ijinfomgt.2014.12.005.

Hennig-Thurau, T., Gwinner, K.P. and Gremler, D.D. (2002), "Understanding relationship marketing outcomes: an integration of relational benefits and relationship quality", *Journal of Service Research*, Vol. 4 No. 3, pp. 230-247.

Homans, G.C. (1961), *Social Behavior: Its Elementary Forms*, Harcourt Brace, New York, NY.

Honigman, B. (2012), "100 fascinating social media statistics and figures from 2012", *The Huffington Post*, November 29, available at: www.huffingtonpost.com/brian-honigman/100-fascinating-social-me_b_2185281.html (accessed March 27, 2017).

Hood, M. and Day, T. (2014), "Tech trends for 2014: don't get left behind", available at: http://directsellingnews.com/index.php/view/tech_trends_for_2014_dont_get_left_behind#.WJRv4zhEDis (accessed February 3, 2017).

Hsu, L.C., Wang, K.U. and Chih, W.H. (2013), "Effects of web site characteristics on customer loyalty in B2B e-commerce: evidence from Taiwan", *The Service Industries Journal*, Vol. 33 No. 11, pp. 1026-1050.

Hwang, I.J., Lee, B.G. and Kim, K.Y. (2014), "Information asymmetry, social networking site word of mouth, and mobility effects on social commerce in Korea", *Cyberpsychology, Behavior, and Social Networking*, Vol. 17 No. 2, pp. 117-124.

Internet World Stats (2018), "World internet usage and population statistics", Internet World Stats: usage and population statistics, December 31, available at: www.internetworldstats.com/stats.htm (accessed March 17, 2018).

Islam, J.U. and Rahman, Z. (2017), "The impact of online brand community characteristics on customer engagement: an application of stimulus–organism–response paradigm", *Telematics and Informatics*, Vol. 34 No. 4, pp. 96-109.

Islam, J. and Rahman, Z. (2016), "Linking customer engagement to trust and word-of-mouth on Facebook brand communities: an empirical study", *Journal of Internet Commerce*, Vol. 15 No. 1, pp. 40-58.

Islam, J.U., Rahman, Z. and Hollebeek, L.D. (2017), "Personality factors as predictors of online consumer engagement: an empirical investigation", *Marketing Intelligence & Planning*, Vol. 35 No. 4, pp. 510-528.

Ismail, A.R. (2017), "The influence of perceived social media marketing activities on brand loyalty the mediation effect of brand and value consciousness", *Asia Pacific Journal of Marketing and Logistics*, Vol. 29 No. 1, pp. 129-144, doi: 10.1108/APJML-10-2015-0154.

Jacoby, J. (2002), "Stimulus–organism–response reconsidered: an evolutionary step in modeling (consumer) behavior", *Journal of Consumer Psychology*, Vol. 12 No. 1, pp. 51-57.

Jiang, Z., Chan, J., Tan, B.C.-Y. and Chua, W.S. (2011), "Effects of interactivity on website involvement and purchase intention", *Journal of the Association for Information Systems*, Vol. 11 No. 1, pp. 34-59.

Kaplan, A.M. and Haenlein, M. (2010), "Users of the world, unite! The challenges and opportunities of social media", *Business Horizons*, Vol. 53 No. 1, pp. 59-68, doi: 10.1016/j.bushor.2009.09.003.

Kassim, N.M. and Ismail, S. (2009), "Investigating the complex drivers of loyalty in e-commerce settings", *Measuring Business Excellence*, Vol. 13 No. 1, pp. 56-71.

Keller, K.L. (1993), "Conceptualizing, measuring, and managing customer-based brand equity", *Journal of Marketing*, Vol. 57 No. 1, pp. 1-22.

Keller, K.L., Parameswaran, A.M. and Jacob, I. (2015), *Strategic Brand Management: Building, Measuring, and Managing Brand Equity*, Pearson, Noida.

Khan, I., Dongping, H. and Wahab, A. (2016), "Does culture matter in effectiveness of social media marketing strategy? An investigation of brand fan pages", *Aslib Journal of Information Management*, Vol. 68 No. 6, pp. 694-715.

Kim, A.J. and Ko, E. (2010), "Impacts of luxury fashion brand's social media marketing on customer relationship and purchase intention", *Journal of Global Fashion Marketing*, Vol. 1 No. 3, pp. 164-171, doi: 10.1080/20932685.2010.10593068.

Kim, A.J. and Ko, E. (2012), "Do social media marketing activities enhance customer equity? An empirical study of luxury fashion brand", *Journal of Business Research*, Vol. 65 No. 10, pp. 1480-1486, doi: 10.1016/j.jbusres.2011.10.014.

Kim, J.B. (2015), "The mediating role of presence on consumer intention to participate in a social commerce site", *Journal of Internet Commerce*, Vol. 14 No. 4, pp. 424-454.

Kim, J.U., Kim, W.J. and Park, S.C. (2010), "Consumer perceptions on web advertisements and motivation factors to purchase in the online shopping", *Computers in Human Behavior*, Vol. 26 No. 5, pp. 1208-1222.

Kim, S. and Park, H. (2013), "Effects of various characteristics of social commerce (s-commerce) on consumers' trust and trust performance", *International Journal of Information Management*, Vol. 33 No. 2, pp. 318-332.

Koo, D.M. and Ju, S.H. (2010), "The interactional effects of atmospherics and perceptual curiosity on emotions and online shopping intention", *Computers in Human Behavior*, Vol. 26 No. 3, pp. 377-388.

Kotler, P. and Keller, K.L. (2016), *Marketing Management*, 15th ed., Pearson, Noida.

Kwahk, K.Y. and Ge, X. (2012), "The effects of social media on E-Commerce: a perspective of social impact theory", *45th Hawaii International Conference on System Sciences, IEEE, Maui, HI*, pp. 1814-1823.

Lam, S.Y., Shankar, V., Erramilli, M.K. and Murthy, B. (2004), "Customer value, satisfaction, loyalty, and switching costs: an illustration from a business-to-business service context", *Journal of the Academy of Marketing Science*, Vol. 32 No. 3, pp. 293-311.

Lee, S.-Y.T. and Phang, C.D. (2015), "Leveraging social media for electronic commerce in Asia: research areas and opportunities", *Electronic Commerce Research and Applications*, Vol. 14 No. 3, pp. 145-149, doi: 10.1016/j.elerap.2015.02.001.

Lemon, K.N., Rust, R.T. and Zeithaml, V.A. (2001), "What drives customer equity?", *Marketing Management*, Vol. 10 No. 1, pp. 20-25.

Liang, T.P. and Turban, E. (2014), "Introduction to the special issue social commerce: a research framework for social commerce", *International Journal of Electronic Commerce*, Vol. 16 No. 2, pp. 5-13, doi: 10.2753/JEC1086-4415160201.

Liang, T.P., Lai, H.J. and Ku, Y.C. (2006), "Personalized content recommendation and user satisfaction: theoretical synthesis and empirical findings", *Journal of Management Information Systems*, Vol. 23 No. 3, pp. 45-70.

Liang, T.P., Ho, Y.T., Li, Y.W. and Turban, E. (2011), "What drives social commerce: the role of social support and relationship quality", *International Journal of Electronic Commerce*, Vol. 16 No. 2, pp. 69-90, doi: 10.2753/JEC1086-4415160204.

Lichtenstein, D.R., Netemeyer, R.G. and Burton, S. (1990), "Distinguishing coupon proneness from value consciousness: an acquisition-transaction utility theory perspective", *Journal of Marketing*, Vol. 54 No. 3, pp. 54-67.

Lin, H.F. (2007), "The impact of website quality dimensions on customer satisfaction in the B2C e-commerce context", *Total Quality Management*, Vol. 18 No. 4, pp. 363-378.

Malhotra, N.K. and Dash, S. (2016), *Marketing Research: An Applied Orientation*, 7th ed., Pearson, Noida.

Martin, H.S. and Herrero, A. (2012), "Influence of the user's psychological factors on the online purchase intention in rural tourism: integrating innovativeness to the UTAUT framework", *Tourism Management*, Vol. 33 No. 2, pp. 341-350, doi: 10.1016/j.tourman.2011.04.003.

Martin, K. and Todorov, I. (2010), "How will digital platforms be harnessed in 2010, and how will they change the way people interact with brands?", *Journal of Interactive Advertising*, Vol. 10 No. 2, pp. 61-66.

Mehrabian, A. and Russell, J.A. (1974), *An Approach to Environmental Psychology*, MIT Press, Cambridge, MA.

Mollen, A. and Wilson, H. (2010), "Engagement, telepresence and interactivity in online consumer experience: reconciling scholastic and managerial perspectives", *Journal of Business Research*, Vol. 63 Nos 9-10, pp. 919-925.

Morgan, R.M. and Hunt, S.D. (1994), "The commitment-trust theory of relationship marketing", *Journal of Marketing*, Vol. 58 No. 3, pp. 20-38.

Muntinga, D.G., Moorman, M. and Smit, E.G. (2011), "Introducing COBRAs: exploring motivations for brand-related social media use", *International Journal of Advertising*, Vol. 30 No. 1, pp. 13-46.

Naaman, M., Becker, H. and Gravano, L. (2011), "Hip and trendy: characterizing emerging trends on twitter", *Journal of the American Society for Information Science and Technology*, Vol. 62 No. 5, pp. 902-918.

Nadeem, W., Andreini, D., Salo, J. and Laukkanen, T. (2015), "Engaging consumers online through websites and social media: a gender study of Italian Generation Y clothing consumers", *International Journal of Information Management*, Vol. 35 No. 4, pp. 432-442.

Nambisan, P. and Watt, J.H. (2011), "Managing customer experiences in online product communities", *Journal of Business Research*, Vol. 64 No. 8, pp. 889-895.

Nunnally, J.C. and Bernstein, I.H. (1994), "The assessment of reliability", *Psychometric Theory*, Vol. 3 No. 1, pp. 248-292.

Oliver, R.L. (1999), "Whence consumer loyalty?", *Journal of Marketing*, Vol. 63, Special Issue, pp. 33-44.

Oliver, R.L. and DeSarbo, W.S. (1988), "Response determinants in satisfaction judgments", *Journal of Consumer Research*, Vol. 14 No. 4, pp. 495-507.

Ou, Y.C., De Vries, L., Wiesel, T. and Verhoef, P.C. (2014), "The role of consumer confidence in creating customer loyalty", *Journal of Service Research*, Vol. 17 No. 3, pp. 339-354, doi: 10.1177/1094670513513925.

Palmatier, R.W., Dant, R.P., Grewal, D. and Evans, K.R. (2006), "Factors influencing the effectiveness of relationship marketing: a meta-analysis", *Journal of Marketing*, Vol. 70 No. 4, pp. 136-153.

Parboteeah, D.V., Valacich, J.S. and Wells, J.D. (2009), "The influence of website characteristics on a consumer's urge to buy impulsively", *Information Systems Research*, Vol. 20 No. 1, pp. 60-78.

Park, D.H. and Kim, S. (2008), "The effects of consumer knowledge on message processing of electronic word-of-mouth via online consumer reviews", *Electronic Commerce Research and Applications*, Vol. 7 No. 4, pp. 399-410.

Peppers, D. and Roggers, M. (1995), "A new marketing paradigm: share of customer, not market share", *Planning Review*, Vol. 23 No. 2, pp. 14-18.

Pham, P.H. and Gammoh, B.S. (2015), "Characteristics of social-media marketing strategy and customer-based brand equity outcomes: a conceptual model", *International Journal of Internet Marketing and Advertising*, Vol. 9 No. 4, pp. 321-337, doi: 10.1504/IJIMA.2015.072885.

Podsakoff, P.M., MacKenzie, S.B., Lee, J.-Y. and Podsakoff, N.P. (2003), "Common method biases in behavioral research: a critical review of the literature and recommended remedies", *Journal of Applied Psychology*, Vol. 88 No. 5, pp. 879-903.

Ranganathan, C. and Ganapathy, S. (2002), "Key dimensions of business-to-consumer web sites", *Information & Management*, Vol. 39 No. 6, pp. 457-465.

Ravald, A. and Gronroos, C. (1996), "The value concept and relationship marketing", *European Journal of Marketing*, Vol. 30 No. 2, pp. 19-30.

Reynolds, K.E. and Betty, S.E. (1999), "Customer benefits and company consequences of customer–salesperson relationships in retailing", *Journal of Retailing*, Vol. 75 No. 1, pp. 11-32.

Rust, R.T., Lemon, K.N. and Zeithaml, V.A. (2004), "Return on marketing: using customer-equity to focus marketing strategy", *Journal of Marketing*, Vol. 68 No. 1, pp. 109-127.

Sautter, P., Hyman, M.R. and Lukosius, V. (2004), "E-tail atmospherics: a critique of the literature and model extension", *Journal of Electronic Commerce Research*, Vol. 5 No. 1, pp. 14-24.

Senders, A., Govers, R. and Neuts, B. (2013), "Social media affecting tour operators' customer loyalty", *Journal of Travel & Tourism Marketing*, Vol. 30 Nos 1-2, pp. 41-57.

Sharma, P. (2011), "Country of origin effects in developed and emerging markets: exploring the contrasting roles of materialism and value consciousness", *Journal of International Business Studies*, Vol. 42 No. 2, pp. 285-306.

Srinivasan, S.S., Anderson, R. and Ponnavolu, K. (2002), "Customer loyalty in e-commerce: an exploration of its antecedents and consequence", *Journal of Retailing*, Vol. 78 No. 1, pp. 41-50.

Srivastava, R.K., Shervani, T.A. and Fahey, L. (1998), "Market-based assets and shareholder value: a framework for analysis", *Journal of Marketing*, Vol. 62 No. 1, pp. 2-18.

Statista (2015), "Average numbers of hours per day spent by social media users on all social media channels as of 4th quarter 2015, by country", Statista: the statistics portal, available at: www.statista.com/statistics/270229/usage-duration-of-social-networks-by-country/ (accessed March 3, 2017).

Tam, K.Y. and Ho, S.Y. (2006), "Understanding the impact of web personalization on user information processing and decision outcomes", *MIS Quarterly*, Vol. 30 No. 4, pp. 865-890.

Tuten, T.L. and Solomon, M.R. (2016), *Social Media Marketing*, 2nd ed., Sage Texts, New Delhi.

Verhoef, P.C., Langerak, F. and Donkers, B. (2007), "Understanding brand and dealer retention in the new car market: the moderating role of brand tier", *Journal of Retailing*, Vol. 83 No. 1, pp. 97-113.

Vogel, V., Evanschitzky, H. and Ramaseshan, B. (2008), "Customer equity drivers and future sales", *Journal of Marketing*, Vol. 72 No. 6, pp. 98-108.

Wang, T., Yeh, R.K. and Yen, D.C. (2015), "Influence of customer identification on online usage and purchasing behaviors in social commerce", *International Journal of Human Computer Interaction*, Vol. 31 No. 11, pp. 805-814.

Yadav, M. (2017), "Social media as a marketing tool: opportunities and challenges", *Indian Journal of Marketing*, Vol. 47 No. 3, pp. 16-28.

Yadav, M. and Rahman, Z. (2016), "The social role of social media: the case of Chennai rains-2015", *Social Network Analysis and Mining*, Vol. 6 No. 1, pp. 1-12.

Yadav, M. and Rahman, Z. (2017a), "Social media marketing: literature review and future research directions", *International Journal of Business Information Systems*, Vol. 25 No. 2, pp. 213-240.

Yadav, M. and Rahman, Z. (2017b), "Measuring consumer perception of social media marketing activities in e-commerce industry: scale development & validation", *Telematics and Informatics*, Vol. 34 No. 7, pp. 1294-1307.

Yadav, M., Kamboj, S. and Rahamn, Z. (2016), "Customer co-creation through social media: the case of 'Crash the Pepsi IPL 2015", *Journal of Direct, Data and Digital Marketing Practice*, Vol. 17 No. 4, pp. 259-271, doi: 10.1057/dddmp.2016.4.

Yan, Q., Wu, S., Wang, L., Wu, P., Chen, H. and Wei, G. (2016), "E-WOM from e-commerce websites and social media: which will consumer adopt", *Electronic Commerce Research and Applications*, Vol. 17 No. 3, pp. 62-73, doi: 10.1016/j.elerap.2016.03.004.

Yang, Z. and Peterson, R.T. (2004), "Customer perceived value, satisfaction, and loyalty: the role of switching costs", *Psychology & Marketing*, Vol. 21 No. 10, pp. 799-822.

Zeithaml, V.A., Berry, L.L. and Parasuraman, A. (1996), "The behavioral consequences of service quality", *Journal of Marketing*, Vol. 60 No. 2, pp. 31-46.

Zhang, H., Lu, Y., Gupta, S. and Zhao, L. (2014), "What motivates customers to participate in social commerce? The impact of technological environments and virtual customer experiences", *Information & Management*, Vol. 51 No. 8, pp. 1017-1030, doi: 10.1016/j.im.2014.07.005.

Zhang, K.Z. and Benyoucef, M. (2016), "Consumer behavior in social commerce: a literature review", *Decision Support Systems*, Vol. 86 No. 6, pp. 95-108.

Zhang, K.Z.-K., Benyoucef, M. and Zhao, S.J. (2016), "Building brand loyalty in social commerce: the case of brand microblogs", *Electronic Commerce Research and Applications*, Vol. 15 No. 1, pp. 14-25.

Zhang, S., Doorn, J.V. and Leeflang, P.S.-H. (2014), "Does the importance of value, brand and relationship equity for customer loyalty differ between eastern and western cultures?", *International Business Review*, Vol. 23 No. 1, pp. 284-292.

Further reading

American Marketing Association (2013), *Definition of Marketing*, American Marketing Association, Chicago, IL, available at: www.ama.org/AboutAMA/Pages/Definition-of-Marketing.aspx

Chae, H., Ko, E. and Han, J. (2015), "How do customers' SNS participation activities impact on customer equity drivers and customer loyalty? Focus on the SNS services of a global SPA brand", *Journal of Global Scholars of Marketing Science*, Vol. 25 No. 2, pp. 122-141.

Facebook (2017), "Facebook Newsroom", February, available at: http://newsroom.fb.com/company-info/ (accessed March 24, 2017).

Felix, R., Rauschnabel, P.A. and Hinsch, C. (2017), "Elements of strategic social media marketing: a holistic framework", *Journal of Business Research*, Vol. 70 No. 1, pp. 118-126, doi: 10.1016/j.jbusres.2016.05.001.

Appendix

Construct	Items	Source
Interactivity	E-commerce's social media allows me to share and update the existing content	Zhang, Lu, Gupta and Zhao (2014)
	This e-commerce brand interacts regularly with its followers and fans	Zhang *et al.* (2016)
	E-commerce's social media facilitates two-way interaction with family and friends	Kim (2015)
Informativeness	E-commerce's social media offers accurate information on products	Kim and Park (2013)
	E-commerce's social media offers useful information	Lin (2007)
	The information provided by e-commerce's social media is comprehensive	Zhang *et al.* (2016)
Word-of-mouth	I would recommend my friends to visit e-commerce's social media	Hwang *et al.* (2014)
	I would encourage my friends and acquaintances to use e-commerce's social media	Hsu *et al.* (2013)
	I would like to share my purchase experiences with friends and acquaintances on e-commerce's social media	Hwang *et al.* (2014)
Personalization	E-commerce's social media makes purchase recommendations as per my requirements	Srinivasan *et al.* (2002)
	I feel my needs are met by using e-commerce's social media	Kassim and Ismail (2009)
	E-commerce's social media facilitates personalized information search	Kim and Ko (2012)
Trendiness	Contents visible in e-commerce's social media is the latest trend	Yadav and Rahman (2017b)
	Using e-commerce's social media is really trendy	Kim and Ko (2012)
	Anything trendy is available on e-commerce's social media	Yadav and Rahman (2017b)
Value equity	The price-quality ratio of the products at the e-commerce site is good	Ou *et al.* (2014)
	I can purchase products from e-commerce site conveniently	
	I could use e-commerce site 24/7 anywhere	
Brand equity	This e-commerce site is a strong Brand	Verhoef *et al.* (2007)
	This e-commerce site is an innovative brand	
Relationship equity	I feel that the e-commerce site knows my requirements	Ou *et al.* (2014)
	I feel like home with this e-commerce site	
	I feel committed to this e-commerce site	
Customer loyalty	The likelihood of my purchase from this e-commerce site in the future is high	Wang *et al.* (2015)
	The likelihood of my recommending this e-commerce site to my friends is high	
	The likelihood of returning to this e-commerce site is high	

Table AI.
Scale items

About the authors

Mayank Yadav is Assistant Professor of Marketing in the Department of Marketing, School of Business at the University of Petroleum and Energy Studies, Dehradun, Uttarakhand (India). He is PhD in Marketing from Indian Institute of Technology Roorkee (IIT Roorkee), Uttarakhand, India. His research interests include social media marketing, social CRM and consumer behavior. He has published papers in reputed international journals like *Telematics and Informatics*, *Journal of Direct Data & Digital Marketing Practice*, *International Journal of Business Information Systems*, *Social Network Analysis and Mining*, *International Journal of Business Excellence* with indexing in Scopus, SSCI, ESCI, ABDC and ABS. He has presented papers in various international and national conferences. He has also participated and conducted various training programs and FDPs. Mayank Yadav is the corresponding author and can be contacted at: mayankyadavmajor@gmail.com

Dr Zillur Rahman is Associate Professor of Marketing in the Department of Management Studies at the Indian Institute of Technology, Roorkee Uttarakhand (India). He has several publications in reputed international journals indexed in Scopus, SSCI, SCI and ABDC. He has published numerous research papers with heavy citation indices. His research interest is business strategy, international marketing and sustainability. He has also authored the Indian adoption of the book titled *Consumer Behavior*, 10e, Blackwell, Miniard, Engel and Rahman (2018). He is among the top five most productive authors in the field of business, management and accounting as acknowledged by Careers 360 in India, which awarded to him by honorable Union Minister of HRD Shri Prakash Javadekar. He was the recipient of various awards, including the Emerald Literati Club Highly Commended Award in 2004 and Emerald/AIMA research fund award in 2009. One of his papers titled "Internet-based supply chain management: using the internet to revolutionize your business" published in *International Journal of Information Management* was the ScienceDirect top 25 hottest article within the journal for the period October-December, 2004.

For instructions on how to order reprints of this article, please visit our website:
www.emeraldgrouppublishing.com/licensing/reprints.htm
Or contact us for further details: **permissions@emeraldinsight.com**